2019

Forward Osmosis for Algae Dewatering and Electrical Field-driven Membrane Fouling Mitigation

Faris Munshi
University of Central Florida

FORWARD OSMOSIS FOR ALGAE DEWATERING AND ELECTRICAL FIELD-DRIVEN MEMBRANE FOULING MITIGATION

by

FARIS M. A. MUNSHI
M.Eng.Sc University of New South Wales, 2009
B.Sc. Umm Al-Qura University, 2006

A dissertation submitted in partial fulfilment of the requirements
for the degree of Doctor of Philosophy
in the Department of Civil, Environmental, and Construction Engineering
in the College of Engineering and Computer Science
at the University of Central Florida
Orlando, Florida

Spring Term
2019

Major Professor: Woo Hyoung Lee

ABSTRACT

Efficient and low-energy microalgae harvesting is essential for sustainable biofuel production. Forward osmosis (FO) can provide a potential alternative for algae separation with low energy consumption by using osmotic pressure. In this study, an aquaporin-based polyethersulfone (PES) membrane was evaluated for algae dewatering using FO with three different types of draw solutions (DSs: NaCl, KCl and NH_4Cl), and under different cross flow velocities (CFVs). 81% of algae dewatering was achieved with a 29% flux drop. Among three different DSs, although NH_4Cl was the best candidate for improved water flux and low reverse salt flux (RSF), it could accelerate cell division, reducing settleability during the FO process. However, RSF originated from NaCl could increase lipid content (~ 49%) in algal biomass probably due to the osmotic imbalance in algal cells.

During FO operations, membrane fouling would be an inherent problem against sustainable algae dewatering. In this study, a novel approach was investigated by coupling the FO with an electric field for developing repulsion forces that can prolong the filtration cycle and mitigate foulant attachment. Several electric fields (0.33, 0.13 and 0.03 V mm^{-1}) were applied in continuous and pulsing modes (10sec intervals) to mitigate membrane fouling for effective algae dewatering. The electric field FO configuration used in this study was able to produce 3.8, 2.2 and 2.2 times greater flux at the applied potential of -1.0, -0.4, and -0.1 V, respectively, compared to the control (without an electric field). A high potential of -10 V for 60 sec was applied as an optimal cleaning procedure with a high ability to recover flux (99%). The study also investigated the effect of the electric fields on bulk pH, conductivity, settling velocity, lipid content and microalgal morphology. Overall, this study demonstrates a

novel technology for algae dewatering in FO application using the aquaporin-based PES membrane.

ACKNOWLEDGMENTS

First, I would like to give thanks to God Almighty, whom that without, none of this would be possible. I would like to than thank all the great people who have supported me in both my personal and professional life.

I would like to seize this opportunity to express my deepest regards and gratitude to Dr. Woo Hyoung Lee, for his dedication and sincere effort throughout my PhD degree and bringing this work to light. Dr. Lee has been a great inspiration who I have admired for his ambitious and supportive attitude. I would also like to thank my dissertation committee, Dr. Steven Duranceau, Dr. Karin Chumbimuni-Torres, and Dr. Anwar Sadmani for their point of views and guidance.

I express my deep gratitude to the KSU and EPA P3 program for funding this research.

I would like thank Maria Real-Robert for her guidance in the lab, from whom I learned the analytic techniques needed for the completion of this research. I would also like to thank my research group friends: Dr. Jaehoon Hwang, Dr. Faisal Al-Quaied, Dr. Xiangmeng Ma, Dr. Jared Church, Rebecca McLean, Rakib UlAlam, AnnMarie Ricchino and Daniela Diaz for their help and support in the laboratory.

Finally, I dedicate my work to my parents and family, Ghadah, Zaid, Nusaibah, Maryam and Ahmad for their devotion and being with me throughout this journey. I also thank my brothers Ahmed, Fadi and Shadi and my sisters Shatha and Shahad for standing with me in all times. Sincere thanks to all my relatives, teachers, mentors, and friends whom help shape me to who I am.

TABLE OF CONTENTS

LIST OF FIGURES

LIST OF TABLES

LIST OF ABBREVIATIONS (OR) ACRONYMS

Algae Biofuel Osmosis Dewatering	ABODE
Biochemical oxygen demand	BOD
Bovine serum albumin	BSA
Canadian Phycological Culture Centre	CPCC
Cellulose triacetate	CTA
Chemical oxygen demand	COD
Cross flow velocities	CFV
Dissolved organic carbon	DOC
Draw solution	DS
Electrical membrane bioreactor	EMBR
Electric Field Forward Osmosis	EFFO
Energy dispersive X-ray	EDX
Environmental Protection Agency	EPA
External concentration polarization	ECP
Extracellular organic matter	EOM
Extracellular polymeric substances,	EPS
Feed solution	FS
Forward osmosis	FO
Hydration Technologies Inc.	HTI
Internal concentration polarization	ICP
Liter per meter square · hour; L m^{-2} h^{-1}	LMH
National Aeronautics and Space Administration	NASA
Optical density	OD
People, Prosperity and the Planet	P3
Polyamide	PA
Polyethersulfone	PES
Pressure-retarded osmosis	PRO
Relative hydrophobicity	RH
Reverse osmosis	RO
Scanning electron microscope	SEM
Sludge volume index	SVI
Soluble microbial products	SMP
Suspended solids	SS
Thin film composite	TFC
Total suspended solids	TSS
Volatile suspended solids	VSS

CHAPTER 1: INTRODUCTION

Dewatered microalgae can be processed to produce biofuel. Microalgae are difficult to remove from solution, and hence, cost effective harvesting of algae is considered to be the most problematic area of algal biofuel production and limits the commercial use of algae (Pahl et al., 2013; Uduman, Qi, Danquah, & Hoadley, 2010). It is estimated that up 20-30 percent of the total cost for algal biomass production in open systems come from harvesting and dewatering (Amer, Adhikari, & Pellegrino, 2011) and about 90 percent of the equipment costs are associated with dewatering (Pahl et al., 2013). The cost of continuous harvesting of dilute suspensions of algae is the major barrier in the advancement of a microalgae based fuel production (McGinnis & Elimelech, 2007; Uduman, Qi, Danquah, Forde, & Hoadley, 2010; Uduman, Qi, Danquah, & Hoadley, 2010).

Traditionally, microalgae have been removed by methods including sedimentation, flocculation, air floatation, filtration, electrophoresis, and centrifugation (Buckwalter, Embaye, Gormly, & Trent, 2013; Mo, Soh, Werber, Elimelech, & Zimmerman, 2015; Uduman, Qi, Danquah, Forde, et al., 2010). Recently, micro and ultrafiltration have been used because of the ease of use and high separation efficiency (Shao et al., 2015). The major drawbacks in pressure driven membrane processes for the separation of algae are biofouling and associated energy costs. Forward osmosis (FO) is a technology that has the potential to conserve energy and produce clean water. Osmosis refers to the phenomenon of spontaneous passage or diffusion of solvents or water through a semipermeable membrane (Ge, Ling, & Chung, 2013; Phuntsho, Shon, Hong, Lee, & Vigneswaran, 2011; Shon, Phuntsho, Zhang, & Surampalli, 2015). FO is a semi-permeable membrane that is placed between two solutions of different osmotic pressures. The osmotic pressure gradient drives water across the membrane

from the less concentrated “feed solution (FS)” (Noffsinger, Giustino, Louie, & Cohen) to the more concentrated “draw solution (DS)”. Several studies have investigated FO as a viable option for desalination, wastewater treatment, irrigation, biomass concentration, and food processing (Cath, Childress, & Elimelech, 2006; Chung, Zhang, Wang, Su, & Ling, 2012; Li et al., 2012; McCutcheon, McGinnis, & Elimelech, 2006; Phuntsho et al., 2011; Yangali-Quintanilla, Li, Valladares, Li, & Amy, 2011). FO can offer excellent dewatering efficiency with that is comparable to pressure driven membrane processes but is less prone to fouling (Kwan, Bar-Zeev, & Elimelech, 2015). Another advantage of FO is its low energy demand. There is a study on algae dewatering using different FO membranes at high cross flow velocity (CFV) of 22.3 cm/sec and using bag FO units (Buckwalter et al., 2013; Zou et al., 2013). NASA offshore membrane enclosures for growing algae project also proposed the use of semi-permeable tubes to dewater algae (Hoover, Phillip, Tiraferri, Yip, & Elimelech, 2011; Wiley, 2013). FO requires very little energy input compared to most conventional dewatering processes, because the DS produces the osmotic pressure which drives the dewatering process (Buckwalter et al., 2013). This makes FO a suitable option for algae biofuel production.

FO draw solutions can be natural resources, waste streams, or high purity solutions. Under FO process, the separation of the solute tends to dilute the DS through the semipermeable membrane (Achilli, Cath, Marchand, & Childress, 2009; Cath et al., 2006). FO can further produce energy by utilizing the diluted DS that, in certain FO process designs, can develop retarded pressure drive forces that can be utilized to generate power (Ge et al., 2013; Hoover et al., 2011). FO requires no hydraulic pressure, leading to a potential to either reduce energy consumption or produce energy (pressure-retarded osmosis, PRO).

Nevertheless, FO requires special membranes, to mitigate internal and external concentration polarization (ICP and ECP). The membrane is usually made from polymeric materials with the capacity to allow passage of small molecules such as water, and block large molecules such as salts, sugars, starches, proteins, viruses, bacteria, and parasites (Shon et al., 2015). Selecting an appropriate DS is important, as the membrane material and draw solutes closely correlate with each other and affect FO performance. Draw solutions that are abundant and require no regeneration are recommended as the diluted DS product can directly be utilized in other applications such as fertigation and feed water in desalination plants. The recommended manufacturer start value of CFV in FO systems is 5 cm/s to control settling and ECP, while high CFV can damage the FO membrane.

Problem Statement

Overview

The objective of using FO is to dewater algae water and to develop a better understanding of FO as a multipurpose sustainable approach. This system is used to achieve a number of outcomes; the secondary wastewater effluent can be used as nutrient media to cultivate the algae specie *Chlorella vulgaris*. This would provide a means of polishing of the wastewater. The FO system would separate the algae from water to produce concentrate algae and diluted DS. The concentrate algae with at least 80% dewatering would require further dewatering and processing to be converted to biofuel or biodiesel (Buckwalter, Embaye, Gormly, & Trent, 2013). The diluted DS is to be used directly in irrigation via fertigation or introduced in a desalination treatment plant.

Research Questions

- What are the effects of varied cross flow velocities (CFV) and different draw solutions (DS) on FO membrane performance for dewatering microalgae?
- How will the fouling be mitigated for flux production in a FO separation system?
- What is the impact of the reverse salt flux (RSF) during FO operation on the algal feed solution (FS)?
- What are the optimal cleaning procedures that would provide maintain flux and high flux recovery rates while being economic?
- What is the effect of an electrical field in the feed chamber on water flux, fouling control and the algal morphology?

Hypotheses

- The increase in CFV would be associated with higher water flux rates with the external concentration polarization and formation of the cake layer being reduced. DS concentration increase would cause an increase in permeate flux. Each DS might have different water flux, reverse salt flux, and reaction with the feed solution.
- While most works in literature only showed short-term tests (e.g., several hours), longer term fouling experiments can show the behaviour of fouling over time. The application of cleaning and fouling control measures can maintain higher average flux rates.
- Optimal cleaning procedure is based on high recovery rates with long cleaning intervals and shorter cleaning intensity and duration. Shorter cleaning intervals and the increase in intensity and duration of cleaning can provide higher recovery rates.

- The applied negative charged electrical field under the support layer of the FO membrane can repel and reduce the negatively charged algal biofouling development.

Opportunities and Challenges of the Study

The membrane used in the study is new in the market and thus have not been studied in the dewatering of algae. The study was also directed to use moderate CFV with conditions which fill in the gaps in the FO work done in literature. Several studies were performed on algae dewatering both using cellulose triacetate (CTA) from Hydration Technology Inc. (Hydrowell Filter, HTI, Albany, OR). One study was conducted with a high CFV of 22.3 cm sec^{-1} (Zhao, Zou, and Mulcahy, 2011). The other study used bag FO units and wave motion to promote mixing and simulate seashore conditions (Buckwalter, Embaye, Gormly, & Trent, 2013). Long term experiments are key to analyse the FO system for fouling control and the development of extracellular organic matter (EOM) in the system that would require special treatment.

FO coupled with and electrical field is a novel approach to control fouling during membrane treatment. The amount of energy input is marginal compared to regular pumping or backwash. On the other hand, pressure gradient loss happens by concentration polarization, fouling, increase of FS concentration, and dilution of the DS occur in the same time. This makes it difficult to clearly quantify the effect of ICP or each one individually.

In addition to the flux loss due to the blockage caused by the cake/foulant layer on the surface of the FO membrane, reverse salt flux (RSF) absorbed by the foulant layer can also abrupt the osmosis pressure gradient. All these factors are usually combined as flux loss due to fouling.

Low flux of FO systems may be a drawback when utilizing this technology. The continued works in developing appropriate and well-designed FO membranes are required for the industry to adapt this technology. Membranes structure and material should maintain a low ICP formation in addition to high mechanical strength, stability and selective permeate flux (Zhang, Wang, Chung, Chen, Jean, and Amy, 2010).

Objective and Aims

Overall Objective

The overall objective of the study is to evaluate the algae separation using a FO system and develop antifouling strategies for sustainable algae dewatering. The specific tasks are: 1) to investigate the effect of different cross flow velocities and different draw solutions, 2) to determine the effect of reverse salt flus in the FO operations on the quality of the algal feed solution, 3) to evaluate a modified configuration of the FO unit by employing an electrical field to abrupt concentration polarization, and 4) to determine the effect of the electric field on the algal biomass.

Dissertation Organization

This dissertation incorporates six chapters. Chapter 1 presents introductory information and overview of this study. Chapter 2 provides a literature review on FO and relevant components in the system in addition to the application of electric fields in membrane filtration systems.

Chapter 3 focuses on providing a better understanding of algae dewatering when using a specific aquaporin PES membrane. Under different cross flow velocities (i.e., 1.5, 5.0, and 10.7 cm sec^{-1}) which have not been examined in other work related to algae dewatering. Also, three draw solutions were examined (e.g. NH_4Cl, NaCl and KCl). The

work furthermore discussed FO membrane fouling and fouling control with algae as a foulant. Chapter 4 discusses the effect of reverse salt flux on the algae culture. The three different salts were tested to understand their effect on the characteristics and morphology of the algae culture.

Chapter 5 demonstrates the use of a modified FO system which was coupled with an electric field to reduce FO fouling and enhance the performance of the FO system. In this section, the development, characterization and evaluation of the electric filed FO system (EFFO) was conducted, with attention to the FS chamber to mitigate fouling and cleaning requirements. The effect of different electrical field intensities in continuous and pulsing modes were evaluated in relation to permeate flux and reverse salt flux. Algae agglomeration activity was covered, in addition to the effect of the electric field on the algae solution with different electric field intensities, different salinity levels and two types of mesh electrodes (e.g. stainless steel and carbon fiber).

Chapter 6 has a comprehension of the dissertation, displaying a summery and. Chapter 7 proposes potential impacts of the work and future potential work developed of this research. This document also includes appendices that provide supplemental information.

References

Achilli, A., Cath, T. Y., Marchand, E. A., & Childress, A. E. (2009). The forward osmosis membrane bioreactor: A low fouling alternative to MBR processes. *Desalination, 239*(1–3), 10-21. doi:http://dx.doi.org/10.1016/j.desal.2008.02.022

Amer, L., Adhikari, B., & Pellegrino, J. (2011). Technoeconomic analysis of five microalgae-to-biofuels processes of varying complexity. *Bioresource Technology, 102*(20), 9350-9359. doi:http://dx.doi.org/10.1016/j.biortech.2011.08.010

Buckwalter, P., Embaye, T., Gormly, S., & Trent, J. D. (2013). Dewatering microalgae by forward osmosis. *Desalination, 312,* 19-22. doi:http://dx.doi.org/10.1016/j.desal.2012.12.015

Cath, T. Y., Childress, A. E., & Elimelech, M. (2006). Forward osmosis: Principles, applications, and recent developments. *Journal of Membrane Science, 281*(1–2), 70-87. doi:http://dx.doi.org/10.1016/j.memsci.2006.05.048

Chung, T.-S., Zhang, S., Wang, K. Y., Su, J., & Ling, M. M. (2012). Forward osmosis processes: Yesterday, today and tomorrow. *Desalination, 287*, 78-81. doi:http://dx.doi.org/10.1016/j.desal.2010.12.019

Ge, Q., Ling, M., & Chung, T.-S. (2013). Draw solutions for forward osmosis processes: Developments, challenges, and prospects for the future. *Journal of Membrane Science, 442*, 225-237. doi:http://dx.doi.org/10.1016/j.memsci.2013.03.046

Hoover, L. A., Phillip, W. A., Tiraferri, A., Yip, N. Y., & Elimelech, M. (2011). Forward with Osmosis: Emerging Applications for Greater Sustainability. *Environmental Science & Technology, 45*(23), 9824-9830. doi:10.1021/es202576h

Kwan, S. E., Bar-Zeev, E., & Elimelech, M. (2015). Biofouling in forward osmosis and reverse osmosis: Measurements and mechanisms. *Journal of Membrane Science, 493*, 703-708. doi:http://dx.doi.org/10.1016/j.memsci.2015.07.027

Li, Z.-Y., Yangali-Quintanilla, V., Valladares-Linares, R., Li, Q., Zhan, T., & Amy, G. (2012). Flux patterns and membrane fouling propensity during desalination of seawater by forward osmosis. *Water Research, 46*(1), 195-204. doi:http://dx.doi.org/10.1016/j.watres.2011.10.051

McCutcheon, J. R., McGinnis, R. L., & Elimelech, M. (2006). Desalination by ammonia–carbon dioxide forward osmosis: Influence of draw and feed solution concentrations on process performance. *Journal of Membrane Science, 278*(1–2), 114-123. doi:http://dx.doi.org/10.1016/j.memsci.2005.10.048

McGinnis, R. L., & Elimelech, M. (2007). Energy requirements of ammonia–carbon dioxide forward osmosis desalination. *Desalination, 207*(1), 370-382. doi:http://dx.doi.org/10.1016/j.desal.2006.08.012

Mo, W., Soh, L., Werber, J. R., Elimelech, M., & Zimmerman, J. B. (2015). Application of membrane dewatering for algal biofuel. *Algal Research, 11*, 1-12. doi:http://dx.doi.org/10.1016/j.algal.2015.05.018

Noffsinger, J., Giustino, F., Louie, S. G., & Cohen, M. L. (2009). Origin of superconductivity in boron-doped silicon carbide from first principles. *Physical Review B, 79*(10), 104511.

Pahl, S. L., Lee, A. K., Kalaitzidis, T., Ashman, P. J., Sathe, S., & Lewis, D. M. (2013). Harvesting, thickening and dewatering microalgae biomass. In *Algae for biofuels and energy* (pp. 165-185): Springer.

Phuntsho, S., Shon, H. K., Hong, S., Lee, S., & Vigneswaran, S. (2011). A novel low energy fertilizer driven forward osmosis desalination for direct fertigation: Evaluating the

performance of fertilizer draw solutions. *Journal of Membrane Science, 375*(1–2), 172-181. doi:http://dx.doi.org/10.1016/j.memsci.2011.03.038

Shao, P., Darcovich, K., McCracken, T., Ordorica-Garcia, G., Reith, M., & O'Leary, S. (2015). Algae-dewatering using rotary drum vacuum filters: Process modeling, simulation and techno-economics. *Chemical Engineering Journal, 268*, 67-75. doi:http://dx.doi.org/10.1016/j.cej.2015.01.029

Shon, H., Phuntsho, S., Zhang, T., & Surampalli, R. (2015). *Forward Osmosis*: American Society of Civil Engineers.

Uduman, N., Qi, Y., Danquah, M. K., Forde, G. M., & Hoadley, A. (2010). Dewatering of microalgal cultures: a major bottleneck to algae-based fuels. *Journal of renewable and sustainable energy*, *2*(1), 012701.

Uduman, N., Qi, Y., Danquah, M. K., & Hoadley, A. F. (2010). Marine microalgae flocculation and focused beam reflectance measurement. *Chemical Engineering Journal, 162*(3), 935-940.

Wiley, P. E. (2013). Microalgae cultivation using offshore membrane enclosures for growing algae (OMEGA).

Yangali-Quintanilla, V., Li, Z., Valladares, R., Li, Q., & Amy, G. (2011). Indirect desalination of Red Sea water with forward osmosis and low pressure reverse osmosis for water reuse. *Desalination, 280*(1–3), 160-166. doi:http://dx.doi.org/10.1016/j.desal.2011.06.066

Zou, S., Wang, Y.-N., Wicaksana, F., Aung, T., Wong, P. C. Y., Fane, A. G., & Tang, C. Y. (2013). Direct microscopic observation of forward osmosis membrane fouling by microalgae: Critical flux and the role of operational conditions. *Journal of Membrane Science, 436*, 174-185. doi:http://dx.doi.org/10.1016/j.memsci.2013.02.030

CHAPTER 2: BACKGROUND AND SIGNIFICANCE OF FORWARD OSMOSIS IN RELATION TO ALGAE DEWATERING

Forward Osmosis (FO)

Prosperity and prevalence of life is based on water security. The relatively small fraction of water that is available as fresh water requires great efforts to be manage and maintain for municipal, commercial, agricultural and industrial purposes while being economically and environmentally conservative. In forward osmosis (FO), the osmosis property can driver water to permeate through the membrane from the less concentrated "feed solution" to the more concentrated "draw solution". FO known applications include separation processes, pressure generation and electrical production. It has been used in various applications including desalination, wastewater treatment, biomass concentration, and food processing. FO requires no hydraulic pressure and has the potential to contribute in seawater and brackish water desalination, wastewater treatment, biomass concentration, and food processing (Buckwalter, Embaye, Gormly and Trent, 2013). The renewed interest in FO processes comes from its potential to either reduce energy consumption or produce energy (pressure retarded osmosis).

Energy Conservation

In terms of reducing energy consumption in desalination, a study used FO membranes to dilute seawater from the Red Sea using secondary wastewater effluent as FS. The energy required to apply reverse osmosis (RO) desalination to the diluted seawater was reduced from 2.5–4 kWh m^{-3} to 1.5 kWh/m^3 (Yangali-Quintanilla, Li, Valladares, Li, & Amy, 2011).

Water Production

FO membranes can be used to assist in desalination by utilizing FO before the desalination of seawater, seawater is used as a DS and will be diluted via impaired water feed solution (brackish or advanced treated wastewater). This can ease the process of desalination as diluted seawater would produce more permeate and reduce fouling in the reverse osmosis (RO) stage. FO is currently utilized by resting the RO; the permeate backflows through the membrane due to salt gradient difference which helps release the fouling formation on the RO membrane. Lastly, the high concentrated brine from the desalinated plant can be diluted to meet the standards of waste water discharge into the sea (Hoover, Phillip, Tiraferri, Yip, & Elimelech, 2011). In agriculture, FO can increase the availability of water for irrigation through extraction of freshwater from brackish sources. Fertilizer is used to generate the concentrated DS, and brackish groundwater is used as the FS. The diluted fertilizer solution is subsequently applied to crops through a fertigation distribution network. A study estimated that 1 kg of fertilizer can extract 2,459 L of freshwater from a simulated brackish water of very high salinity (Hoover et al., 2011; Phuntsho, Shon, Hong, Lee, & Vigneswaran, 2011).

Concentration Polarization

FO membranes are specially designed to control concentration polarization (i.e. external and internal concentration polarization (ECP & ICP)). This is done by developing thin membranes and special support structures that can reduce the effect of ICP. The orientation of the FO membrane, surface characteristics and the applied CFV can affect ECP (McCutcheon & Elimelech, 2006). When the conventional structure of membranes (reverse osmosis or nano-filters) are used solely under osmotic forces, internal concentration

polarization is developed which inhibits the performance of the FO unit reducing the water flux (Chou et al., 2010; Ge, Ling, & Chung, 2013).

Draw Solution

Draw solutions are typically composed of salts that naturally occur in brackish water, seawater, or hypersaline water, but they can include any osmolyte, such as glucose and fructose. The requirements of selecting a suitable DS are specific to the purpose of FO and the subsequent applications (Fig. 2-1 & Table 2-1). This process would ensure the feasibility and long-term performance of the DS. Studies done on FO for different draw solutions and concentration showed flux that varied widely (4-22.6 L m^{-2} h^{-1}) (Holloway, Childress, Dennett, & Cath, 2007).

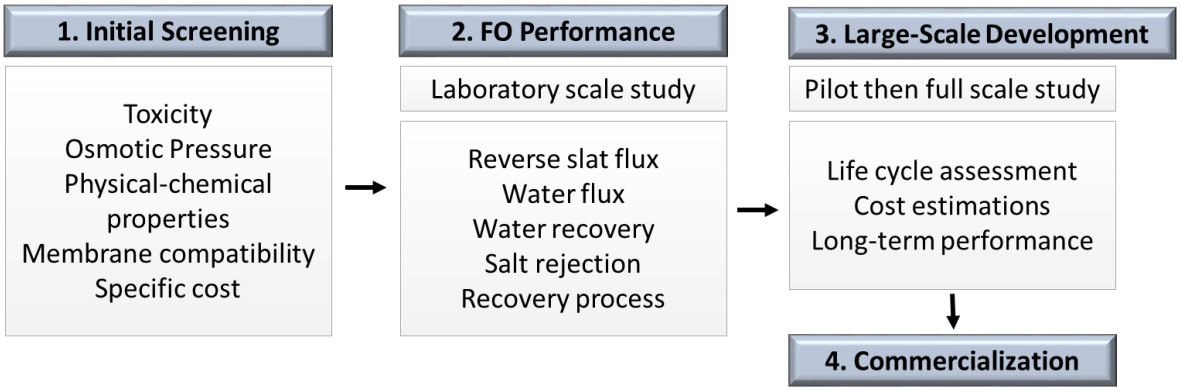

Figure 2-1: General criteria for selecting a DS (Shon, Phuntsho, Zhang, & Surampalli, 2015).

Algae Growth and Dewatering

The harvesting cycle of microalgae is from 1 - 10 days. Microalgae can be grown with minimal impact on fresh water resources and require less land area compared to crops (Chisti, 2007). In the present of light, algae can grow using flue gas from power plants as a carbon source, and secondary effluent from wastewater treatment plants as nutrients. Attention is

drawn to algae cultivation and harvesting for its high biomass to oil fraction (Chisti, 2007; Tornabene, Holzer, Lien, & Burris, 1983).

The dewatering of cultivated algae can be assisted with the use of FO. More than 75% and up to 85% of the water can be removed from the algae solution by FO when using abundant seawater as a DS (Buckwalter, Embaye, Gormly, & Trent, 2013; Hoover et al., 2011). For FO to be considered as a viable treatment or process stage, it should be constructed near other facilities and geolocations that provide quality draw and feed solutions. Direct use of the final concentrated feed water and the diluted DS should be considered without further high energy input. The algae specie *Chlorella vulgaris* was selected as a potential FS for its ability be used as a tertiary treatment stage for nutrient removal. When dewatered algae can be processed to produce biofuel. Microalgae are difficult to remove from solution and cost effective harvesting of microalgae is considered to be the most problematic area of algal biofuel production and limits the commercial use of algae as a biofuel source (Pahl et al., 2013; Uduman, Qi, Danquah, & Hoadley, 2010). Experts estimate up 20-30% of the total cost for algal biomass production in open systems come from harvesting and dewatering (Amer, Adhikari, & Pellegrino, 2011) and 90% of the equipment costs are associated with dewatering (Pahl et al., 2013). The cost of continuous harvesting of dilute suspensions of algae is the main impediment to advance the commercial use of microalgae (McGinnis & Elimelech, 2007; Uduman, Qi, Danquah, Forde, & Hoadley, 2010; Uduman, Qi, Danquah, & Hoadley, 2010).

Membrane Fouling and Fouling Control

Organic fouling occurring on the membrane surface starts with the attachment of small cultures of the organisms on the surface and which can further grow and accumulate.

At first, reversible fouling is achieved by bacteria being attracted to the surface under physical forces including Brownian motion, electrostatic interaction, gravity, and Van-der Waals. Irreversible fouling starts when bacteria produce extracellular polymeric substances (EPS) which cement the microorganisms to the surface of the membrane (Shon, Phuntsho, Zhang, & Surampalli, 2015). On the surface of FO membranes, the organic foulants form a less compact layer due to the absence of hydraulic pressure. This would reduce the tendency of using harsh cleaning procedures.

There are a couple of studies that compared between organic fouling in FO and RO membranes. Cleaning was done by only applying physical scouring cleaning; The study showed that the cellulose triacetate (CTA) membrane performance was fully reversible for the FO membrane and only 70% for the RO mode (Valladares Linares, Yangali-Quintanilla, Li, & Amy, 2012; Cath, Childress, and Elimelech, 2006). The full understanding of the complex FO fouling mechanisms is yet found; further research should include all factors that comprehend the FO system (Kwan, Bar-Zeev and Elimelech, 2015). These findings support the riddance of any chemical requirement for FO membrane performance recovery.

Arkhangelsky (2011) introduced inorganic foulants ($CaSO_4$) and studied several cleaning procedures such as hydraulic backwash, surface flushing and osmotic backwash. Only hydraulic backwash was able to restore water flux of the flat sheet FO membrane to 75% and up to 100% for the FO hollow fibres (Arkhangelsky et al., 2012). They found that the inorganic scaling caused pore blocking which could be a result of the penetration of crystals from the FS into the support matrix of the membrane, or the formation of crystals inside the porous support layer. Another study showed that draw solutions containing Mg^{+2}

can negatively impact the FO membrane as it severely causes less reversible fouling and increases reverse salt diffusion into the FS (Buckwalter, Embaye, Gormly, & Trent, 2013).

FO membranes cleaning and fouling control are of major importance for the adaptation of this technology. There is a lack in long term studies that have a well-rounded approach in maintaining flux. FO has the advantage of concentrating high organic and inorganic loadings. Most organic fouling studies used alginate as an organic foulant (Lee, Boo, Elimelech, & Hong, 2010; Liu & Mi, 2012; Mi & Elimelech, 2010). Lee (2010) used a combination of alginate, humic acid, and bovine serum albumin (BSA). These three studies used low total organic concentration of 200 mg/L. Other organic foulants tested for fouling control were raw centrate mixed with influent raw wastewater (Holloway et al., 2007), secondary wastewater effluent (Valladares Linares, Yangali-Quintanilla, Li, & Amy, 2012), synthetic municipal wastewater that was sludge seeded, and BSA with NaCl (Zhao & Zou, 2011).

Most papers that conducted fouling cleaning used a cellulose triacetate (CTA) FO membranes from Hydration Technologies Inc. (Körbahti & Artut) (Albany, OR). Zhang et al. (2012), developed their own ultra-thin polyamide membrane with an active layer (~300 nm) on an inner surface of hollow fibre. The FO membrane was used in a membrane bioreactor to treat synthetic municipal wastewater. In addition to HTI FO membranes, Mi (2010) used a polyamide (PA) which was a RO membrane from Dow Chemical Company (Midland, MI).

The cleaning methods used to remove the organic fouling had recovery rates from 90-100%. However, most of the previous studies varied widely when defining cleaning points. The duration between cleaning varied 8, 16, 24, 32 and 48 hours. Zaho (2011) chose to clean the FO system when flux reached 40-60% of the initial flux. A better approach would take in

consideration maintaining flux with the longest cleaning intervals while being able to achieve high recovery of the system. Table 2-1 displays FO experimental conditions and variables used in fouling cleaning. Furthermore, Table 2-2 contains FO cleaning procedures in relation to feed solutions with inorganic components

Chlorella vulgaris are microalgae with an average diameter of 5 μm. The behaviour of the algae biofouling is yet to be studied. The effect of the selected draw solution should be taken in consideration as it may react with the foulant layer (i.e. shrink or enhance growth after attachment).

Table 2-1: Forward osmosis cleaning procedures using feed solutions containing organic components.

Membranes Type	Draw solution	Feed solution	Cleaning after (h)	Cleaning method	Recovery (%)	Flux (LMH)	Ref.
Flat-sheet CTA, HTI	4.0 M NaCl	Sodium alginate 200 mg L^{-1}	48	Flush: DI water for 21 min; CFV 21 cm sec^{-1}; continuous air bubble with 5 min interval	90-100 %	14-16	(Liu, 2012)
Flat-sheet CTA, HTI	3.0 M NaCl	200 mg L^{-1} total organic foulant concentration (Alginate, humic acid, and BSA)	12	Flush: increase CFV to 25.6 cm sec^{-1} till full recovery (20-50 min)	99%	25.2	(Lee, 2010)
Flat-sheet CTA, HTI	1.2 M NaCl	High nutrient raw centrate; mixed with raw wastewater	32	Flush: DI (FS); 4 Liter flush - NaOH solution (FS); 30 min - DI (FS); 4 Liter flush Osmotic backwashing: 50 g L^{-1} NaCl (FS) & DI water (DS); 10 & 20 min - Flush with DS & FS	90%	6-8	(Holloway, 2007)
Flat-sheet CTA, HTI	4.0 M NaCl	200 mg L^{-1} alginate, 50 mM NaCl, and 0.5 mMCa^{2+}	20 - 24	Flush: 50mM NaCl; 15 min; CFV: 21 cm sec^{-1} DI water; 15 min; CFV: 21 cm sec^{-1} Bubble DI; 5 min; CFV: 21 cm sec^{-1}	97%	27	(Mi, 2010)
Flat-sheet CTA, HTI	Seawater; (TDS) was 0.7 g/L, the conductivity 54.3 mS cm^{-1}	Secondary wastewater effluent	24	Submerged FO membrane system: Air scouring for 15 min. Chemical cleaning (1% NaOCl)	90% 93%	-	(Valladares, 2012)
Flat-sheet CTA, HTI	0.6 M NaCl	0.436 M NaCl and 2 g L^{-1} BSA.	at flux loss of 40-60%	Flush: DI water; 1 - 5 h; CFV 25 cm sec^{-1}	90%	5-6	(Zhao, 2011)
Ultra-thin polyamide skin layer (~300 nm) on the inner surface of the hollow fibre	0.5 M NaCl	Synthetic municipal Wastewater, Seed sludge	8 - 16	Flush: ultrapure water; 48 hr; - Soak in a HNO_3 solution at pH 2; 1 hr (dissolve the inorganic scaling)	99%	5.5	(Zhang, 2012)

Table 2-2: Forward osmosis cleaning procedures using feed solutions containing inorganic components.

Membranes Type	Draw solution	Feed solution	Cleaning after (hr)	Cleaning method	Recovery	Flux (LMH)	Ref.
Flat-sheet CTA, HTI	1.5 M Na_2SO_4	Brackish water; TDS= 3970 mg L^{-1}	23	Flush: DI water; 30 min; CFV 33.3 cm sec^{-1}	FO: 70%	8.8	(Zhao, 2012)
Flat-sheet CTA, HTI + Plastic mesh spacers	1.5 M $Na2_SO_4$	Brackish water (0.06 M NaCl solution-simulated); TDS= 3970 mg L^{-1}	28	Flush: DI water; 20 min; CFV 33.3 cm sec^{-1}	92 – 97%; 25 - 45°C	15	(Zhao, 2011)
Flat-sheet CTA, HTI	4 M NaCl	35 mM $CaCl_2$, 20 mM Na_2SO_4, and 19 mM NaCl with a gypsum	24	Flush: DI; 15 min; CFV 21 cm sec^{-1}	96%	6-7	(Mi, 2010)
Flat-sheet CTA, HTI	4.4 M NaCl	Drilling wastewater	3 - 7	Flush: DI (FS); 30 min Osmotic back wash: DI (DS) & DS (FS); 21 min	99%	14	(Hickenbottom, 2013)
Flat-sheet CTA, HTI	5 M NaCl	Calcium sulphate ($CaSO_4$) scaling with sodium chloride as draw solution, $CaCl_2$ (3.88 g L^{-1}), Na_2SO_4 (2.84 g L^{-1}) and NaCl (1.11g L^{-1}) with 130% saturated $CaSO_4$	5.8	Flush: Ultra-pure water; 1 hr; CFV: 48 cm sec^{-1} Backwash: Ultra-pure water; 1 bar; 450 mL min^{-1}	47, 80, 41% respectively	14-18	(Arkhangelsky, 2012)
Thin film composite (TFC) FO hollow fibres, Polyamide	1 M NaCl			Osmotic Backwash: Ultra-pure water (DS) & 5 M NaCl (FS); 1 hr; 48 cm sec^{-1}	99% (backwash)	19	(Arkhangelsky, 2012)

Electrical Field

The concept of applying an electrical field has been used in membrane bioreactors. Bechhold (1926) used an electric field in ultrafiltration to serve as an additional force for separation (Zumbusch, Kulcke, & Brunner, 1998). The concept of electrical membrane bioreactor (EMBR) in treating wastewater is attributed to developing an electrostatic field on the membrane surface to build repulsion forces that would prolong the filtration cycle and inhibit foulant attachment, Figure 2-2 displays the principle of membrane electro-filtration. Membrane positioned at a potential of -300 to -500 mV is expected to have a higher foulant rejection compared to the low potential on membrane surfaces (L. Liu, J. Liu, B. Gao, & F. Yang, 2012). The applied electrical fields used in literature varied between 0.036 – 6 V cm^{-1} with 2 - 5.5 cm between the cathode and anode electrodes. Different applied patterns were used of continuous and pulsing electric fields (Bani-Melhem & Elektorowicz, 2011; J. Liu, L. Liu, B. Gao, & F. Yang, 2012). Fluctuating intensities can be used to control the formation of the biofouling layer. Algae has a negative charge with a zeta potential of -10 to -35 mV (Henderson, Parsons, & Jefferson, 2008). Introducing a neutralizing or higher negative charge can repel particles and further reduce the compaction of the forming foulant layer.

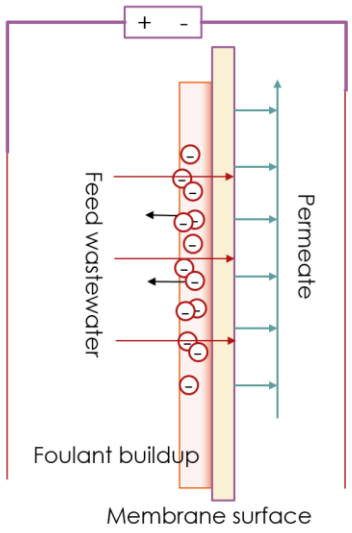

Figure 2-2: Principles of Membrane electro-*filtration*

Factors Effecting the Efficiency of the Electrical Field:

The selected electric field intensity can be strongly influenced by biomass characteristics, mainly the density of negative charged (Akamatsu, Lu, Sugawara, & Nakao, 2010). Other factors are the membrane characteristics including the applied electric field density, operating conditions, membrane type and surface, the position of the electrodes and configuration of membrane modules. Side reaction may occur (i.e. electro coagulation). Liu et. al. (2012) analyzed the performance of an EMBR, a low electrical field was utilized (~0.2 V cm^{-1}) and the EMBR settled sludge appeared to be denser compared to MBR sludge. Furthermore, the results showed higher fluxes and a reduction in COD and total phosphorous, but not NH_3-N in the effluent.

Fouling prevention using an electric system could increase sludge size and reduce particle zeta potential, cause electrophoresis and generate an electrostatic repulsion/rejection against electronegative colloids or particles (Liu, 2012 #417). Meng (2006) found that the effect of

soluble microbial products (ss), suspended solids (SSs) in supernatant, dynamic viscosity (μ), relative hydrophobicity (RH), and zeta potential are interrelated and can be represented by the extracellular polymeric substances (EPS).

Configuration

Researches investigating EMBR had designs that varied in terms of the elements of the EMBR system include membrane module assemble, membrane type, electrode selection of material, shape and position, and electrical current intensity (electrical field). The operational concepts and overall results in the literature indicate prolong running cycle on the MBR due to the presence of an electrical field around the membrane surface.

References

Akamatsu, K., Lu, W., Sugawara, T., & Nakao, S.-i. (2010). Development of a novel fouling suppression system in membrane bioreactors using an intermittent electric field. *Water Research, 44*(3), 825-830. doi:http://dx.doi.org/10.1016/j.watres.2009.10.026

Amer, L., Adhikari, B., & Pellegrino, J. (2011). Technoeconomic analysis of five microalgae-to-biofuels processes of varying complexity. *Bioresource Technology*, *102*(20), 9350-9359. doi:http://dx.doi.org/10.1016/j.biortech.2011.08.010

Arkhangelsky, E., Wicaksana, F., Chou, S., Al-Rabiah, A. A., Al-Zahrani, S. M., & Wang, R. (2012). Effects of scaling and cleaning on the performance of forward osmosis hollow fiber membranes. *Journal of Membrane Science, 415–416*, 101-108. doi:http://dx.doi.org/10.1016/j.memsci.2012.04.041

Bani-Melhem, K., & Elektorowicz, M. (2011). Performance of the submerged membrane electro-bioreactor (SMEBR) with iron electrodes for wastewater treatment and fouling reduction. *Journal of Membrane Science, 379*(1–2), 434-439. doi:http://dx.doi.org/10.1016/j.memsci.2011.06.017

Buckwalter, P., Embaye, T., Gormly, S., & Trent, J. D. (2013). Dewatering microalgae by forward osmosis. *Desalination, 312*, 19-22. doi:http://dx.doi.org/10.1016/j.desal.2012.12.015

Chisti, Y. (2007). Biodiesel from microalgae. *Biotechnology Advances, 25*(3), 294-306. doi:http://dx.doi.org/10.1016/j.biotechadv.2007.02.001

Chou, S., Shi, L., Wang, R., Tang, C. Y., Qiu, C., & Fane, A. G. (2010). Characteristics and potential applications of a novel forward osmosis hollow fiber membrane. *Desalination, 261*(3), 365-372. doi:http://dx.doi.org/10.1016/j.desal.2010.06.027

Ge, Q., Ling, M., & Chung, T.-S. (2013). Draw solutions for forward osmosis processes: Developments, challenges, and prospects for the future. *Journal of Membrane Science, 442*, 225-237. doi:http://dx.doi.org/10.1016/j.memsci.2013.03.046

Henderson, R. K., Parsons, S. A., & Jefferson, B. (2008). Successful Removal of Algae through the Control of Zeta Potential. *Separation Science and Technology*, *43*(7), 1653-1666. doi:10.1080/01496390801973771

Holloway, R. W., Childress, A. E., Dennett, K. E., & Cath, T. Y. (2007). Forward osmosis for concentration of anaerobic digester centrate. *Water Research, 41*(17), 4005-4014. doi:http://dx.doi.org/10.1016/j.watres.2007.05.054

Hoover, L. A., Phillip, W. A., Tiraferri, A., Yip, N. Y., & Elimelech, M. (2011). Forward with Osmosis: Emerging Applications for Greater Sustainability. *Environmental Science & Technology, 45*(23), 9824-9830. doi:10.1021/es202576h

Körbahti, B. K., & Artut, K. (2013). Bilge Water Treatment in an Upflow Electrochemical Reactor using Pt Anode. *Separation Science and Technology, 48*(14), 2204-2216. doi:10.1080/01496395.2013.791852

Lee, S., Boo, C., Elimelech, M., & Hong, S. (2010). Comparison of fouling behavior in forward osmosis (FO) and reverse osmosis (RO). *Journal of Membrane Science, 365*(1–2), 34-39. doi:http://dx.doi.org/10.1016/j.memsci.2010.08.036

Liu, J., Liu, L., Gao, B., & Yang, F. (2012). Cathode membrane fouling reduction and sludge property in membrane bioreactor integrating electrocoagulation and electrostatic repulsion. *Separation and Purification Technology, 100*(0), 44-50. doi:http://dx.doi.org/10.1016/j.seppur.2012.08.029

Liu, L., Liu, J., Gao, B., & Yang, F. (2012a). Minute electric field reduced membrane fouling and improved performance of membrane bioreactor. *Separation and Purification Technology, 86*, 106-112. doi:http://dx.doi.org/10.1016/j.seppur.2011.10.030

Liu, L., Liu, J., Gao, B., & Yang, F. (2012b). Minute electric field reduced membrane fouling and improved performance of membrane bioreactor. *Separation and Purification Technology, 86*(0), 106-112. doi:http://dx.doi.org/10.1016/j.seppur.2011.10.030

Liu, Y., & Mi, B. (2012). Combined fouling of forward osmosis membranes: Synergistic foulant interaction and direct observation of fouling layer formation. *Journal of Membrane Science, 407–408*, 136-144. doi:http://dx.doi.org/10.1016/j.memsci.2012.03.028

McCutcheon, J. R., & Elimelech, M. (2006). Influence of concentrative and dilutive internal concentration polarization on flux behavior in forward osmosis. *Journal of Membrane Science, 284*(1–2), 237-247. doi:http://dx.doi.org/10.1016/j.memsci.2006.07.049

McGinnis, R. L., & Elimelech, M. (2007). Energy requirements of ammonia–carbon dioxide forward osmosis desalination. *Desalination, 207*(1), 370-382. doi:http://dx.doi.org/10.1016/j.desal.2006.08.012

Mi, B., & Elimelech, M. (2010). Gypsum Scaling and Cleaning in Forward Osmosis: Measurements and Mechanisms. *Environmental Science & Technology, 44*(6), 2022-2028. doi:10.1021/es903623r

Pahl, S. L., Lee, A. K., Kalaitzidis, T., Ashman, P. J., Sathe, S., & Lewis, D. M. (2013). Harvesting, thickening and dewatering microalgae biomass. In *Algae for biofuels and energy* (pp. 165-185): Springer.

Phuntsho, S., Shon, H. K., Hong, S., Lee, S., & Vigneswaran, S. (2011). A novel low energy fertilizer driven forward osmosis desalination for direct fertigation: Evaluating the performance of fertilizer draw solutions. *Journal of Membrane Science, 375*(1–2), 172-181. doi:http://dx.doi.org/10.1016/j.memsci.2011.03.038

Shon, H., Phuntsho, S., Zhang, T., & Surampalli, R. (2015). *Forward Osmosis*: American Society of Civil Engineers.

Sing, S. F., Isdepsky, A., Borowitzka, M., & Lewis, D. (2014). Pilot-scale continuous recycling of growth medium for the mass culture of a halotolerant Tetraselmis sp. in raceway ponds under increasing salinity: a novel protocol for commercial microalgal biomass production. *Bioresource Technology, 161*, 47-54.

Tornabene, T. G., Holzer, G., Lien, S., & Burris, N. (1983). Lipid composition of the nitrogen starved green alga Neochloris oleoabundans. *Enzyme and Microbial Technology, 5*(6), 435-440. doi:http://dx.doi.org/10.1016/0141-0229(83)90026-1

Uduman, N., Qi, Y., Danquah, M. K., Forde, G. M., & Hoadley, A. (2010). Dewatering of microalgal cultures: a major bottleneck to algae-based fuels. *Journal of renewable and sustainable energy, 2*(1), 012701.

Uduman, N., Qi, Y., Danquah, M. K., & Hoadley, A. F. (2010). Marine microalgae flocculation and focused beam reflectance measurement. *Chemical Engineering Journal, 162*(3), 935-940.

Valladares Linares, R., Yangali-Quintanilla, V., Li, Z., & Amy, G. (2012). NOM and TEP fouling of a forward osmosis (FO) membrane: Foulant identification and cleaning. *Journal of Membrane Science, 421–422*, 217-224. doi:http://dx.doi.org/10.1016/j.memsci.2012.07.019

Yangali-Quintanilla, V., Li, Z., Valladares, R., Li, Q., & Amy, G. (2011). Indirect desalination of Red Sea water with forward osmosis and low pressure reverse osmosis for water reuse. *Desalination, 280*(1–3), 160-166. doi:http://dx.doi.org/10.1016/j.desal.2011.06.066

Zhao, S., & Zou, L. (2011). Effects of working temperature on separation performance, membrane scaling and cleaning in forward osmosis desalination. *Desalination, 278*(1–3), 157-164. doi:http://dx.doi.org/10.1016/j.desal.2011.05.018

Zumbusch, P. v., Kulcke, W., & Brunner, G. (1998). Use of alternating electrical fields as anti-fouling strategy in ultrafiltration of biological suspensions – Introduction of a new experimental procedure for crossflow filtration. *Journal of Membrane Science, 142*(1), 75-86. doi:http://dx.doi.org/10.1016/S0376-7388(97)00310-4

CHAPTER 3: DEWATERING ALGAE USING AN AQUAPORIN-BASED POLYETHERSULFONE FORWARD OSMOSIS MEMBRANE

This paper has been previously published as: Munshi, F. M., Church, J., McLean, R., Maier, N., Sadmani, A. A., Duranceau, S. J., & Lee, W. H. (2018). Dewatering algae using an aquaporin-based polyethersulfone forward osmosis membrane. *Separation and Purification Technology, 204,* 154-161.

Abstract

Low energy requirement in algae harvesting is necessary for sustainable biofuel production. Forward osmosis (FO) can provide a potential alternative for low energy consumption by using osmotic pressure between the draw solution (DS) and feed solution (FS). In this study, an aquaporin-based polyethersulfone (PES) membrane was evaluated for algal dewatering using FO. Three different types of DS (NaCl, KCl and NH_4Cl), different cross flow velocities (CFVs), and configuration variations were compared to determine the FO performance to dewater *Chlorella vulgaris*. For short-term operation (500 min), the average water fluxes were 5.6, 4.8, and 4.3 L m^{-2} h^{-1} for NaCl, KCl, and NH_4Cl, respectively and all DSs showed increased fluxes with increased CFVs. In particular, this study found that NH_4Cl is the best candidate among the three tested DSs for improved water flux and low reverse salt flux for the aquaporin-based PES FO membrane. Natural seawater was also tested and revealed well-defined DS performance compatible with NaCl. For a longer duration experiment, 81% of algae dewatering was achieved with a 29% flux drop which may be attributed to the increasing FS concentration, concentration polarization and the loosely attached algal biofilm on the membrane surface.

Overall, this study demonstrates a new iteration of the aquaporin-based PES membrane for algal dewatering in FO application.

Introduction

Given that water resource management and renewable energy production are two major challenges faced by modern society, there is clear motivation to use microalgae as a biofuel feedstock due to their high lipid to biomass ratio and their ability to utilize secondary wastewater effluent for cultivation (Hwang, Church, Lee, Park, & Lee, 2016). However, microalgae are difficult to remove from their suspension in water and developing cost-effective harvesting methods for microalgae is among the most challenging aspects of algal biofuel production, limiting the commercial use of algae (Pahl et al., 2013; Uduman, Qi, Danquah, & Hoadley, 2010). It is estimated that 20–30% of the total cost of algal biomass production in open systems are from harvesting and dewatering (Amer, Adhikari, & Pellegrino, 2011), while 90% of the equipment costs are associated with dewatering (Pahl et al., 2013). The cost of harvesting dilute algae suspensions continuously is a major 'bottleneck' hindering the development of a microalgae-based fuel industry (McGinnis & Elimelech, 2007; Uduman, Qi, Danquah, Forde, & Hoadley, 2010; Uduman, Qi, Danquah, & Hoadley, 2010).

Traditionally, microalgae have been removed by sedimentation, flocculation, air floatation, filtration, electrophoresis, and centrifugation (Buckwalter, Embaye, Gormly, & Trent, 2013; Mo, Soh, Werber, Elimelech, & Zimmerman, 2015; Uduman, Qi, Danquah, Forde, et al., 2010). More recently, microfiltration (MF) (Simstich, Beimfohr, & Horn) and ultrafiltration (UF) have been used because of their ease of use and high separation efficiency (Shao et al., 2015),

however, these pressure driven membrane processes (e.g. MF and UF) are prone to fouling which can increase energy costs. Forward osmosis (FO) is an emerging membrane separation technology that has the potential to reduce the overall costs of harvesting microalgae by using osmotic pressure to concentrate microalgae. Osmosis refers to the spontaneous movement of water through a semi-permeable membrane from a solution of lower solute concentration into a solution of higher solute concentration. (Ge, Ling, & Chung, 2013; Phuntsho, Shon, Hong, Lee, & Vigneswaran, 2011; Shon, Phuntsho, Zhang, & Surampalli, 2015). The osmotic pressure gradient drives water across the membrane from the less concentrated "feed solution" (FS) to the more concentrated "draw solution" (DS) (Noffsinger, Giustino, Louie, & Cohen). FO draw solutions can be natural resources (ocean water), waste streams (brine), or high purity solutions. Membranes used in FO processes are usually made from polymeric materials with the capacity to allow passage of small molecules such as water and block large molecules such as salts, sugars, starches, proteins, viruses, bacteria, and parasites (Shon et al., 2015).

Several studies have investigated FO as a viable option for desalination, wastewater treatment, irrigation, biomass concentration, and food processing (Cath, Childress, & Elimelech, 2006; Chung, Zhang, Wang, Su, & Ling, 2012; Li et al., 2012; McCutcheon, McGinnis, & Elimelech, 2006; Phuntsho et al., 2011; Yangali-Quintanilla, Li, Valladares, Li, & Amy, 2011). FO can offer excellent dewatering efficiency with less fouling potential compared to pressure driven membrane processes (Kwan, Bar-Zeev, & Elimelech, 2015). For example, NASA's OMEGA project proposed the use of semi-permeable tubes to dewater algae cultivated in offshore membrane enclosures (Hoover, Phillip, Tiraferri, Yip, & Elimelech, 2011; Wiley,

2013). However, only a handful of studies have explored the potential of FO for dewatering algae (Table S1) and are limited to the use of one membrane type (i.e. cellulose triacetate FO membrane) or commercial FO bags without further operational parameters evaluations (Buckwalter et al., 2013; Zou et al., 2013).

Aquaporin FO membrane is a relatively new type of membrane in the field of biofuel or algae dewatering. It has been used for testing synthetic saline waters (200 ppm NaCl) and seawater as FS with different DSs (e.g., NaCl and sucrose) in a FO desalination hybrid system (Wang et al., 2012). Aquaporin has also been used in removing trace organics/pesticides (1–10 ppm) with a DS of 1 M of NaCl (Madsen, Bajraktari, Helix-Nielsen, Van der Bruggen, and Søgaard, 2015).

In this study, we evaluated a new aquaporin polyethersulfone (PES) FO membrane for algae dewatering under various operational conditions. The effects of different types and concentrations of DSs and different cross flow velocities (CFVs) on FO performance for algae dewatering were extensively investigated. In addition, the fouling potential, changes in flux, and reverse salt flux of this new membrane were monitored over short (8 hrs.) and long-term experiments (170 hrs.). Lastly, the membrane was characterized using a scanning electron microscopy (SEM) to determine fouling and overall durability.

Materials and methods

Algal species and cultivation

Chlorella vulgaris (UTEX 2714, Austin, Texas) was selected to represent microalgae that are difficult to harvest and commonly used in biofuel cultivation. Upon arrival, *C. vulgaris* was

cultivated in a mother photobioreactor (4L) using modified bold basal media (BBM) (Kline, Hayes, Womac, & Labbe) adapted from the Canadian Phycological Culture Centre (CPCC), University of Waterloo (Stein, 1979). BBM was selected to maintain optimal growth conditions (EL-Moslamy, Kabeil, & Hafez, 2016). For FO bench scale tests, the *C. vulgaris* from the mother photobioreactor was used to inoculate 1L glass bottles (13951L, Corning Inc.) containing 500 mL of BBM. The 1L glass bottles were then incubated at 25±3 °C under continuous white fluorescent light illumination with a light intensity of 27–33 µmol m^{-2} s^{-1} PAR and stirred using a magnetic stirrer at 50 rpm. The light intensity was measured by a dual-range digital light meter (06-662-63, Fisher). The culture was aerated using an aquarium air pump to supply CO_2 (0.04%) to the algae. Biomass weight was monitored daily until it reached about 1 g L^{-1} dry algal biomass. Approximately three days were required to achieve the target algal concentration (1 g L^{-1} dry algal biomass).

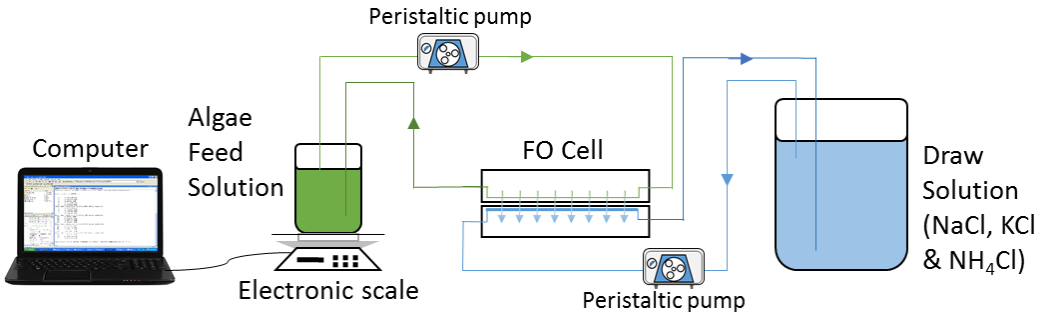

Figure 3-1: A schematic of the algae dewatering process.

Bench scale test system

Bench-scale tests were performed to investigate water flux, reverse salt flux, and fouling of a new flat sheet PES membrane (Aquaporin–Sterlitech, Kent, WA) with an active surface area of 12.5 cm^2. The custom-made FO system used for this study consisted of a FS tank (0.5 L), DS

tank (15 L), peristaltic pumps, and the FO unit (Fig. 3-1). The FO unit was fabricated using ¾" plexiglass (ePlastics, San Diego, CA) with custom flow channels to allow even flow across both sides of the membrane. A 5-mm thick rubber gasket (50A, Rubber-Cal, Santa Ana, CA) was used to separate the plexiglass and hold the membrane in place. A 0.33 mm thick polypropylene permeable mesh (FM100, Diversified Biotech, Dedham) was placed on the DS side to support the FO membrane. The FO membrane active semi-permeable layer faced the FS. The volume of the FO chamber was 3.75 cm^3 (1 cm [W]×12.5 cm [L]×0.3 cm [H]). 0.5 L BBM with *C. vulgaris* (1 g L^{-1} dry biomass weight) was used as a FS throughout the study, while various concentrations of sodium chloride (NaCl), potassium chloride (KCl), and ammonium chloride (NH_4Cl) were used as DS. The DS volume was 15 L to maintain the initial concentration with a negligible dilution effect. A peristaltic pump (Masterflex L/S economy pump drive, Cole Parmer, Vernon Hills, IL) was used to recirculate the FS and DS in opposite directions with the same CFVs. The pump was periodically calibrated to maintain designed CFVs. The FS tank was positioned on an electronic analytical balance (PCE-PCS 6 Counting Scale, PCE Americas, Inc., Jupiter, FL) connected to logging software (MATLAB). The rate of change of the FS weight was recorded every four-minutes for real-time with an accuracy of 0.1 g (equivalent to 0.1 mL of dilute water) and used to calculate water flux through the membrane.

Physical cleaning was achieved by increasing the CFV to 21 cm s^{-1} for 10–15 minutes (Mi & Elimelech, 2010). Furthermore, both orientations of the FO membrane (e.g., an active layer facing the FS and an active layer facing to the DS) were tested to evaluate the effect of the

membrane orientation on the FO performance (35.5 g L^{-1} NaCl as DS and 1 g L^{-1} of algae FS at a CFV of 5 cm s^{-1}).

Table 3-1: Operating conditions for testing of FO membranes

Draw solution	Cross flow velocity, cm s^{-1}	Concentration, g L^{-1} (M)	Note
NaCl	1.5, 5.0 and 10.7	35.5 (0.6M)	Conductivity equivalent to seawater (60.2 mS cm^{-1})
KCl	1.5, 5.0 and 10.7	37.0 (0.5M)	
NH_4Cl	1.5, 5.0 and 10.7	27.2 (0.5M)	
NaCl	5.0	58.4 (1.0M)	89.1 mS cm^{-1}
KCl	5.0	74.6 (1.0M)	109.0 mS cm^{-1}
NH_4Cl	5.0	53.5 (1.0M)	109.0 mS cm^{-1}
Seawater (Florida's east coast beach)	5.0	N/A*	56.6 mS cm^{-1}
NaCl	5.0	35.5	Extended run (170 hrs)

*Not available

Evaluation of CFV and DS on FO performance

Table 3-1 shows the experimental trials used to evaluate the FO system for harvesting microalgae. Different CFVs and different types and concentrations of DS were tested over 8-hour batch experiments. DSs were selected based on their availability without need of regeneration which include NaCl, KCl, and NH_4Cl. NaCl (Fisher Scientific, Hampton, NH) was selected to simulate seawater and KCl (Gateway Products, Holly, CO) and NH_4Cl (Fisher Scientific, Hampton, NH) were selected as representative fertilizer salts. The salts were dissolved in deionized (DI) water to prepare target DS concentrations.

The optimization of CFVs specific to algae dewatering is required for improved FO efficiency. The recommended manufacturer value of CFV in FO operations is 5 cm s^{-1} to control

settling and external concentration polarization; however, high CFV can damage the FO membrane. In this study, the three DSs with concentration equivalent to the conductivity of seawater were tested under different CFVs of 1.5, 5.0 and 10.7 cm s^{-1}. In addition, the same molar concentration of DS (1.0 M) with a constant CFV (5 cm s^{-1}) was tested at a given temperature (23±0.2 °C). 5 cm s^{-1} was selected as a representative CFV based on preliminary experiments. Two concentrations (0.5–0.6 M and 1.0 M) were selected to compare NaCl, KCl, and NH_4Cl as DS with equivalent concentration of abundant saline resources: seawater (0.6 M of NaCl) and brine water (1 M of NaCl). A fresh FO membrane was used for every experiment to ensure similar initial FO membrane integrity.

Other FO validation experiments were conducted under the condition of CFV: 5.0 cm s^{-1}, DS: 35.5 g L^{-1} of NaCl (15 L), FS: 1 g L^{-1} of dry algae biomass (0.5 L), FO mode, and an aquaporin PES FO membrane unless stated otherwise. Under this condition, effect of the polypropylene permeable support mesh was evaluated in an extended FO operation. In addition, actual seawater taken from Florida's east coast beach (Canaveral National seashore beyond Mosquito lagoon, Titusville, Florida, USA) as a natural DS was tested to validate NaCl experiments.

FO performance analysis

The water flux (L m^{-2} h^{-1}) was determined by the following Eq. (3-1).

$$J_w = \frac{\Delta V}{A\,t} \tag{3-1}$$

where, ΔV: the volume (L) of the water permeated from the feed to the DS (L), A: the effective membrane surface area (m^2), and t: duration of the experiment (h). The FS volumetric change was monitored at 1 h intervals using the electronic analytical balance.

Reverse salt flux (g m^{-2} h^{-1}) is the amount of the dissolved salt that passes from the DS to the FS across FO membrane per unit time. The factors that affect salt concentration in the FS include dewatering, reverse salt flux, applied CFV, and membrane service time. In this study, the reverse salt flux was determined by Eq. (3-2).

$$J_s = \frac{\Delta C_t V_t}{A\, t} \tag{3-2}$$

where, V_t: the volume of FS at a certain period in the experiment (L), A: the effective membrane surface area (m^2), t: duration of the experiment (h), and ΔC_t: the change in salt concentration over the experiment period (g L^{-1}) (Zhang et al., 2010). Conductivity in FS was monitored using a portable multimeter (HQ40d, Hach, Loveland, CO) and then converted to corresponding salt concentration (g L^{-1}). Standard curves of salt concentration and conductivity were developed for each salt (Fig. B1) which was used to determine the cross-transfer of salts (e.g. reverse salt flux) from the DS to the FS. pH was also monitored using a portable multimeter (HQ40d, Hach, Loveland, CO) during the tests. Conductivity of the FS were monitored every hour to determine the salt transfer from the DS. Total suspended solids (TSS) were determined by Standard Methods (2540-Solids) (Association, Association, Federation, & Federation, 1915) and optical density (OD) was measured using a spectrophotometer (DR1900, Hach, Loveland, CO) to determine the dry biomass of the algal solution. Selective microscopic and naked eye

observations of the surface of the membranes were carried out to identify the color change and formation of the fouling layer.

FO membrane characterization

The FO flat sheet membrane tested is composed of a selective synthetic protein layer and a polymeric support layer of PES. As per specifications from the manufacturer, the average thickness of the membrane is 110 µm, providing an average permeate flux of 7 L m^{-2} h^{-1} with pure water as a FS and 1 M NaCl as a DS and a reverse salt flux less than 2 g m^{-2} h^{-1}. Prior to test, the FO membrane was soaked in DI water for over 30 minutes to remove the protective filling material (e.g. glycerine) within the pores and structure. SEM (Zeiss ULTRA-55 FEG) was used to analyze the membrane surface, cross-sectional area, and measure surface pore size of the FO membrane. The FO test for longer duration was conducted to evaluate FO performance with regards to potential membrane fouling and water flux recovery upon cleaning.

Contact angle was measured to determine hydrophilicity/hydrophobicity of the FO membrane surface using a goniometer (Model 100-00, Ramé-hart Instrument Co., Succasunna, NJ) (Yuan & Lee, 2013). The aquaporin side of the FO membrane was found to be hydrophilic (contact angle varied from 24˚ to 45˚) (Fig. B2). The aquaporin surface with the attached foulant (FO mode) had a contact angle of 44˚ (Fig. B3), indicating a flux decline potential. The fresh PES support layer was found to be hydrophilic (contact angle ~21˚) (Fig. B4).

Results and discussion

Effect of orientation on membrane flux

Internal concentration polarization in FO membrane is developed in the support layer and is influenced by membrane thickness, support structures, FS, DS and the orientation of the FO membrane (McCutcheon & Elimelech, 2006). The aquaporin PES FO membrane was tested for both orientations (i.e. active layer facing the FS and active layer facing to the DS) to determine the internal concentration polarization effect on the membrane flux. Water flux and reverse salt flux were measured for both modes and 35.5 g L^{-1} of NaCl and 1 g L^{-1} of algal solution were used as DS and FS, respectively. The average water flux for a 50-hour run was found to be 4.4 L m^{-2} h^{-1} in both the cases. The identical water flux for both modes implies that the aquaporin FO membrane is designed to minimize internal concentration polarization (K. Y. Wang, Ong, & Chung, 2010). The reverse salt flux was 0.714 g m^{-2} h^{-1} in the active layer facing to the FS, while it was 50% lower (0.374 g m^{-2} h^{-1}) in the active layer facing to the DS, indicating that membrane operation in the active layer facing to the DS would minimize the reverse salt effect. It was reported that when the support layer faces the DS, salts would be accumulated in the support layer, resulting in higher salt passage. For the active layer facing the DS, it seems that the CFV on the active surface would prevent any accumulation of salt at the FS side (Phillip, Yong, & Elimelech, 2010; Zhao & Zou, 2011). For all tests in this study, active layer was faced to FS.

Effect of mesh support

A polypropylene permeable mesh support was applied to prevent membrane rupture. The mesh support had two distinct sides: a rough sharp screen edge surface and a smooth surface.

The hydrodynamics of the spacers were often reported to affect the FO membrane flux and flux stability during fouling (Y. Wang, Wicaksana, Tang, & Fane, 2010). In this study, the effect of the mesh support was investigated under the condition of CFV: 5.0 cm s^{-1}, DS: 35.5 g L^{-1} of NaCl (15 L), FS: 1 g L^{-1} of dry algae biomass (0.5 L). Two tests were conducted: 1) with mesh support on the DS side (active layer facing to FS) and 2) without mesh support. The support with the rough surface on the membrane surface and the no mesh support showed similar average fluxes of 4.5 L m^{-2} h^{-1}, demonstrating that the rough surface mesh support, when in contact with the membrane, had no negative impact on flux. However, the smooth surface attachment to the membrane surface resulted in a loss of flux and half of the average flux was reduced from 4.5 to 2.5 L m^{-2} h^{-1}. This may be due to reduced interactions between DS and membrane. It was suggested that the mesh support should be applied with the rough surface toward membrane surface. The tests in this study used the mesh support with the suggested direction.

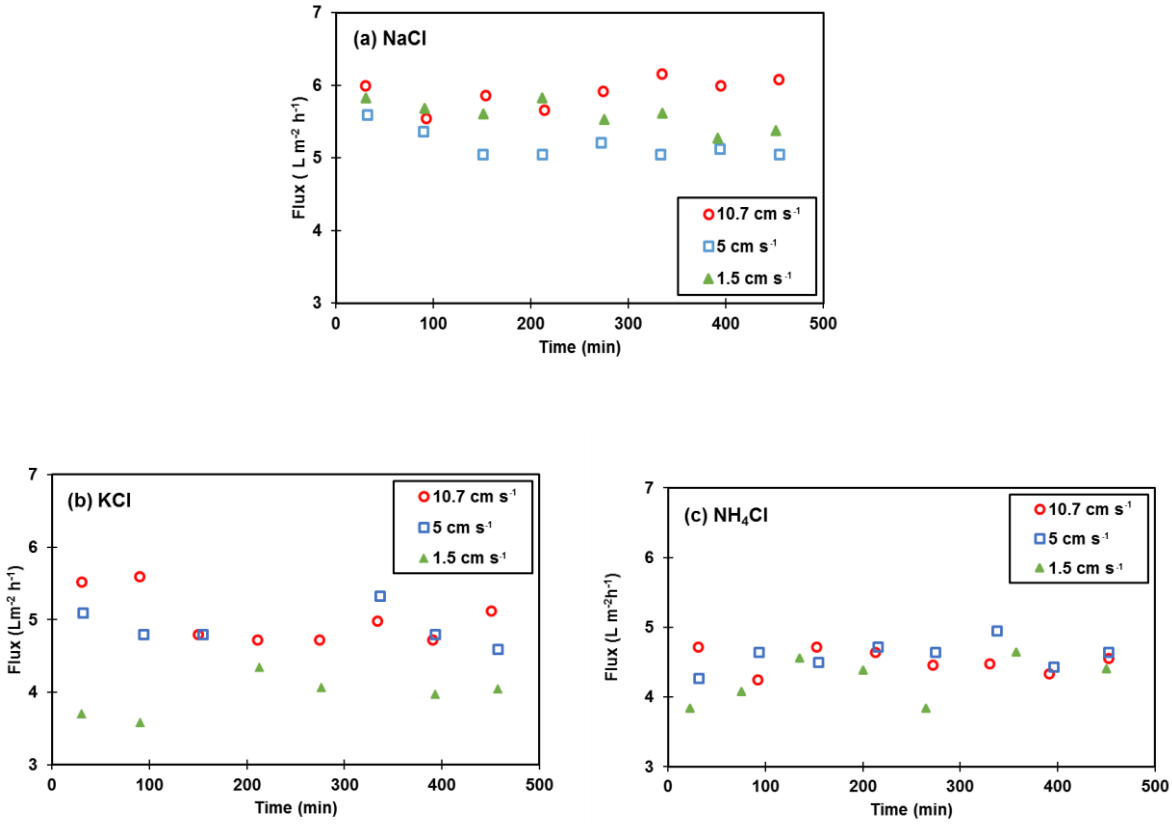

Figure 3-2: Effects of different cross flow velocities and draw solutions on the water flux of the FO membrane: (a) 35.5 g L^{-1} of NaCl, (b) 37.0 g L^{-1} of KCl and (c) 27.2 g L^{-1} of NH_4Cl. Algae concentration was 1 g L^{-1} (dry biomass).

Effects of different salts and CFVs on FO performance

The membrane flux trends over the 8-hour batch experiment under given CFVs and DS concentrations are shown in Fig. 3-2. For the duration of FO operation, the flux showed no abrupt drop, not requiring membrane cleaning. Each DS demonstrated a distinctive flux pattern depending on the CFVs. Duplicate experiments were performed and showed 15–22% variation in average flux. Average fluxes using NaCl as a DS were 5.6, 5.2, and 5.9 L m^{-2} h^{-1} for CFVs of 1.5, 5.0, and 10.7 cm s^{-1}, respectively (Fig. 3-2(a)). At the lowest CFV of 1.5 cm s^{-1}, although depositions of algae biomass were visibly observed on the selective layer of the membrane, the

water flux was not significantly changed throughout the test period. The average fluxes for KCl were 4.6, 4.8, and 5.0 L m^{-2} h^{-1} (Fig. 3-2(b)), while for NH_4Cl the fluxes were 4.1, 4.2, and 4.5 L m^{-2} h^{-1} at 1.5, 5.0, and 10.7 cm s^{-1} of CFVs, respectively (Fig. 3-2(c)). The changes in CFVs from 1.5 to 10.7 cm s^{-1} resulted in flux increases of approximately 5.3% (5.6 to 5.9 L m^{-2} h^{-1}) for NaCl, 8.7% (4.6 to 5.0 L m^{-2} h^{-1}) for KCl, and 9.8% (4.1 to 4.5 L m^{-2} h^{-1}) for NH_4Cl. All DSs showed increased fluxes with increased CFVs and this can be explained by the assumption that external concentration polarization can decrease with increase CFVs, resulting in increased water flux.

With the increased CFVs from 1.5 to 10.7 cm s^{-1}, the reverse salt flux for NaCl was reduced by 8.2% (from 0.660 to 0.606 g m^{-2} h^{-1}), for KCl by 73% (from 2.41 to 0.636 g m^{-2} h^{-1}), and for NH_4Cl by 50.6% (from 0.810 to 0.468 g m^{-2} h^{-1}). NH_4Cl showed the lowest reverse salt fluxes at high CFV (i.e. 10.7 cm s^{-1}) and it was observed that the color of the algal FS became darker, indicating possible ammonia uptake by the algae unlike NaCl and KCl (Choi, H.J. and Lee, S.M., 2012; Church et al., 2017). NaCl showed a minimal effect of changes of CFVs on the reverse salt flux at the equivalent conductivity and a given algae biomass (i.e. 1 g L^{-1}). The pHs of the algal FS during the batch tests were constantly stable with 8.4 ± 0.2 with a minimal effect by reverse salt fluxes. The variation of initial flux at each CFV and DS (Fig. 3-2 and 3-3(a)) can be explained by relatively short duration (i.e. 500 min) for the membrane performance stabilization. In a long-term operation (Fig. 3-5), the water flux decrease was clearly observed.

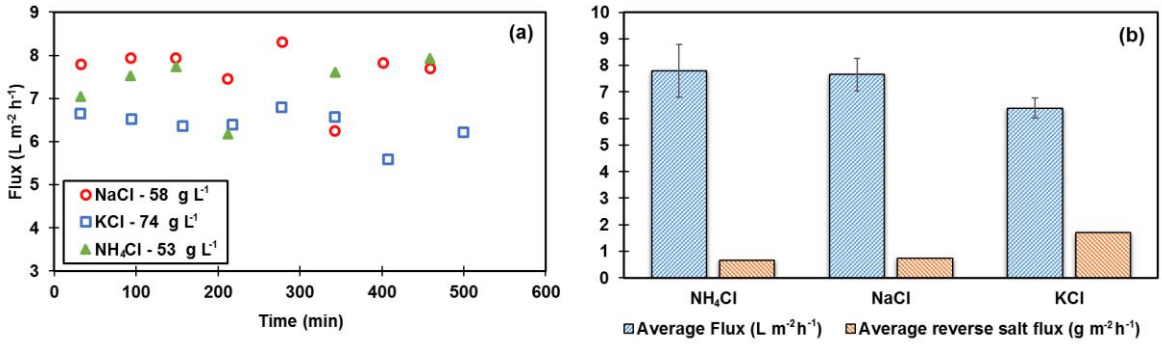

Figure 3-3: (a) Water flux and (b) reverse salt flux during FO tests with different salts as draw solutions under the same molar concentration (1.0 M). The cross-flow velocity was constant at 5 cm s^{-1}.

The algal layer deposited on the surface of the FO membrane during the 8-hour runs showed a minimal impact on the fluxes and the reverse salt fluxes probably due to the loosely attached algal layer (Kim, Elimelech, Shon, & Hong, 2014; Lee, Boo, Elimelech, & Hong, 2010; Mi & Elimelech, 2008, 2010). At the lowest CFV of 1.5 cm s^{-1}, a greenish fouling layer formation was observed within the first hour and the layer was continuously formed in dark green with time (Fig. B5); however, at higher CFV (e.g. 10.7 cm s^{-1}), the algae fouling layer was barley formed during the initial few hours (Fig. B5). This fouling layer was further evaluated with longer period tests (see section 3.5).

Effect of different types of salt on FO performance

Given that osmotic pressure is a major driving force for FO operations, conductivity may not be a comparable parameter for evaluating the effect of different types of salts in FO performance. It is expected that the increase in salt concentrations provides a proportional effect on the applied osmotic pressure, increasing average fluxes and reverse salt fluxes. Therefore, in this test, molar concentration for three types of salt was kept constant at 1.0 M at a room

temperature (23±0.2 °C). The middle value of the tests CFVs (5 cm s^{-1}) was selected to compare the effect of different types of salt on the FO performance. As shown in Fig. 3-3, 1.0 M of NH_4Cl, NaCl, and KCl produced relatively high fluxes of 7.8, 7.7, and 6.4 L m^{-2} h^{-1}, respectively. With the equivalent molar concentration, NH_4Cl showed higher flux in FO operations than NaCl and KCl. It seems that the lowest reverse salt flux by NH_4Cl resulted in a larger osmotic pressure gradient and thus a higher water flux compared to NaCl and KCl.

Comparing it to the previous tests with the same conductivity, an increase in NaCl concentration from 0.6 to 1.0 M resulted in 47.3% increase in flux (from 5.2 to 7.7 L m^{-2} h^{-1}). For KCl, an increase in the concentration from 0.5 to 1.0 M resulted in 33.2% increase in flux (from 4.8 to 6.4 L m^{-2} h^{-1}). Lastly, the increase in NH_4Cl concentration from 0.5 to 1.0 M resulted in 85.5% increase in flux (from 4.2 to 7.8 L m^{-2} h^{-1}). As per increased salt concentrations, NH_4Cl showed the greatest flux improvement (0.88 = 83.3%/96.7%) compared to other two salts (0.33 for KCl and 0.73 for NaCl).

The average reverse salt flux under the equivalent molar concentration (1.0 M) was inversely proportional to water flux with 0.67, 0.75 and 1.70 g m^{-2} h^{-1} for NH_4Cl, NaCl and KCl, respectively (Fig. 3-3(b)). Possible ammonia uptake by the algae may explain the lowest reverse salt flux and this can be further evaluated separately. With the concepts of algal biofuel production and advanced wastewater treatment using algae, the reverse salt flux in FO operations would increase the salinity in FS and thus affect the lipid contents accumulated in algae biomass and phosphate (P) uptake. Mohleji and Verhoff (1980) showed that the presence of Na^+ increases P consumption by *Selenastrum capricornutum* under very low salt concentration (e.g. 0–100 mg

L^{-1} Na^{+} with initial P ≈ 50 μg L^{-1}) (Mohleji & Verhoff, 1980). While the current study used *C. vulgaris*, given that as Na^{+} is known to be involved in the cotransport of P in green algae (Schachtman, Reid, & Ayling, 1998), the potential effect of Na^{+} on P uptake will be possible in low salinities.

FO simulation with seawater

Seawater was tested as a representative natural DS in a FO operation under a CFV of 5 cm s^{-1}. The salinity of the seawater was 56.6 mS cm^{-1} and 1 g L^{-1} of dry algal biomass was used as a FS. For natural seawater, the average water flux of 4.9 L m^{-2} h^{-1} was observed with a reverse salt flux of 0.515 g m^{-2} h^{-1} which is similar with NaCl under the same conductivity (5.2 L m^{-2} h^{-1} for water flux and 0.633 g m^{-2} h^{-1} for reverse salt flux) (Fig. 3-4). This observation shows that natural seawater is a good candidate of algae dewatering which is compatible with NaCl as a DS. In addition, as seawater is abundant, non-toxic, and affordable natural source, it is expected to satisfy the criteria of an ideal DS and the diluted seawater (as s results of FO operation) can be further processed to produce clean water in a desalination processes.

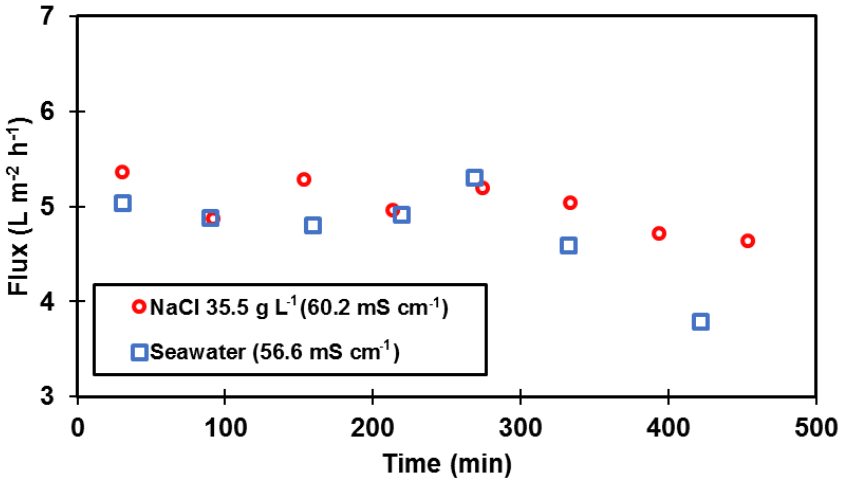

Figure 3-4: Average flux using seawater and pure NaCl 35.5 g L^{-1} (simulated seawater) as draw solution and algae as feed solution with a concentration of about 1 g L^{-1} of dry biomass and at 5 cm s^{-1} cross flow velocities.

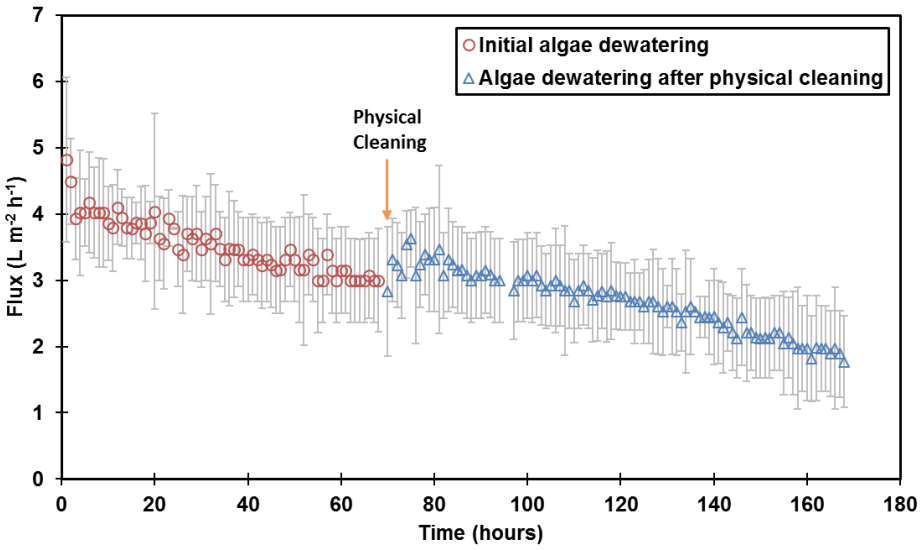

Figure 3-5: Extended batch reactor experiment with about 1 g L^{-1} of dry biomass algae (*C. vulgaris*) as feed solution and 35.5 g L^{-1} of NaCl as draw solution and 5 cm s^{-1} cross flow velocity.

Extended run

A batch experiment was conducted for an extended period of 170 hours (Fig. 3-5). During the period, the hourly averaged permeate flux was slowly declined with minor fluctuations which can also be found in the previous studies using bench-scale FO systems (Cath et al., 2013, Coday, Heil, Xu, and Cath, 2013). The change of FS concentration and the accumulation of algal biomass on the membrane surface seems to result in a flux decline by approximately 0.0175 L m^{-2} h^{-1} per hour. At the end of the first algae batch at 70 hours, 81% dewatering was achieved with only 29% flux drop from an initial flux of 4.1 L m^{-2} h^{-1}. While this was bench-scale test that was conducted using FO membranes with small active surface area (12.5 cm^2), similar performance may be obtained at shorter duration than 70 hours by using larger surface area (Seman, Kei, & Yusoff, 2015). The membrane was physically cleaned after the 70-hour run by increasing the CFV to 21 cm s^{-1} for 10 minutes (Mi and Elimelech, 2010). After cleaning, the flux was recovered and reached at 83% (3.4 L m^{-2} h^{-1}) of the initial flux.

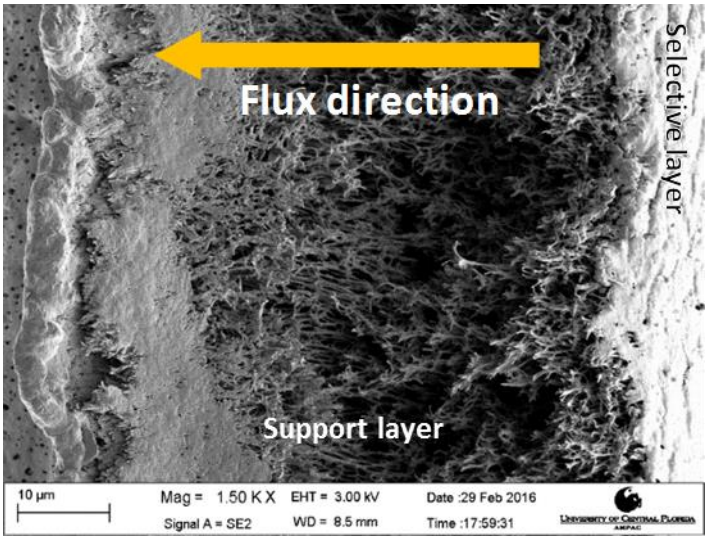

Figure 3-6: SEM image of the vertical cross section of a fresh aquaporin active layer and PES based FO membrane

Surface characterization

For fresh membrane analysis, the membrane was initially soaked in DI water to remove unattached particles on the membrane surface and sacrificed for SEM analysis. The cross-sectional image visualized that the initially soaked fresh FO membrane has a support material similar to a sponge structure (Fig. 3-6). The selective (active) surface of the FO membrane showed a moderately homogeneous surface pore size distribution (Fig. 3-7(a) and (b)). The average surface pore size observed was 200 nm. SEM images after 100 hour-duration showed a slightly fouled membrane surface with an increased pore size (400 nm) before (Fig. 3-7(c) and (d)) and after being washed using DI water (Fig. 3-7(e) and (f)). The membrane selective layer used in this study mimics aquaporin, which is a protein layer that has an hourglass shape across the membrane thickness. Therefore, it must be noted that the observed surface pore diameters do not represent the effective pore size given that active pore sizes are less than 1.5 nm in a semi-permeable membrane.

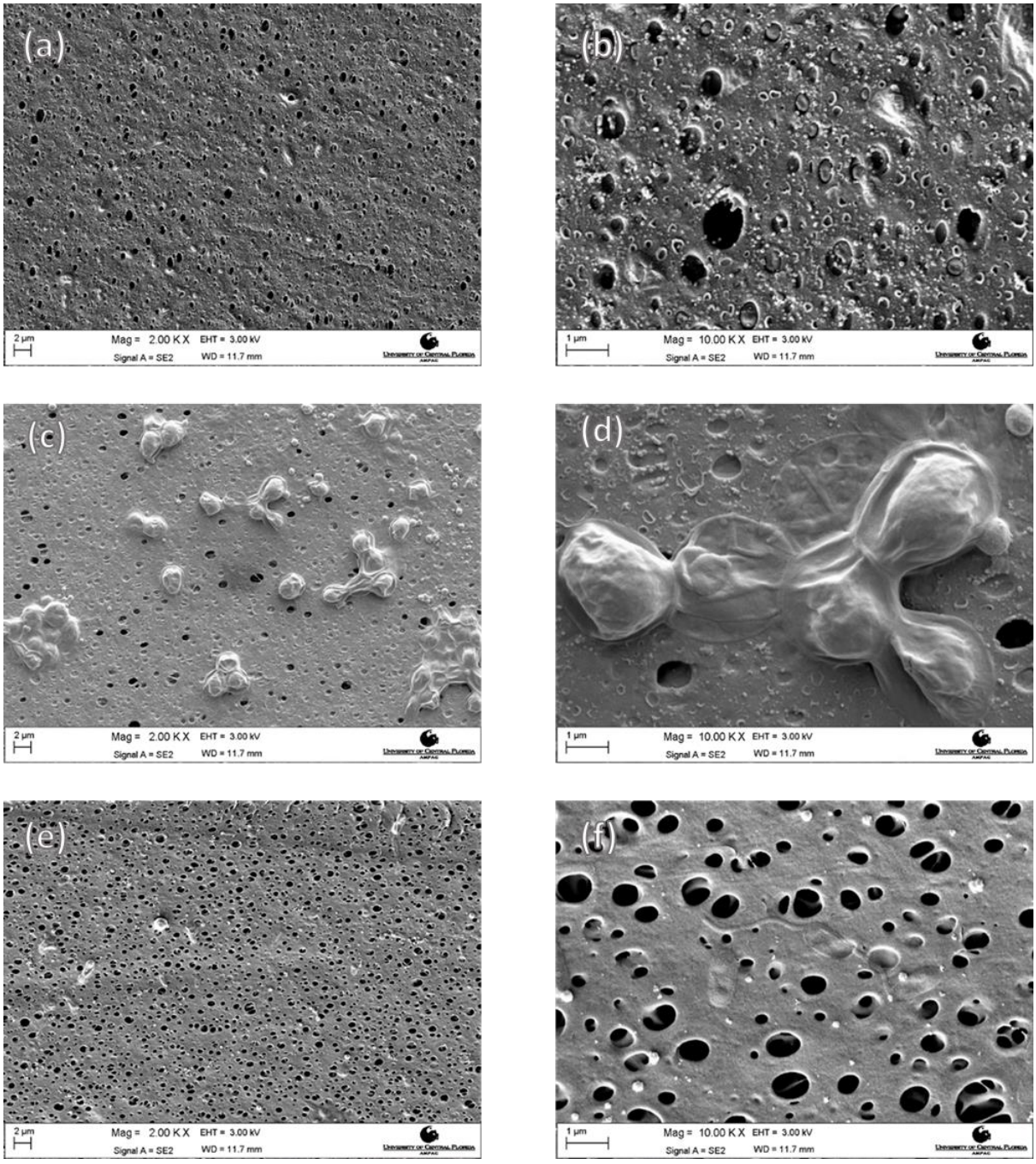

Figure 3-7: SEM images of FO membrane performance for algae separation: fresh FO sample ((a) × 2,000, (b) ×10,000), used (100 hours) FO membranes with attached algae cells ((c)× 2,000, (d) ×10,000), and used (100 hours) FO membranes after being washed ((e)× 2,000, (f) ×10,000). The active layer of the FO membrane was faced to the algal solution as a FS.

SEM images showed the accumulation of both singled and grouped algal cells on the membrane surface (Fig. 3-7(c) and (d)). Approximately only 20–30% of the membrane active surface area were covered by the foulants related to algae. This demonstrates the ability of FO systems to tolerate biofouling for long durations and recover water flux easily. Although the build-up of algae aggregates may intensify concentration polarization inside the membrane, most of foulants on the membrane surface were cleaned off when simply soaked in DI water (Fig. 3-7(e) and (f)), indicating that a temporal physical cleaning (e.g. increasing CFVs) will be feasible to prevent fouling layer development. The formation of this relatively 'loose' layer of algae fouling that can be dislodged without any chemical cleaning may serve as an explanation for the overall fluctuating flux pattern or sudden recovery of flux.

Conclusions

FO processes require lower energy input compared to most conventional dewatering processes, because the osmotic pressure gradient is the driving force for the dewatering process. This makes FO a suitable option for algae dewatering aimed at biofuel production. In general, the increase in CFVs from 1.5 to 10.7 cm s^{-1} resulted in increased average permeate flux by 5–10% depending on the DSs tested in this study. The accumulation of *C. vulgaris* microalgae had a minimal impact on flux throughout the duration of 8-hour experiment. The increase of DS concentration from 0.5–0.6 to 1.0 M increased the flux by 85.5% for NH_4Cl, whereas for NaCl and KCl the flux increase was only 47.3 and 33.2%, respectively. In the continuous long-term run, while the fluxes declined with time, sudden recovery of flux was periodically observed,

which may be attributed to dislodging of relatively 'loose' layers of algal biofilm without additional cleaning processes.

Selecting an appropriate DS is critical as the membrane material and DS closely correlate with each other and affect FO performance. This study suggests that NH_4Cl is the best candidate among three tested DSs for an aquaporin-based PES FO membrane in terms of improved water flux and low reverse salt flux with increased DS concentrations. DSs that are abundant and require no regeneration like natural seawater are recommended as the diluted DS product can directly be utilized in other applications such as feed water in desalination plants. In this study, NaCl and natural seawater also showed well-defined DS performance. Although the current study showed no significant flux drop from membrane fouling in the 170 hours experiment, future work is suggested to develop an appropriate protocol of physical and chemical FO membrane cleaning for continuous and effective algae dewatering.

References

Amer, L., Adhikari, B., & Pellegrino, J. (2011). Technoeconomic analysis of five microalgae-to-biofuels processes of varying complexity. *Bioresource technology, 102*(20), 9350-9359. doi:http://dx.doi.org/10.1016/j.biortech.2011.08.010

Association, A. P. H., Association, A. W. W., Federation, W. P. C., & Federation, W. E. (1915). *Standard methods for the examination of water and wastewater* (Vol. 2): American Public Health Association.

Buckwalter, P., Embaye, T., Gormly, S., & Trent, J. D. (2013). Dewatering microalgae by forward osmosis. *Desalination, 312*, 19-22. doi:http://dx.doi.org/10.1016/j.desal.2012.12.015

Cath, T. Y., Childress, A. E., & Elimelech, M. (2006). Forward osmosis: Principles, applications, and recent developments. *Journal of Membrane Science, 281*(1–2), 70-87. doi:http://dx.doi.org/10.1016/j.memsci.2006.05.048

Cath, T. Y., Elimelech, M., McCutcheon, J. R., McGinnis, R. L., Achilli, A., Anastasio, D., ... & Lampi, J. (2013). Standard methodology for evaluating membrane performance in osmotically driven membrane processes. *Desalination*, *312*, 31-38.

Chung, T.-S., Zhang, S., Wang, K. Y., Su, J., & Ling, M. M. (2012). Forward osmosis processes: Yesterday, today and tomorrow. *Desalination*, *287*, 78-81. doi:http://dx.doi.org/10.1016/j.desal.2010.12.019

Choi, H. J., & Lee, S. M. (2012). Effects of microalgae on the removal of nutrients from wastewater: various concentrations of Chlorella vulgaris. *Environmental Engineering Research*, *17*(S1), 3-8.

EL-Moslamy, S., Kabeil, S., & Hafez, E. (2016). Bioprocess Development for Chlorella vulgaris Cultivation and Biosynthesis of Anti-phytopathogens Silver Nanoparticles. J Nanomater Mol Nanotechnol 5: 1. *of*, *9*, 2.

Ge, Q., Ling, M., & Chung, T.-S. (2013). Draw solutions for forward osmosis processes: Developments, challenges, and prospects for the future. *Journal of Membrane Science*, *442*, 225-237. doi:http://dx.doi.org/10.1016/j.memsci.2013.03.046

Hoover, L. A., Phillip, W. A., Tiraferri, A., Yip, N. Y., & Elimelech, M. (2011). Forward with Osmosis: Emerging Applications for Greater Sustainability. *Environmental science & technology*, *45*(23), 9824-9830. doi:10.1021/es202576h

Hwang, J.-H., Church, J., Lee, S.-J., Park, J., & Lee, W. H. (2016). Use of microalgae for advanced wastewater treatment and sustainable bioenergy generation. *Environmental engineering science*, *33*(11), 882-897.

Kim, Y., Elimelech, M., Shon, H. K., & Hong, S. (2014). Combined organic and colloidal fouling in forward osmosis: fouling reversibility and the role of applied pressure. *Journal of Membrane Science*, *460*, 206-212.

Kline, L. M., Hayes, D. G., Womac, A. R., & Labbe, N. (2010). Simplified determination of lignin content in hard and soft woods via UV-spectrophotometric analysis of biomass dissolved in ionic liquids. *BioResources*, *5*(3), 1366-1383.

Kwan, S. E., Bar-Zeev, E., & Elimelech, M. (2015). Biofouling in forward osmosis and reverse osmosis: Measurements and mechanisms. *Journal of Membrane Science*, *493*, 703-708. doi:http://dx.doi.org/10.1016/j.memsci.2015.07.027

Lee, S., Boo, C., Elimelech, M., & Hong, S. (2010). Comparison of fouling behavior in forward osmosis (FO) and reverse osmosis (RO). *Journal of Membrane Science*, *365*(1–2), 34-39. doi:http://dx.doi.org/10.1016/j.memsci.2010.08.036

Li, Z.-Y., Yangali-Quintanilla, V., Valladares-Linares, R., Li, Q., Zhan, T., & Amy, G. (2012). Flux patterns and membrane fouling propensity during desalination of seawater by forward osmosis. *Water Research, 46*(1), 195-204. doi:http://dx.doi.org/10.1016/j.watres.2011.10.051

Madsen, H. T., Bajraktari, N., Helix-Nielsen, C., Van der Bruggen, B., & Søgaard, E. G. (2015). Use of biomimetic forward osmosis membrane for trace organics removal. *Journal of Membrane Science, 476*, 469-474.

McCutcheon, J. R., & Elimelech, M. (2006). Influence of concentrative and dilutive internal concentration polarization on flux behavior in forward osmosis. *Journal of Membrane Science, 284*(1–2), 237-247. doi:https://doi.org/10.1016/j.memsci.2006.07.049

McCutcheon, J. R., McGinnis, R. L., & Elimelech, M. (2006). Desalination by ammonia–carbon dioxide forward osmosis: Influence of draw and feed solution concentrations on process performance. *Journal of Membrane Science, 278*(1–2), 114-123. doi:http://dx.doi.org/10.1016/j.memsci.2005.10.048

McGinnis, R. L., & Elimelech, M. (2007). Energy requirements of ammonia–carbon dioxide forward osmosis desalination. *Desalination, 207*(1), 370-382. doi:http://dx.doi.org/10.1016/j.desal.2006.08.012

Mi, B., & Elimelech, M. (2008). Chemical and physical aspects of organic fouling of forward osmosis membranes. *Journal of Membrane Science, 320*(1–2), 292-302. doi:http://dx.doi.org/10.1016/j.memsci.2008.04.036

Mi, B., & Elimelech, M. (2010). Organic fouling of forward osmosis membranes: Fouling reversibility and cleaning without chemical reagents. *Journal of Membrane Science, 348*(1–2), 337-345. doi:http://dx.doi.org/10.1016/j.memsci.2009.11.021

Mo, W., Soh, L., Werber, J. R., Elimelech, M., & Zimmerman, J. B. (2015). Application of membrane dewatering for algal biofuel. *Algal Research, 11*, 1-12. doi:http://dx.doi.org/10.1016/j.algal.2015.05.018

Mohleji, S. C., & Verhoff, F. H. (1980). Sodium and potassium ions effects on phosphorus transport in algal cells. *Journal (Water Pollution Control Federation)*, 110-125.

Noffsinger, J., Giustino, F., Louie, S. G., & Cohen, M. L. (2009). Origin of superconductivity in boron-doped silicon carbide from first principles. *Physical Review B, 79*(10), 104511.

Pahl, S. L., Lee, A. K., Kalaitzidis, T., Ashman, P. J., Sathe, S., & Lewis, D. M. (2013). Harvesting, thickening and dewatering microalgae biomass. In *Algae for biofuels and energy* (pp. 165-185): Springer.

Phillip, W. A., Yong, J. S., & Elimelech, M. (2010). Reverse draw solute permeation in forward osmosis: modeling and experiments. *Environmental Science & Technology, 44*(13), 5170-5176.

Phuntsho, S., Shon, H. K., Hong, S., Lee, S., & Vigneswaran, S. (2011). A novel low energy fertilizer driven forward osmosis desalination for direct fertigation: Evaluating the performance of fertilizer draw solutions. *Journal of Membrane Science, 375*(1–2), 172-181. doi:http://dx.doi.org/10.1016/j.memsci.2011.03.038

Schachtman, D. P., Reid, R. J., & Ayling, S. M. (1998). Phosphorus uptake by plants: from soil to cell. *Plant physiology, 116*(2), 447-453.

Seman, M. A., Kei, L., & Yusoff, M. (2015). Synthesis and Performance of Polyamide Forward Osmosis Membrane for Natural Organic Matter (NOM) Removal. *World Academy of Science, Engineering and Technology, International Journal of Environmental, Chemical, Ecological, Geological and Geophysical Engineering, 9*(2), 160-163.

Shao, P., Darcovich, K., McCracken, T., Ordorica-Garcia, G., Reith, M., & O'Leary, S. (2015). Algae-dewatering using rotary drum vacuum filters: Process modeling, simulation and techno-economics. *Chemical Engineering Journal, 268*, 67-75. doi:http://dx.doi.org/10.1016/j.cej.2015.01.029

Shon, H. K., Phuntsho, S., Zhang, T. C., & Surampalli, R. Y. (2015). *Forward osmosis: fundamental and applications*: American Society of Civil Engineers (ASCE).

Simstich, B., Beimfohr, C., & Horn, H. (2012). Lab scale experiments using a submerged MBR under thermophilic aerobic conditions for the treatment of paper mill deinking wastewater. *Bioresource technology, 122*, 11-16. doi:http://dx.doi.org/10.1016/j.biortech.2012.04.029

Stein, J. R. (1979). *Handbook of phycological methods: culture methods and growth measurements* (Vol. 1): CUP Archive.

Uduman, N., Qi, Y., Danquah, M. K., Forde, G. M., & Hoadley, A. (2010). Dewatering of microalgal cultures: a major bottleneck to algae-based fuels. *Journal of renewable and sustainable energy, 2*(1), 012701.

Uduman, N., Qi, Y., Danquah, M. K., & Hoadley, A. F. (2010). Marine microalgae flocculation and focused beam reflectance measurement. *Chemical Engineering Journal, 162*(3), 935-940.

Wang, H., Chung, T. S., Tong, Y. W., Jeyaseelan, K., Armugam, A., Chen, Z., ... & Meier, W. (2012). Highly permeable and selective pore-spanning biomimetic membrane embedded with aquaporin Z. *small, 8*(8), 1185-1190.

Wang, K. Y., Ong, R. C., & Chung, T.-S. (2010). Double-Skinned Forward Osmosis Membranes for Reducing Internal Concentration Polarization within the Porous Sublayer. *Industrial & Engineering Chemistry Research, 49*(10), 4824-4831. doi:10.1021/ie901592d

Wang, Y., Wicaksana, F., Tang, C. Y., & Fane, A. G. (2010). Direct Microscopic Observation of Forward Osmosis Membrane Fouling. *Environmental Science & Technology, 44*(18), 7102-7109. doi:10.1021/es101966m

Wiley, P. E. (2013). Microalgae cultivation using offshore membrane enclosures for growing algae (OMEGA).

Yangali-Quintanilla, V., Li, Z., Valladares, R., Li, Q., & Amy, G. (2011). Indirect desalination of Red Sea water with forward osmosis and low pressure reverse osmosis for water reuse. *Desalination, 280*(1–3), 160-166. doi:http://dx.doi.org/10.1016/j.desal.2011.06.066

Yuan, Y., & Lee, T. R. (2013). Contact angle and wetting properties. In *Surface science techniques* (pp. 3-34): Springer.

Zhang, S., Wang, K. Y., Chung, T.-S., Chen, H., Jean, Y. C., & Amy, G. (2010). Well-constructed cellulose acetate membranes for forward osmosis: Minimized internal concentration polarization with an ultra-thin selective layer. *Journal of Membrane Science, 360*(1–2), 522-535. doi:http://dx.doi.org/10.1016/j.memsci.2010.05.056

Zhao, S., & Zou, L. (2011). Relating solution physicochemical properties to internal concentration polarization in forward osmosis. *Journal of Membrane Science, 379*(1), 459-467. doi:https://doi.org/10.1016/j.memsci.2011.06.021

Zhao, S., Zou, L., & Mulcahy, D. (2011). Effects of membrane orientation on process performance in forward osmosis applications. *Journal of membrane science, 382*(1-2), 308-315.

Zou, S., Wang, Y.-N., Wicaksana, F., Aung, T., Wong, P. C. Y., Fane, A. G., & Tang, C. Y. (2013). Direct microscopic observation of forward osmosis membrane fouling by microalgae: Critical flux and the role of operational conditions. *Journal of Membrane Science, 436*, 174-185. doi:http://dx.doi.org/10.1016/j.memsci.2013.02.030

CHAPTER 4: REVERSE SALT FLUX EFFECT ON *CHLORELLA VULGARIS* IN A FORWARD OSMOSIS SYSTEM

Abstract

The effect of reverse salt flux (RSF) which can be found during forward osmosis (FO) algae dewatering on *Chlorella vulgaris* microalgae was investigated. Three draw solution (DS) salts (NaCl, KCl and NH_4Cl) were evaluated in RSF simulating batch tests. The salt diffusion from the DS to the algae FS caused a static growth rate while increasing in lipid content from -22.2 to 57.6% within two days. With the addition of the different salts, pH was maintained to the optimal algae thriving range of 8-11, but the presence of salt stressed the algal cells which inhibited photosynthesis and algal growth within the experimental conditions. The settling velocity of the algal cells improved with the increase of salt content from 8 to 80 mM of each DS. It seemed that cell division can be accelerated in the presence of NH_4Cl and microscopic images showed the change in the algal cell size distribution which may negatively affect algal settleability. DS salt in a FO-algae harvesting system should be selected based on the final algal properties and constituents required.

Introduction

Microalgae have a high potential to produce biofuel, biodiesel, supplemental nutrient and feedstock. Depending on the conditions of cultivation, microalgae can vary in the constituent ratios of carbohydrates, lipid and protein (Lv, Cheng, Xu, Zhang, & Chen, 2010; Wang et al., 2015). The cultivation of microalgae can be achieved with low impact on natural resources. Algae can grow using secondary treated wastewater as a nutrient source which can serve as a polishing stage. In the presence of sunlight, algae can utilize high concentrations of carbon

dioxide from power plants (Azov, 1982; Hwang, Church, Lee, Park, & Lee, 2016). The use forward osmosis (FO) membranes as an attempt to harvest grown algae in a sustainable way has been studied for this last decade. FO has the capacity to preserve energy by utilizing osmotic pressure to concentrate/harvest microalgae while producing clean water. FO requires two salt concentration gradient solutions (draw solution [DS] and feed solution [FS]) to interact on the opposite sides of the membrane surface. This can allow the FO system to reduce the volume of the algal FS to 20% by extracting clean water using the DS (Munshi et al., 2018). However, during this process, salts can reverse flux from the DS to the algal FS by diffusion (Fig. S1). The concentration of the salts transferring from the DS to the algal FS vary depending on the concentration gradient, type of salt and membrane configuration. It was found that at a DS concentration between 0.5 – 4 M the reverse salt flux (RSF) can vary between 8 to 80 mM after running for 1-2 days (Munshi et al., 2018). The concentration and type of salt can affect algal growth, composition, metabolism, photosynthesis and morphology (Sudhir & Murthy, 2004; Wang et al., 2015). Specific salts can have different interaction with enzyme channel use and the ratio between potassium and sodium can stress the bioenergetic processes of photosynthesis (Sudhir & Murthy, 2004). NaCl, KCl and NH_4Cl were selected to represent RSF in a FO system for practical reasons (Munshi et al., 2018). NaCl simulates seawater or brine effluent from desalination plants. KCl and NH_4Cl represent fertilizer salts that can be used as DS to extract water and later to be used in fertigation. RSF in FO has been studied in terms of membrane fouling and permeate flux loss (Phillip, Yong, & Elimelech, 2010), while the effect of the RSF on the algal biomass has not been reported yet.

In this work, the effect of different types and salt concentrations of RSF which can be found in a FO operation during algae watering on *C. vulgaris* microalgae were investigated using batch tests. The conditions and the time frames were specific and essential to provide a better understanding of the effect of the RSF salts on the algae FS, which further can contribute in understanding the fouling and biofouling mechanism in a membrane system.

Materials and Methods

FO System

A custom-made bench-scale FO system was used to investigate water flux, RSF, and fouling of a new flat sheet PES FO membrane (Aquaporin–Sterlitech, Kent, WA) with an active surface area of 12.5 cm^2. The system consisted of a FS tank (0.5 L), DS tank (15 L) (Munshi et al., 2018). In the previous study (Munshi et al., 2018), the salts used in the FO operation showed effects on water flux and the final algal biomass properties such as color. The RSF was considered to be a potential contributor in stressing algal biomass in FS and possibly altering algal metabolism in FS. Upon that, the experiments were designed to investigate the effect of the NaCl, KCl and NH_4Cl salts on the algal culture. The RSF concentrations used in the experiments were determined in the previous FO operation with 2 days of hydraulic retention time (HRT).

Draw solution (DS)

The DSs used in FO systems are preferred to be economic, abundant, non-toxic and easy to regenerate. In best practice, the diluted DS would be directly utilized in other applications like fertigation or as a FS in desalination plants (Ge, Ling, & Chung, 2013; Phuntsho, Shon, Hong, Lee, & Vigneswaran, 2011). The hypothesis taken in account is that the RSF can enhance the

growth rate of algae during the algae dewatering, as it can be considered as an additional nutrient source in case of NH_4Cl and KCl. Moreover, specific salt concentrations can cause algal toxicity which can lead to algal degradation. The low RSF concentrations may enhance algal growth and lipid content for some salts, while the salts might create a growth inhibition with the high concentration (Church et al., 2017; Lv et al., 2010; Yeesang & Cheirsilp, 2011; Yeh & Chang, 2012). pH can change with each salt, which can also affect algal characteristics. The added salts can also affect algae excretion (dissolved organic content) (Discart, Bilad, Marbelia, & Vankelecom, 2014), which can adversely impact the process of algal separation via membranes or settling.

Algae species and cultivation

Chlorella vulgaris microalgae (UTEX 2714, Austin, Texas) was cultivated in a 4 L photo-bioreactor at room temperature (25.0 ± 1.0 ˚C). The system was aerated with filtered ambient air to supply CO_2 (0.04%) under continuous white fluorescent light illumination (light intensity: 159-189 µmol m^{-2} s^{-1} PAR) (06-662-63, Fisher). Modified Bold's Basal Medium (BBM) was used as growth media which consisted of (mg per liter): 175 KH_2PO_4; 25 $CaCl_2.2H_2O$; 75 $MgSO_4.7H_2O$; 250 $NaNO_3$; 75 Na_2HPO_4; 25 NaCl; 10 $Na_2EDTA.\ 2H_2O$; 6.2 NaOH; 4.98 $FeSO_4.7H_2O$; 0.001 mL H_2SO_4 (concentrated); 11.5 H_3BO_3, and a Trace Metal Solution of 2.86 H_3BO_3; 1.81 $MnCl_2.4H_2O$; 0.222 $ZnSO_4.7H_2O$; 0.079 $CuSO_4.5H_2O$; 0.0494 $Co(NO_3)_2.6H_2O$ (Kline, Hayes, Womac, & Labbe, 2010; Stein, 1979). The algal concentration was monitored to be maintained in the exponential growth phase at a concentration of about 0.37

g L^{-1} dry algal biomass. The pH and conductivity of the algal solution were 10.0 ± 0.5 and 700-800 µS cm^{-1}, respectively.

Analytical tools

Conductivity was measured to monitor salt depletion or uptake (Hach HQ40d Portable multi-parameter meter) in the FS. pH change was monitored over time (Hach HQ40d). pH values of healthy *C. vulgaris* solutions range from 8 – 11. Total suspended solids (standard methods, *2540*) and optical density (Hach – DR5000 Portable Spectrophotometer) were measured to determine the dry biomass of the algal solution. Microscopic and visual observations of the bulk algal solution were carried out to identify the color change and morphology of the microalgae using a microscope (Omax 40-2500X LED digital trinocular lab microscope, China). Settling velocity was measured using graduated cylinders (100 mL Borosilicate, Karter Scientific, LA), which was monitored using an image time-lapse recorder. Lipid cell content was determined at the end of the experiments by using a modified gravimetric determination of total lipids from Bligh and Dyer (1959).

The osmotic pressure was calculated using the following equation:

$$\Pi = n\ C\ R\ T \tag{4-1}$$

Where, Π: osmotic pressure (kPa); n: number of osmotically active particles (OAP) per mole; C: molar concentration (mol L^{-1}); R: universal gas constant (8.31441 L kPa mol^{-1} K^{-1}) T: temperature (K)

Experimental protocol

In a jar test set up, salts were added to a 500 mL algal FS. The algae in the experiment was in the exponential growth phase (OD=3 abs @ wavelength of 685nm; 0.37 g L^{-1}). The experiment duration was two days to simulate the HRT used in the previous FO system (Munshi et. al., 2018). Based on previous experiments (part 1), the RSF in the FO system was found for different CFVs and DS concentrations. The highest RSF that concentrated in the FS was found to be 0.470 g L^{-1} and the lowest was 0.048 g L^{-1} with the relatively low concentrations of the DSs (e.g., 0.5 and 1.0 M). Several batch experiments were conducted to understand the effect of each draw solution salt on the algal FS after dewatering 80% of the FS volume. Dewatering of 80% will lead to a five time increase in salt concentration in the algae product which ranged between 0.243 – 2.35 g L^{-1} of salt in the FS. The RSF concentrations that had were used in this work were 8, 32, and 80 mM for each salt (Covers the spectrum of the RSF concentration found the dewatered algae). The associated algal morphological changes from the RSF in FS were also determined for three DSs. Table 4.1 displays the matrix of conditions with different applied salt dosing.

Table 4.1 displays the matrix of conditions with different applied salt dosing.

Table 4-1: Experimental conditions to test the effect of DS salts on algae

Draw solution	Concentration (mM)	Feed solution (g L^{-1})
NaCl	8, 32, 80	0.37 dry *C. vulgaris* biomass
KCl		
NH_4Cl		

Results

In this section, different variables were monitored and are reported with minor interpretation as the results will be incorporated in a combined discussion in section 4.

pH

pH was found to slightly decrease with time. The initial pH of cultivated algal solution was around 10.0 without salt. When NaCl was added to the algal solution, there was a 0.3 increase in pH and for KCl, pH increase was about 0.2 to 0.6. Whereas, NH_4Cl had immediately decreased pH, for the different concentrations to a pH drop to 7.2-7.9. Figure 4-1 displays the changes of pH over time and the effect of each salt on the micro-algal solution.

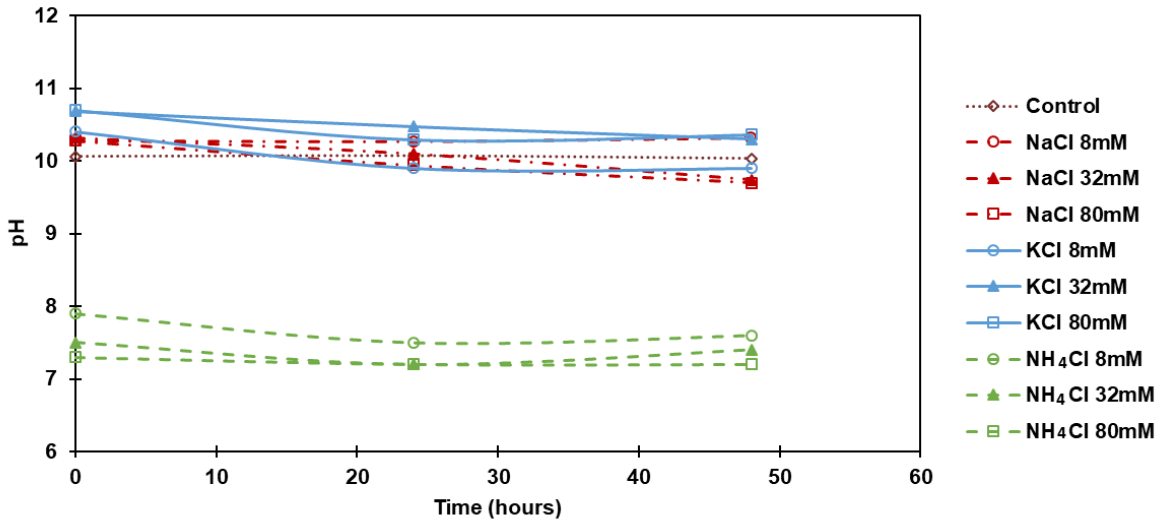

Figure 4-1: pH changes over time for NaCl, KCl and NH_4Cl under different salt concentrations.

The growth of *C. vulgaris* microalgae containing ammonia nitrogen (NH_4Cl) was different compared to NaCl and KCl. Visibly, the different dose concentrations of NH_4Cl effected the color of the algal solution making the solution dark green possibly from mitosis (McAuley & Cook, 1994). The addition of NH_4Cl altered pH to the range of 7.2-7.9; the medium

became neutral in the logarithmic phase of growth, in long term, it is expected to become alkaline when cells pass the lag phase (Przytocka-Jusiak, Mlynarczyk, Kulesza, & Mycielski, 1977; Tam & Wong, 1996). The drop in pH would not influence the growth nor algae viability as algae can thrive in even lower pH changes (Hargreaves & Whitton, 1976; Mayo, 1997).

Conductivity

After 24 hours, when the algal culture was dosed with 32 and 80 mM, KCl and NH_4Cl observed conductivity change (Fig. 4-2). With KCl, there was a clear trend of salt assimilation, the conductivity in the solution decreased as the KCl dose increased. At 8, 32 and 80 mM the conductivity decreased 10, 160 and 300 µS cm^{-1} respectively, this is equivalent to about 0.4, 70 and 155 mg L^{-1} of KCl being removed. On the other hand, NH_4Cl had an increase in conductivity around 160-250 µS cm^{-1}.

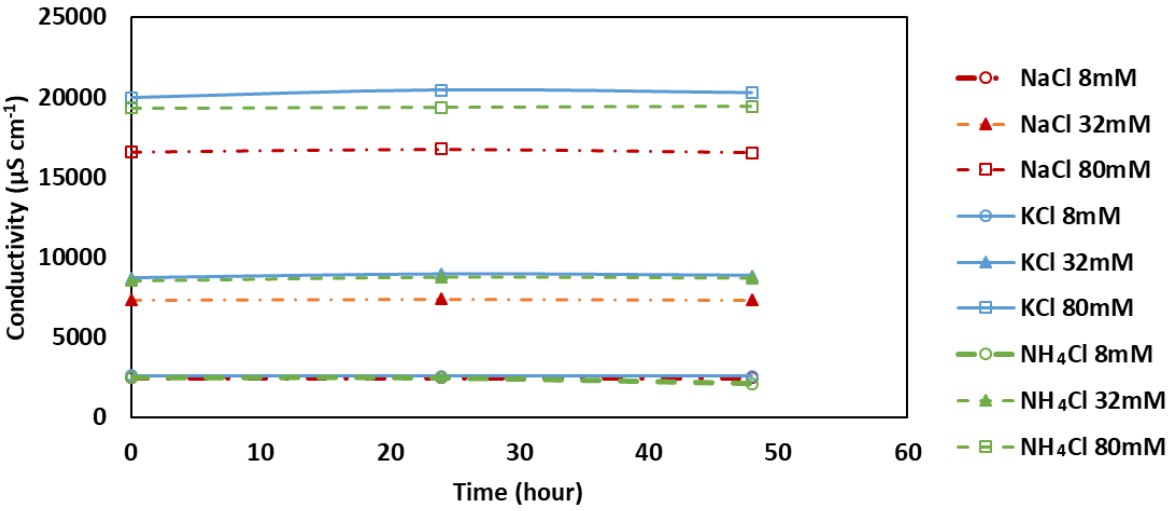

Figure 4-2: Conductivity changes over time for NaCl, KCl and NH_4Cl under different salt concentrations; Original algae conductivity 750 ± 50 µS cm^{-1}.

NH_4Cl had an increase in conductivity around 160-250 µS cm^{-1}. It seems that the algal cells may release organic matters which contribute to increase in conductivity (equivalent to 20 mg L^{-1} of NaCl). It was also reported that electrolyte leakage from damaged cells can increase conductivity in the presence of NH_4Cl (Liu, Xiong, Li, & Huang, 2004). Another explanation can be that the addition of NH_4Cl had accelerated cell division (McAuley & Cook, 1994), this would have led to micro-releases of electrolytes adding to conductivity.

Lipid content

Lipid analysis was conducted at the end of the experiment (after 48 hours) (Fig. 4-3). For the initial concentration of 0.37 g/L of dry algal biomass (OD_{685}: 3 abs), the lipid content was about 9.5%.

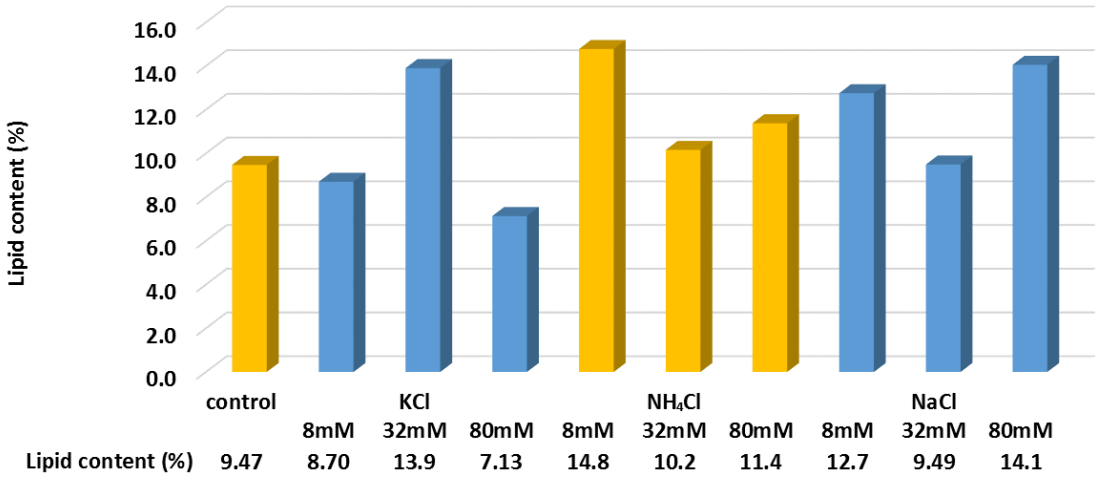

Figure 4-3: Lipid content (%) change after NaCl, KCl and NH_4Cl under different salt concentrations.

Each salt had each d different effect on the *C. vulgaris* algal cells lipid accumulation. KCl dose within the time frame of the experiment with the low doses that simulate RSF in a FO

system showed an adverse effect on lipid accumulation. From visual observation, the color of the algal solution lightened which indicates loss of chlorophyll. Microscopic images showed minimal variations on the algal morphology and cell colony formation, this may be caused by nitrate reductase inhibition which is triggered by the presence on KCl (Heimer, 1973), limiting the formation of protein in the algal cells and later stressing the algae to promote lipid accumulation. The two-day duration was not enough for KCl to show a clear trend in lipid cell generation. NaCl showed an increase in lipid content ranging from 0.2 to 49% for the different salt concentrations, typically, the increase in NaCl caused growth loss while enhancing lipid accumulation (Church et al., 2017; Heredia-Arroyo, Wei, Ruan, & Hu, 2011; Yeesang & Cheirsilp, 2011). This work showed that low concentrations in a short time frame can also affect lipid accumulation in the algal cell. In other work, it was determined that the presence of ammonia (e.g., 2.0-2.5 mM) functioned as a growth and photosynthesis inhibitor for different species of algae (Abeliovich & Azov, 1976). In this study, the concentrations of ammonia were much higher (e.g., 8, 32 and 80 mM), but like NaCl, NH_4Cl had no growth increase, but an enhanced lipid accumulation within the two days from 8 to 56 %.

Microscopic Imaging

The microscopic images were collected with magnification of 100 and 1,000 times. The average size of *C. vulgaris* was 3-5 μm. The images with 100 times magnification could show an overall picture of algal cell distribution (e.g., aggregates or scattering). The microscopic images with 1,000 times magnification provided details of the algal cell morphology. The control algal sample had scattered algal cells throughout the 2-day period. Duplicates samples were examined

at time 0, 24 and 48 hours for each salt concentration. Again, based on the short retention time in a FO system, it was sufficient to monitor the reactions for 48 hours. A long-term exposer is expected to further affect growth, morphology and aggregate formation. For the initial concentration, all samples had similar algal distribution to the control (Fig. C2(a)).

The dosing of low concentrations for the three salts showed no clear formation of coagulation or aggregate of cells (Fig. C2(b)) and no clear morphological variation was noticed for all salts (Fig. C2(c)). At a magnification of 100 times, the increase in dose to 32 mM developed more aggregates of algal cells (Fig. C2(d)). This can be an indicator of the destabilizing of the algal cells surface charge which lead to the coagulation and agglomeration of algal cells. The algal aggregate formation was observed in the solutions dosed with NaCl and less in KCl and NH_4Cl, while KCl had the least aggregate formation compared to NH_4Cl (Fig. C2(e)). At the high concentrations of 80 mM, NH_4Cl showed large algal aggregate formation. NaCl also had an increase in the formation of algal aggregates compared to 8 mM (Fig. C2(f)). KCl had some aggregate formation. The microscopic images with magnification of 1,000 times showed that the increase of dose to 80 mM showed a more complex aggregate of algal cells (Fig. C2(g)). In the algal solution dosed with NH_4Cl, the algae had two different colorations (Fig. 4-4, C2(f and g)). The cells appeared to develop plasmolysis in the hypertonic solution (Fig. 4-5, C2(e and g)), the transparent parts of the circular cell were developed from cell wall shrinkage and loss of cytoplasm. Cell divisions was also accelerated as small size algal cells were present with large cells that had multiple cells within.

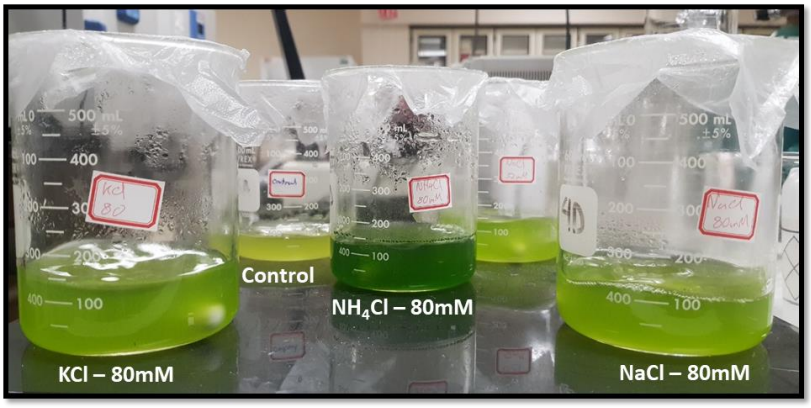

Figure 4-4: The effects of different salts (simulating RSF in a FO operation) on *C. vulgaris* solution.

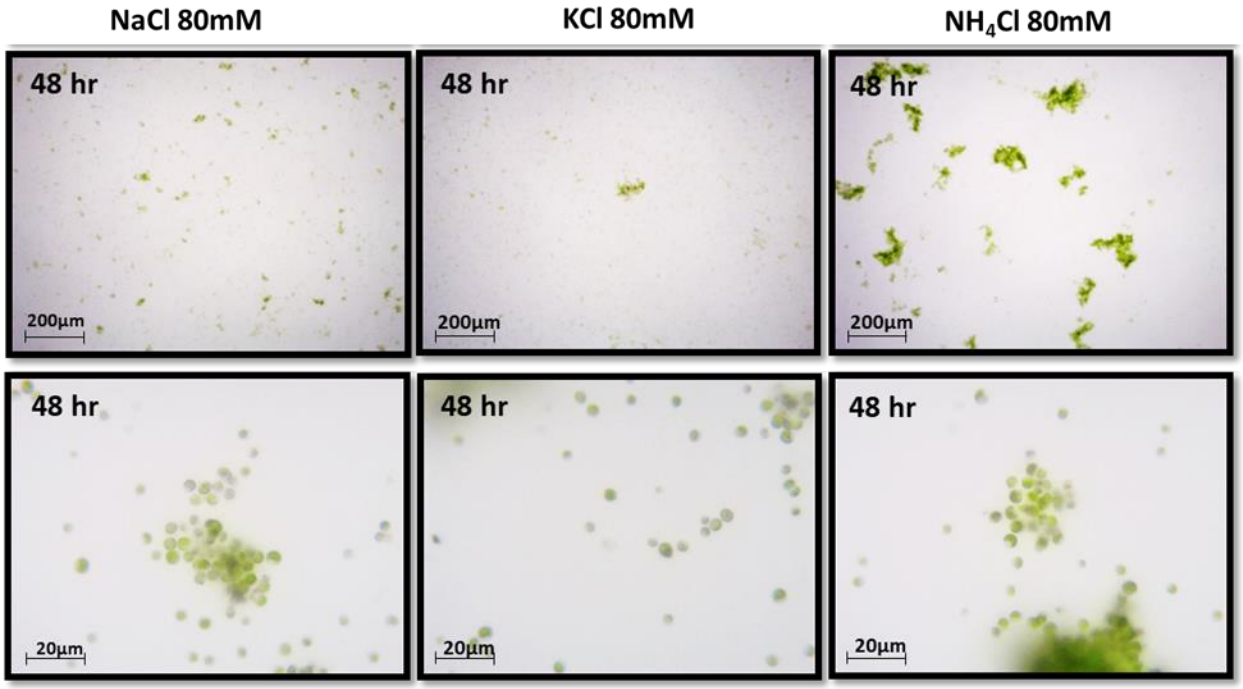

Figure 4-5: Microscopic images of the algal FS after two days of being subjected to different salts and concentrations. Top (x100) bottom (x1,000) magnification.

Settling Velocity

The overall trend showed that with the addition of KCl and NaCl increased the settling velocity. In the case of NH_4Cl, the low dose of 8 mM had an adverse effect on the settle-ability, but as the dose increased the settling velocity recovered (Fig. 4-5).

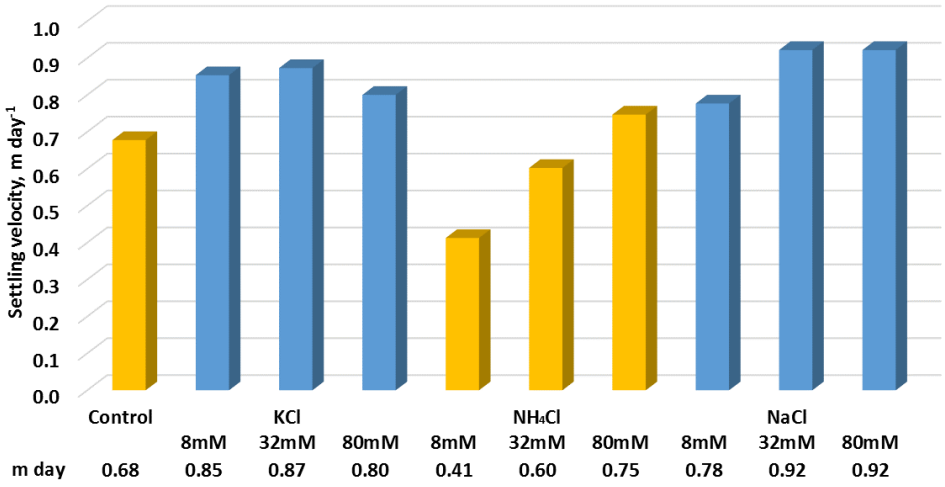

Figure 4-6: Settling velocity of *C. vulgaris* subjected to different salt concentrations of NaCl, KCl and NH_4Cl

Dry Biomass concentration

In the FO simulated conditions, the effect of the added salts was minimal on the algal growth rate. The algal cells seemed to be at the delayed growth station. In the presence of KCl, there was a fluctuating change in the dry algal biomass, the dose of 8 mM had the highest increase 1.9 %. The dose of 32 mM and 80 mM had a decrease in the algal concentration by 2.7% and 0.8%, respectively. When NH_4Cl was added, the concentration of the algal biomass decreased by 4.6 to 6.2% from the initial concentration of 0.37 g L^{-1}. NaCl had an increase in dry

biomass concentration by about 3.5% for doses of 8 and 32mM. The high dose of 80mM NaCl had a null effect on the dry biomass concentration for the two-day period.

Within the short-proposed duration (e.g., 48 hours), the addition of salt would impose algae to a lag growth phase. For the long-term effect of the added salts, when storage of the concentrated algae with the RSF is administrated, further research can include monitoring the different growth phases (i.e., lag and growth phases). Dissolved organic concentration (DOC) was also measured over time. NaCl and KCl had similar changes in DOC compared to control experiments. NH_4Cl dosed algal solution VSS was not determined, as NH_4Cl directly increased the concentration of the dissolved volatile content. This was attributed to ammonium effecting the reading, as it can evaporate at temperatures above 340 ˚C to form ammonia and hydrogen chloride.

There was a correlation with the density of the biomass and dissolved organics released in the solution with settling velocity, the higher the density the lower the settling velocity. The increase in conductivity can develop a hypertonic solution that promotes cell plasmolysis. This would increase the density of the algal cell. Nevertheless, it was found that when the salt concentration increased, the settling velocity was enhanced. Even in very high concentration (e.g., 15, 30, and 45% of NaCl), the settling velocity was also found to increase (Church et al., 2017). The increase in the ionic strength seems to enhance the settling velocity. For NH_4Cl, there was an accelerated cell division, this phenomenon could have caused algal cells to develop settling resistance in addition to algal cell excretions (dissolved organic matter).

Conclusions

C. vulgaris microalgae with its high potential for biofuel production can develop morphological and compositional alteration when subjected to low doses of salts within short time frames. Overall, *C. vulgaris* showed a static growth rate while having an increase in lipid content. The settling velocity of the algal cells was found to improve with the increase of salt content from 8 to 80 mM. NH_4Cl can accelerate *chlorella vulgaris* cell division, altering the cell size distribution and reducing the settleability of the algae particles in the solution. pH was found to be within the optimal algae thriving pH, but the presence of salt stressed the microalgae which inhibited growth and photosynthesis. The RSF caused by DS in FO was found to modify algal cell characteristics, future work should monitor algal cell components (e.g., protein, carbohydrates and lipid content) in FO operations, with microbial fatty acid profiles and amino acid composition analyses to determine the optimal algae use as a final product.

References

Abeliovich, A., & Azov, Y. (1976). Toxicity of ammonia to algae in sewage oxidation ponds. *Applied and Environmental Microbiology, 31*(6), 801-806.

Azov, Y. (1982). Effect of pH on inorganic carbon uptake in algal cultures. *Applied and Environmental Microbiology, 43*(6), 1300-1306.

Church, J., Hwang, J.-H., Kim, K.-T., McLean, R., Oh, Y.-K., Nam, B., . . . Lee, W. H. (2017). Effect of salt type and concentration on the growth and lipid content of Chlorella vulgaris in synthetic saline wastewater for biofuel production. *Bioresource Technology, 243*, 147-153. doi:https://doi.org/10.1016/j.biortech.2017.06.081

Discart, V., Bilad, M. R., Marbelia, L., & Vankelecom, I. F. J. (2014). Impact of changes in broth composition on Chlorella vulgaris cultivation in a membrane photobioreactor (MPBR) with permeate recycle. *Bioresource Technology, 152*, 321-328. doi:https://doi.org/10.1016/j.biortech.2013.11.019

Ge, Q., Ling, M., & Chung, T.-S. (2013). Draw solutions for forward osmosis processes: Developments, challenges, and prospects for the future. *Journal of Membrane Science, 442*, 225-237. doi:http://dx.doi.org/10.1016/j.memsci.2013.03.046

Hargreaves, J., & Whitton, B. (1976). Effect of pH on growth of acid stream algae. *British Phycological Journal, 11*(3), 215-223.

Heimer, Y. M. (1973). The effects of sodium chloride, potassium chloride and glycerol on the activity of nitrate reductase of a salt-tolerant and two non-tolerant plants. *Planta, 113*(3), 279-281. doi:10.1007/bf00390515

Heredia-Arroyo, T., Wei, W., Ruan, R., & Hu, B. (2011). Mixotrophic cultivation of Chlorella vulgaris and its potential application for the oil accumulation from non-sugar materials. *Biomass and Bioenergy, 35*(5), 2245-2253. doi:https://doi.org/10.1016/j.biombioe.2011.02.036

Hwang, J.-H., Church, J., Lee, S.-J., Park, J., & Lee, W. H. (2016). Use of microalgae for advanced wastewater treatment and sustainable bioenergy generation. *Environmental Engineering Science, 33*(11), 882-897.

Kline, L. M., Hayes, D. G., Womac, A. R., & Labbe, N. (2010). Simplified determination of lignin content in hard and soft woods via UV-spectrophotometric analysis of biomass dissolved in ionic liquids. *BioResources, 5*(3), 1366-1383.

Liu, J., Xiong, Z., Li, T., & Huang, H. (2004). Bioaccumulation and ecophysiological responses to copper stress in two populations of Rumex dentatus L. from Cu contaminated and non-contaminated sites. *Environmental and Experimental Botany, 52*(1), 43-51.

Lv, J.-M., Cheng, L.-H., Xu, X.-H., Zhang, L., & Chen, H.-L. (2010). Enhanced lipid production of Chlorella vulgaris by adjustment of cultivation conditions. *Bioresource Technology, 101*(17), 6797-6804. doi:https://doi.org/10.1016/j.biortech.2010.03.120

Mayo, A. W. (1997). Effects of temperature and pH on the kinetic growth of unialga Chlorella vulgaris cultures containing bacteria. *Water environment research, 69*(1), 64-72.

McAuley, P., & Cook, C. (1994). Effects of host feeding and dissolved ammonium on cell division and nitrogen status of zooxanthellae in the hydroid Myrionema amboinense. *Marine Biology, 121*(2), 343-348.

Munshi, F. M., Church, J., McLean, R., Maier, N., Sadmani, A. H. M. A., Duranceau, S. J., & Lee, W. H. (2018). Dewatering algae using an aquaporin-based polyethersulfone forward osmosis membrane. *Separation and Purification Technology, 204*, 154-161. doi:https://doi.org/10.1016/j.seppur.2018.04.077

Phillip, W. A., Yong, J. S., & Elimelech, M. (2010). Reverse Draw Solute Permeation in Forward Osmosis: Modeling and Experiments. *Environmental Science & Technology, 44*(13), 5170-5176. doi:10.1021/es100901n

Phuntsho, S., Shon, H. K., Hong, S., Lee, S., & Vigneswaran, S. (2011). A novel low energy fertilizer driven forward osmosis desalination for direct fertigation: Evaluating the performance of fertilizer draw solutions. *Journal of Membrane Science, 375*(1–2), 172-181. doi:http://dx.doi.org/10.1016/j.memsci.2011.03.038

Przytocka-Jusiak, M., Mlynarczyk, A., Kulesza, M., & Mycielski, R. (1977). Properties ofChlorella vulgaris strain adapted to high concentration of ammonium nitrogen. *Acta Microbiologica Polonica, 26*(2), 185-197.

Stein, J. R. (1979). *Handbook of phycological methods: culture methods and growth measurements* (Vol. 1): CUP archive.

Sudhir, P., & Murthy, S. D. S. (2004). Effects of salt stress on basic processes of photosynthesis. *Photosynthetica, 42*(4), 481-486. doi:10.1007/S11099-005-0001-6

Tam, N., & Wong, Y. (1996). Effect of ammonia concentrations on growth of Chlorella vulgaris and nitrogen removal from media. *Bioresource Technology, 57*(1), 45-50.

Wang, Y., Guo, W., Yen, H.-W., Ho, S.-H., Lo, Y.-C., Cheng, C.-L., . . . Chang, J.-S. (2015). Cultivation of Chlorella vulgaris JSC-6 with swine wastewater for simultaneous nutrient/COD removal and carbohydrate production. *Bioresource Technology, 198*, 619-625. doi:https://doi.org/10.1016/j.biortech.2015.09.067

Yeesang, C., & Cheirsilp, B. (2011). Effect of nitrogen, salt, and iron content in the growth medium and light intensity on lipid production by microalgae isolated from freshwater sources in Thailand. *Bioresource Technology, 102*(3), 3034-3040. doi:https://doi.org/10.1016/j.biortech.2010.10.013

Yeh, K.-L., & Chang, J.-S. (2012). Effects of cultivation conditions and media composition on cell growth and lipid productivity of indigenous microalga Chlorella vulgaris ESP-31. *Bioresource Technology, 105*, 120-127. doi:https://doi.org/10.1016/j.biortech.2011.11.103

CHAPTER 5: THE USE OF ELECTRIC FIELD FORWARD OSMOSIS FOR THE MITIGATION OF FOULING DURING ALGAE HARVESTING

Abstract

Efficient microalgae harvesting is essential to produce sustainable biofuel. Forward osmosis (FO) membrane processes can provide a cost-effective means for algae separation; however, there is a potential of membrane fouling. In this study, a bench scale FO membrane unit was fabricated using an aquaporin thin film composite (TFC) FO membrane and was coupled with an electric field (0.33, 0.13 and 0.03 V mm^{-1}) in a continuous and pulsing mode (10 sec intervals) to mitigate membrane fouling for effective algae dewatering (*Chlorella vulgaris*). The electric field forward osmosis (EFFO) configuration was able to produce 3.8, 2.2, 2.2 times greater flux at the applied potential of -1.0, -0.4, and -0.1 V, respectively, compared to the control (without an electric field). EFFO (-0.4 V; continuous) also increased the settling velocity from 0.30 to 0.33 m day^{-1} during the algae dewatering (50–60%), probably due to electro-flocculation. The study also investigated the effect of the electric field on pH, conductivity, lipid content and morphology of *C. vulgaris* during the FO process for algae dewatering. Generally, higher applied potentials increased fluxes. The different electric field intensities (V mm^{-1}) were found to have the same proportional flux loss trend. A high potential of -10 V was applied as a cleaning scheme, demonstrating the high ability to recover flux (99%) and remove membrane foulant build up.

Introduction

Microalgae have high potential for biofuel production, preferably algae strains that maintain a fast growth rate and high lipid content, which can be harvested. Algal biomass

recovery is one of the most challenging steps in algal biofuel production (Pahl et al., 2013). About 90% of equipment cost is associated with algae harvesting and 20-30% of the total cost of algae biomass production (Faris M. Munshi et al., 2018). Recently, forward osmosis (FO) has emerged as a possible alternative to conventional algae separation methods (e.g., centrifuge, microfiltration [MF] and ultrafiltration [UF]). The high concentration gradient between a draw solution (DS) and feed solution (FS) can produce an osmotic pressure, driving slow, but cost-effective algae dewatering (Buckwalter, Embaye, Gormly, & Trent, 2013). The FO utilizes the osmotic pressure to concentrate the algal solution, while producing clean water in a simple operation that has low energy demands. Fouling and biofouling can decelerate the dewatering process over time and have been usually controlled by physical and chemical cleaning methods such as bubbling, flushing, scraping and immersion in a washing solution (Mi & Elimelech, 2010a, 2010b; Valladares Linares, Yangali-Quintanilla, Li, & Amy, 2012). A simple and easy on-site cleaning procedure would assist sustainable algal dewatering. A novel approach of this would be to couple the FO with an electric field in order to develop repulsion forces that can prolong the filtration cycle and mitigate foulant attachment.

Applying an electric field has been tested for the mitigate of fouling in the operation of membrane bioreactors for decades (v Zumbusch, Kulcke, & Brunner, 1998). The concept of applying an electric field has been conceived in membrane bioreactors for advanced wastewater treatment by Bechhold (1904), where an electric field in an UF system was applied as a repulsive force to assist membrane separation (Bechhold, 1904). The electrical antifouling in a membrane process is attributed to developing an electrostatic field on the membrane surface to build

repulsion forces that would inhibit the foulant layer to build up during wastewater treatment. It was found that a membrane which is polarized at a potential of -300 to -500 mV is expected to have a higher foulant rejection compared to the low potential (e.g., -20 mV) on membrane surfaces (J. Liu, L. Liu, B. Gao, & F. Yang, 2012). Different patterns were also applied with a mode of continuous or pulsing electric fields (e.g., 5 min on and 1 min off) (Bani-Melhem & Elektorowicz, 2011; L. Liu, J. Liu, B. Gao, & F. Yang, 2012). The repulsion forces generated by the electric field were primarily influenced by the membrane surface characteristics and the density of negatively charged biomass (Akamatsu, Lu, Sugawara, & Nakao, 2010). However, most studies on electrical antifouling have been limited to MF and UF, and the application of electric field on FO systems for algae dewatering is still in early stages (Son, Sung, Ryu, Oh, & Han, 2017).

The objective of this study is to introduce electric field to the FO algal dewatering process to mitigate fouling during the process. Algae typically has negative zeta potentials of -10 to -35 mV (Oukarroum, Bras, Perreault, & Popovic, 2012; Rosenhahn et al., 2009), thus introducing a negative charge would repel particles and further reduce the compaction of the algal forming foulant layers. When applying an electric field, fouling prevention using an applied negative potential can further increase sludge size, reduce zeta potential, electrophoresis, and generate an electrostatic repulsion/rejection against electronegative colloids or particles (Ahmad, Yasin, Derek, & Lim, 2011; Liu, Liu, Gao, Yang, & Chellam, 2012). In this study, various electrical fields were applied for dewatering algae using an aquaporin thin film composite (TFC) FO membrane. The influence of applied electric fields on FO membrane flux and fouling and algal

biomass was investigated under different conditions. Two different operating modes were applied and compared between a continuous and pulsing mode for effective algae dewatering. Other factors which can affect the repulsion efficiency were also evaluated and these include the applied electric field, the type of electrodes, and the salinity level. Any side reaction which may occur during the application of an electric field (i.e., electrocoagulation (L. Liu, J. Liu, B. Gao, F. Yang, et al., 2012)) was also investigated.

Materials and methods

Algae species and cultivation

A photo-bioreactor (4 L-Erlenmeyer) growth system was used to cultivate *Chlorella vulgaris* (UTEX 2714, Austin, Texas) at room temperature (25.0 ± 1.0 ˚C) under continuous white fluorescent light illumination with a light intensity (159 – 189 µmoL m^{-2} s^{-1} PAR) and stirred using a magnetic stirrer at 50 rpm. The culture was aerated with filtered ambient air to supply CO_2 (0.04%). A modified Bold's Basal Medium (BBM) was used to cultivate the microalgae composed (per liter) of 175 mg KH_2PO_4; 25 mg $CaCl_2.2H_2O$; 75 mg $MgSO_4.7H_2O$; 250 mg $NaNO_3$; 75 mg Na_2HPO_4; 25 mg NaCl; 10 mg $Na_2EDTA.\ 2H_2O$; 6.2 mg NaOH; 4.98 mg $FeSO_4.7H_2O$; 0.001 mL H_2SO_4 (concentrated); 11.5 mg H_3BO_3, and a Trace Metal Solution of 2.86 mg H_3BO_3; 1.81 mg $MnCl_2.4H_2O$; 0.222 mg $ZnSO_4.7H_2O$; 0.079 mg $CuSO_4.5H_2O$; 0.0494 mg $Co(NO_3)_2.6H_2O$ of which was modified from (Kline, Hayes, Womac, & Labbe, 2010; Stein, 1979). Biomass growth was monitored until it reached about 0.5 g L^{-1} dry algal biomass. The pH and conductivity of the algal solution was 10.5 ± 0.5 and about 700 µS cm^{-1}, respectively.

Electric field forward osmosis (EFFO) system

The FO membrane used was a flat sheet TFC membrane (Aquaporin–Sterlitech, Kent, WA). Zeta potential (mV) was measured using an electro kinetic analyzer (Anton Paar, Graz, Austria). The FO membrane had a steady zeta potential of -11 mV under various pHs between 6.5 and 10 (Fig. D1). Bench-scale tests were performed to investigate the effect of EFFO on water flux, reverse salt flux (RSF), and the fouling of the flat sheet TFC FO membrane. The FO system used for this study consisted of FS tank (0.5 L), DS tank (15 L), peristaltic pumps, scale, DC power supplier (DP821A, Regol, OR) and the home-made FO unit (2x4.35 cm^3) (Fig. 5-1). The FO unit was fabricated using ¾ inch plexiglass. A 3-mm thick rubber gasket was used to create the flow channels and prevent water leaking. The dimensions of the FO flow path were width: 1 cm × length: 12.5 cm× height: 0.3 cm. Peristaltic pumps (Masterflex L/S, Cole Parmer, IL) were used to recirculate the FS and DS. To generate the electric field, two different types of electrode meshes were used: stainless steel (SS) mesh #40 (401212, ASC Stainless Mesh Works) and carbon fiber (CF) 12K Tow (CF-1FTX8IN, Carbon Fiber - FABRIC, NJ), Two electrodes were installed by facing each other; one under the FO membrane surface (cathode) and the other electrode on the other side of the algae channel (anode) (Fig. 5-1). The algal FS was pumped through the top chamber and a DS was pumped in the lower chamber. FO occurred naturally; across the FO membrane. The FS and DS flowed in the opposite direction with a similar cross flow velocity (CFV). The FO active layer was facing the feed solution (FO mode). Water flowed from the FS to the DS, also RSF occurred naturally in the system; where salt moves from the DS to the FS.

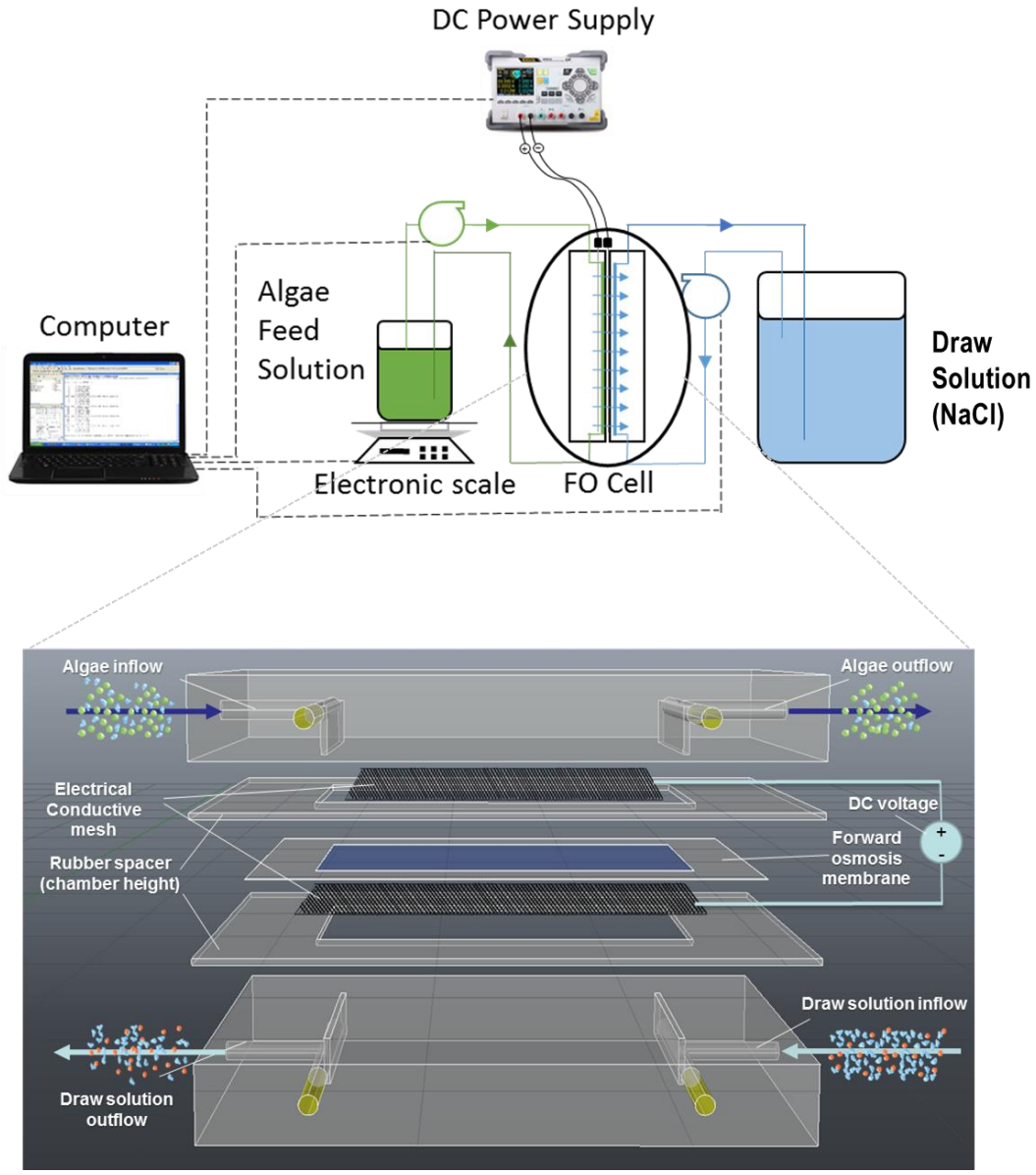

Figure 5-1: A schematic of EFFO system with a FO cell coupled with an electric field.

EFFO fouling tests:

The use of different pattern modes was tested (Table 1) to investigate the effect of electric fields on the FO performance and algae. 0.5 L of microalgae *C. vulgaris* (0.5 g L^{-1}) was used as FS and

4 M NaCl (15 L) was used as DS. The fabricated FO system coupled with electrode sheets were used to evaluate the effect of the EFFO system. Polypropylene (FM100, Diversified Biotech, Dedham) and stainless steel were used to support the FO membrane and their effect on the FO dewatering capacity was investigated. The osmotic pressure was calculated using the following equation:

$$\Pi = n\ C\ R\ T \quad (5\text{-}1)$$

where, π : osmotic pressure (kPa); n: number of osmotically active particles (OAP) per mole; C: molar concentration (mol L^{-1}); R: universal gas constant (8.31441 L kPa mol^{-1} K^{-1}); T: temperature (K).

Table 5-1: The experimental desgin to investigate the effect of electric fields on the FO performance and algae.

Experiment	Feed Solution (FS)	Draw solution (DS)	Applied potential (V)	Electric field (V mm^{-1})	Cross Flow Velocity (cm sec^{-1})
Control	*C. vulgaris* microalgae: ~ 0.5 g L^{-1}	NaCl: 4M	-	-	5.0 and 10.7
Pulsing mode (10 sec pulse & 10 sec intervals)			- 0.4	0.13	5.0 and 10.7
			- 0.1	0.03	5.0
			- 1.0	0.33	
Continuous mode			-0.4 and -1.0	0.33	
High potential cleaning (60 – 120 sec)			-4.0 and -10	1.33 and 3.33	

In an attempt to better understand the effect of fouling, the experiments were conducted for two days (48 hours). A physical cleaning was conducted to remove any temporary deposition and associated concentration polarization by flushing the FO membrane with an increased CFV of 21 cm sec^{-1} for 15 minutes (Chang, Le Clech, Jefferson, & Judd, 2002). In addition, the FS (500 mL) was replaced with a new batch of the stock algal solution to offset the effect of the concentrated FS and eliminate the effect of added salt from RSF, and thus to ensure that the new observed flux loss was mainly attributed to fouling/biofouling.

During the tests, the electric potentials were applied using a DC power supplier to create the desired electric fields. The electric field intensity effect was examined in pulsing and continuous modes for permeate flux and RSF. The effect of the electric field on the algae settling ability (i.e., settling velocity) was also evaluated since the charge disturbance may promote algae agglomeration (Alfafara, Nakano, Nomura, Igarashi, & Matsumura, 2002). The electrodes were closely monitored to control hydrogen and oxygen bubbling from electrolysis. CFV in the DS and FS chambers is one of the important factors that can affect the concentration-polarization and fouling formation (Faris M Munshi et al., 2018). The EFFO system was tested under two CFVs of 5.0 and 10.7 cm sec^{-1}. FS (0.5 L) and DS (15 L) were recirculated in opposite directions at the same CFV.

Draw solution (DS)

The DS in this process was selected to be economic, abundant, non-toxic and easy to regenerate. The best practice when selecting a DS would be to directly utilize the diluted DS in other applications like fertigation and water desalination. The drawbacks associated when using

less favorable approaches include high energy consumption or poor water flux. The DS tested in this work was 4 M of NaCl which generates a high osmotic pressure (π =19.8 MPa). It was used to accelerate the fouling process while simulating brine water from a desalination plant. Such DS would be used in a closed FO-RO system that regenerates the DS. The DS volume selected was 15 L to minimize the dilution of the initial concentration.

Table 5-2: The experimental matrix to investigate the effect of the electric field on pH, lipid content, settling velocity and morphology of *Chlorella vulgaris* microalgae.

Applied potential (V)	Conductivity (µS cm^{-1})	Electrode type
Control	722	-
	1,613*	
-0.1, -0.4 and -1.0	1,613	Stainless Steel mesh (4 × 15 cm) electrode
	4,630**	
-1.0	1,613	Carbon fiber (4 × 15 cm)
	4,630	

*equivalent to 0.5 g L^{-1} NaCl
**equivalent to 2.0 g L^{-1} NaCl

The effect of the electric field on the algal culture

Another set of experiments were conducted in batch setups to determine the effect of the electric field on the *C. vulgaris* algal specie in terms of morphological changes of algae (Fig. D2(a)). The exposure to the electric field is expected to accelerate abiotic redox reactions. Two conductivity levels were used 1,613 and 4,630 µS cm^{-1} (equivalent to 0.5 and 2.0 g L^{-1} of NaCl, respectively) to represent the RSF found in the EFFO system (Faris M. Munshi et al., 2018). An anode carbon fiber (CF) sheet electrode (Fig. D3) was also tested to determine the effect of the different electrode material at an applied potential of -1V. Table 5-2 displays the matrix of conditions with different applied potentials and electrode types.

Analytical approach

The FS tank was positioned on an electronic analytical balance (PCE-PCS 6 Counting Scale, PCE Americas Inc., Jupiter, L) that was connected to a computer to record flux readings (L m^{-2} h^{-1}). RSF was monitored by measuring the conductivity of the feed solution using a portable multi-meter (HQ40d, Hach, Loveland, CO). Total suspended solids (TSS) and optical density (OD) was measured to determine the dry biomass of the algae solution. pH and temperature were also monitored using the portable multi-meter (HQ40d, Hach, Loveland, CO). Membrane surfaces were characterized by microscopic observation (LW Scientific Revelation III, Lawrenceville, GA). The thickness of the membrane fouling layer was determined by drying the fouling layer in room temperature, the (bio)fouling layer was then cracked and the thickness was observed via microscope (× 100 magnification). Zeta potential of the FO membrane was determined using an Electro kinetic analyzer, Paar physical (Anton Paar, Graz, Austria) with a pH range of 2.8-11.4. The settling velocity of algae was determined using a graduated cylinder, the algae setting was recorded using time-lapse photography. Microscopically, the algae morphology was monitored in the batch setups for better understanding of the impact of the electric charges and the oxidized anode on the algal culture. Algal samples were tested at times 0, 3, 24 and 48 hours under the conditions in table 5-2. pH was monitored over time as the pH of the solution containing healthy *C. vulgaris* ranges from 8–11 (Hwang, Church, Lim, & Lee, 2018; Yeh & Chang, 2012). Lipid content was also determined to compare change in lipid content due to different stress conditions using a modified total lipids gravimetric determination method from (Bligh & Dyer, 1959). TSS and volatile dissolved solids (VDS) were conducted to

monitor algal growth and extracellular polymeric substances released (Sing, Isdepsky, Borowitzka, & Lewis, 2014).

Results and discussion

FO membrane support material

The original FO setup used a 0.33 mm thick polypropylene permeable mesh to support the FO membrane (Faris M. Munshi et al., 2018). In this study, the FO unit was modified, a stainless steel (SS) mesh #40 was used as the FO membrane supporter in addition to working as an active electrode (cathode) to create the electric field effect. A separate SS mesh was added as an anode (Fig. 5-1). The FO process was then operated using 0.5 g L^{-1} *C. vulgaris* solution as FS and 4 M NaCl as DS at a cross flow velocity (CFV) of 5.0 cm sec^{-1}. A separate FO system without SS meshes was operated using the polypropylene mesh as a control to compare the effect of the support materials on flux. The percentage of open area was 70% for the polypropylene mesh and 55% for the SS #40 mesh (0.17 mm diameter). While both SS and polypropylene support FO systems showed similar initial fluxes of about 13 L m^{-2} h^{-1}, the average flux after 48 hours for the polypropylene and SS supporter systems was 5.0 and 3.9 L m^{-2} h^{-1}, respectively (Fig. D4(a)). A 21.4% decrease in open surface area of the SS mesh support seemed to contribute in the reduction of permeate flux by roughly 1 L m^{-2} h^{-1}, compared to polypropylene. However, two different support materials showed a similar trend in terms of normalized flux loss (Fig. D4(b)), which may be caused by several factors such as the concentration of the FS over time, salinity increase in the FS from RSF from DS, biofouling, and concentration polarization due to the fouling layer.

Cross flow velocity (CFV) in EFFO

Using the SS supporter mesh, the EFFO system was tested under two CFVs (5.0 and 10.7 cm sec^{-1}) with an applied potential of -0.4 V with 10 sec intervals on/off. At 5.0 cm sec^{-1} of CFV, the EFFO run showed 9% flux recovery, whereas the control (no EFFO) showed only 4% recovery after running for 24 hours (Fig. 5-2 (a)). At 10.7 cm sec^{-1} of CFV, initial flux (10.7 L m^{-2} h^{-1}) was higher compared to 5.0 cm sec^{-1} of CFV (8 L m^{-2} h^{-1}) (Fig. 5-2 (b)). With higher CFV, the effect of EFFO was not significant compared to no EFFO. Both showed about 10% flux recovery (Fig. 5-2 (a)). From the visual observation, a biofouling layer was formed within the first three hours when running at 5.0 cm sec^{-1}, while at higher CFV (10.7 cm sec^{-1}) the foulant layer was not noticeable during the entire duration of the experiment (48 hours). The thickness of the algal fouling layer on the FO membrane was found to be 45–55 and 12 μm for the 5.0 and 10.7 cm sec^{-1} CFV, respectively. In any cases, physical cleaning was required to increase flux recovery. Moreover, running the system with a higher CFV (10.7 cm sec^{-1}) seemed to provide similar fluxes regardless of an electric field (applied potential: -0.4 V; 0.33 V mm^{-1}), but higher CFV can damage the FO membrane, results in short life time, in addition to higher energy demands.

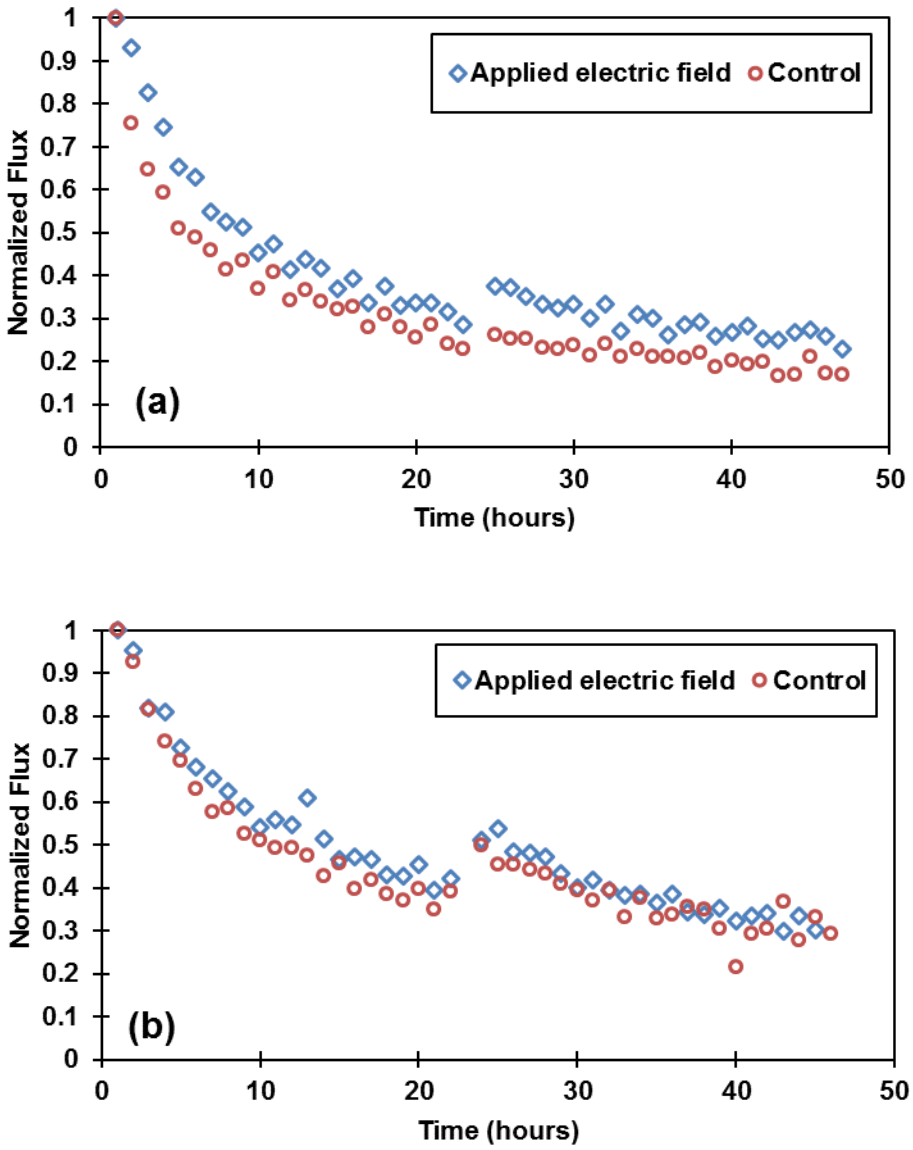

Figure 5-2: Normalized flux with a FS of 0.5 g L^{-1} dry algae biomass (*C. vulgaris*) and a DS of 4 M of NaCl, at a CFV of (a) 5.0 cm sec^{-1} and (b) 10.7 cm sec^{-1}, and an applied potential of -0.4 V with 10 sec intervals on/off. The measured (actual) water flux was normalized by dividing each flux at a given time by the initial flux. No EFFO was used as a control.

Effects of different applied potentials on FO performance

With a lower CFV (5.0 cm sec^{-1}), three different potentials (-0.1, -0.4, and -1.0 V) were applied between two SS meshes and their effect on the algae dewatering was investigated for 48

hours of duration. A similar proportional flux loss trend was observed even with the different electric field intensities. Before physical cleaning after 24 hours, the final flux at -1.0 V was 55% and 45% higher than -0.4 and -0.1 V, respectively (Fig. 5-3). After the FO membrane was physical cleaned and the FS was changed (after 24 hours), flux was about 380, 215 and 215% for the applied potential of -1.0, -0.4, and -0.1 V, respectively, compared to the base line flux (Fig. 5-3). However, at the applied potential of -0.1 V, there was less than 2% recovery even after the physical cleaning. This can indicate that the developed fouling/biofouling layer structure was fixed, while it is less obstructive to the permeate flow as the flux has doubled compared to the control experiment. The low recovery of flux even after physical cleaning indicates that biofouling would be the major cause of flux loss, and that further measures are needed to maintain higher flux rates. At the -0.4 V of applied potential, there was a 12% flux recovery with a minor improvement in permeate flux compared to the low applied potential (-0.1 V), whereas the higher potential (-1.0 V) provided a higher flux of about 55% compared to the applied potential of -0.1 V. The flux recovery at -1.0 V was found to be 25%.

One interesting observation was that the high electric potential resulted in the release of oxidized metals from the anode as a side reaction of electrolysis. It was also found that a higher salinity can further increase the oxidation of the anode. From a preliminary experiment, the higher salinity (4.6 mS cm^{-1}) also increased settling velocity compared to the lower salinity (1.6 mS cm^{-1}) algal solution under the different applied electric potentials. At the potential of -1.0 V, algae cells attached to the released oxidized particles (reddish brown ferric oxides Fe_2O_3). This

allowed the particles and algae cells to coagulate to form dense aggregates of algal biomass which further promoted algal settling.

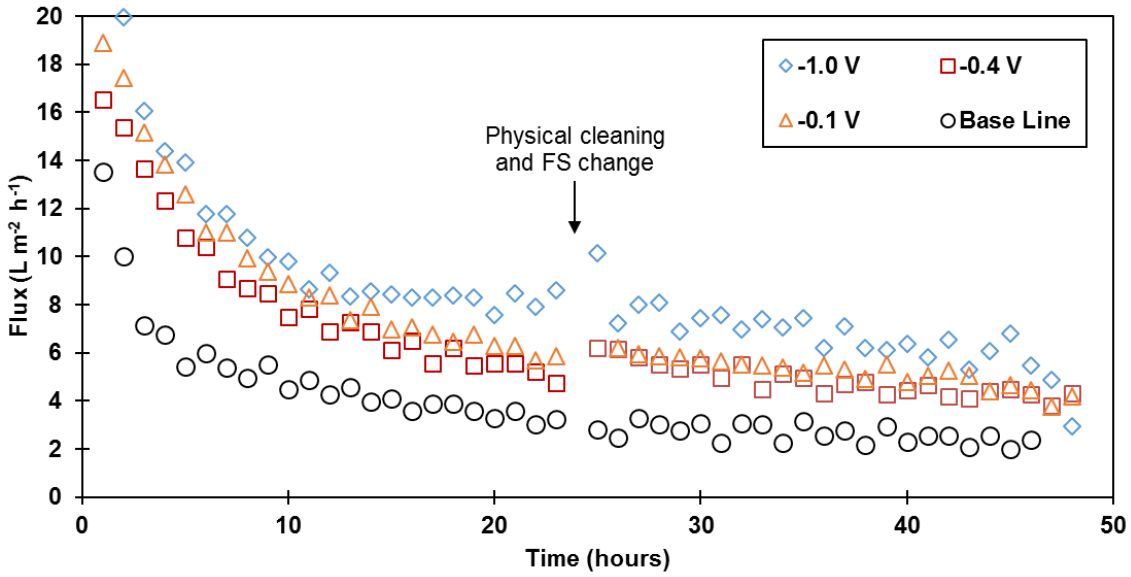

Figure 5-3: Effect of different applied potentials: average flux with a FS of 0.5 g L^{-1} dry algal biomass and a DS of 4 M of NaCl, at a CFV 5.0 cm sec^{-1}, and different applied potentials of -0.1, -0.4 and -1 V with 10 sec intervals on/off. Duration: 48 hours. After 24 hours, FS was changed and physical cleaning (e.g. CFV: 21 cm sec^{-1} for 15 min) was applied. Electrodes: Stainless steel (SS) mesh #40

Effect of electric field patterns on permeate flux

Different patterns of electric fields were tested to see how changing the mode can affect the flux. Particularly, on/off applied electric fields were examined to investigate the effect of pulsing electric current (a beat or frequent repulsion force) on the FO performance, opposed to a continuous repulsion force. Figure 5-4 shows the comparison of flux changes between two different modes of EFFO (pulse [10 sec interval on/off] vs. continuous mode) at two different applied potentials (-0.1 vs. -1.0 V). In general, the higher potential of -1.0 V provided 20-40% more flux than -0.1 V applied potential for both modes. At higher applied electric potential of -1.0 V, the test showed that the continuous mode maintained a higher permeate flux compared to

the intermittent mode (10 sec interval on/off). From Fig. 5-4(a), the continuous applied potential at -1.0 V showed 40 to 60% higher flux (4–5 L m^{-2} h^{-1}), especially for the initial 15 hours. However, after fouling reached a certain point (e.g., 18 hours), the flux was equalized at 8.0 L m^{-2} h^{-1} (Fig. 5-4(a)). Physical cleaning allowed the fouling layer to be rearranged, differentiating the flux with a continuous mode 15 – 25% higher compared to the intermittent mode.

At the lower electric potential of -0.1 V, there was a gradual flux loss trend for both modes (Fig. 5-4(b)). For the initial few hours, it seemed that the low potential was not affected by the change in patterns, but over time, fouling seemed to be further developed in the on/off mode, leading to a drop-in flux without recovery after physical cleaning. After physical cleaning and changing the FS, the flux in the continuous mode showed 10–20% higher flux recovery compared to the intermittent mode.

It was concluded that at higher potential (-1.0V), the mode of the electric field application can be selected based on the design flux, while at lower potential (-0.1V), the flux was similar regardless of the change of the mode, indicating that intermittent mode would be appropriate for improving permeate flux with lower energy requirement.

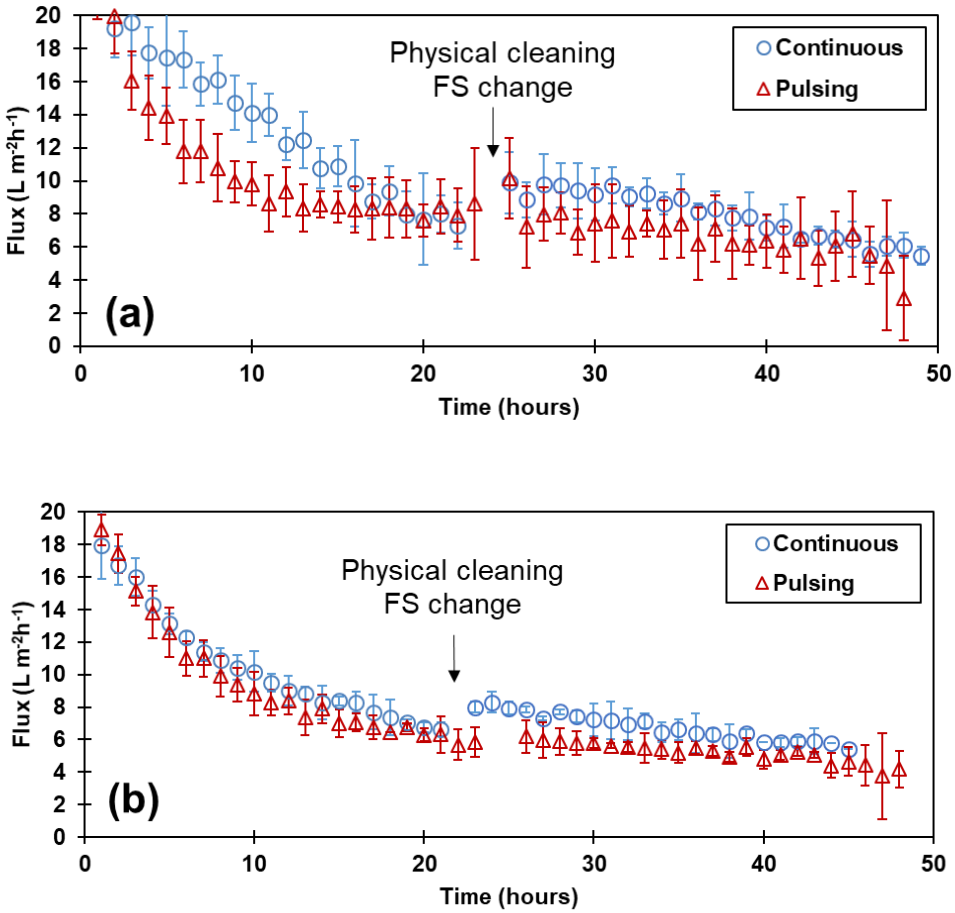

Figure 5-4: Comparison of average flux between pulsing (10 sec intervals on/off) and continuous mode operation of EFFO at the applied potential of (a) -1 V and (b) -0.1 V. for the physical cleaning, the FO system was flushed by increasing the CFV to 21 cm sec^{-1} for 15 minutes.

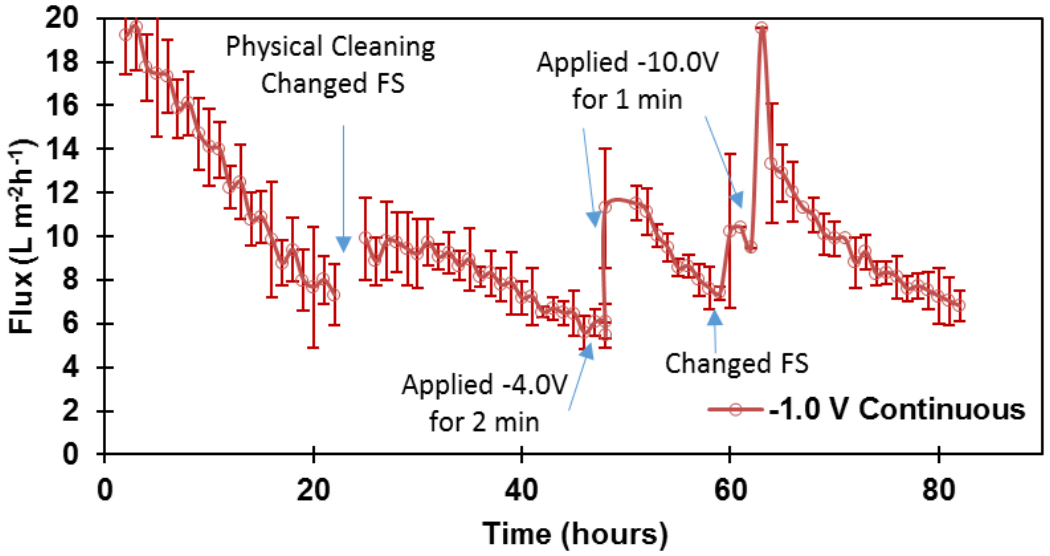

Figure 5-5: The effect of different cleaning methods (physical cleaning vs. extremely high electric potential application on permeate flux recovery; EFFO running continuously under -1.0 V.

Effect of high electric potential on membrane fouling and permeate flux recovery

Different cleaning methods were compared between physical cleaning and extremely high electric potential application on the electrode. A continuous electric potential of -1.0 V was applied for this test. After 24 hours, applying physical cleaning and replacing the FS caused a 15% flux recovery (from 42% to 57% of initial flux) (Fig. 5-5). After about 50 hours of running the EFFO at -1.0V, an extremely high potential of -4.0 V was applied for 2 minutes for the purpose of fouling layer disruption and flux recovery. The short increase of -4.0 V electric potential showed a slight bubble formation (H_2 evolution) on the edge of the anode from electro-hydrolysis, recovering flux 3% (from 30% to 33% of initial flux). In the cathode, a reduction reaction occurred releasing hydrogen gas: $4H^+ + 4e^- \rightarrow 2H_{2(g)}$, while the anode was oxidized, releasing oxygen: $2H_2O - 4e^- \rightarrow O_{2(g)}+4H^+$ (Ursua, Gandia, & Sanchis, 2012). However, there

was no clear observation on detachment of the foulant layer. Then, after 1 hour, another extremely high electric potential was applied at -10.0V for 1 minute and it was observed that H_2 gas bubbles were clearly formed and the foulant/biofoulant layers were peeled off within 30 seconds. The flux was recovered up to about 40%. At 60 hours, a new FS was replaced, and this slightly increased the flux due to lower concentration of the new batch. After 2 hours of the new batch operation, the additional application of -10.0 V improved the flux recovery over 59% (from 40% to 99% of the initial flux). This shows that a short time application of extremely high electric potential of -4 to -10 V can remove the fixed fouling and biofouling layers on the FO membrane that are resistant to removal by physical cleaning.

Portion of the oxidized metals was deposited on the cathode. The presence of the CFV was able to wash the ionic metals released from the anode, allowing the metals to accumulate in the algal FS tank. Figure 5-6 displays the degrading of the anode mesh electrode which happened with extended use. For a durable electric field fouling mitigation and cleaning system, the anode material should be selected to be highly resistant to corrosion and oxidation while being a cost-effective conductive material such as carbon fibers, graphite or silica carbon.

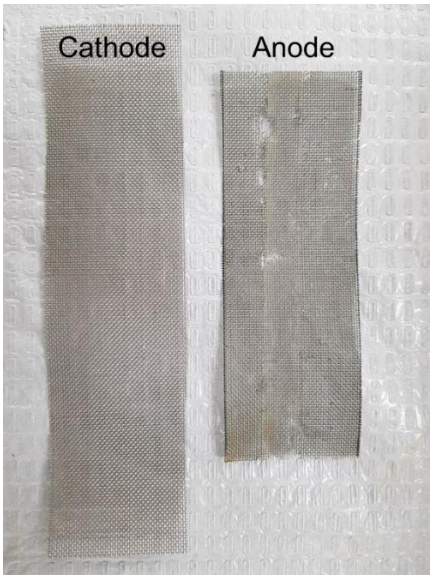

Figure 5-6: Electrodes used in the EFFO system: Running under low and high intensities for about 10 days; The anode releases stainless steel particles due to electrolysis.

Algae characteristics and morphology

pH

The initial pH of the algal FS ranged between pH 10 and 11. Despite running with or without the electric field, the operation of a FO system reduced the initial pH of the FS to 8.5 – 9.5. In the batch experiment runs (Fig. 5-7), pH was also found to decrease with time. The initial pH of the cultivated algal solution was around 10.5, when the algal culture was introduced to the low applied potential (-0.1 and -0.4 V) or contained lower salinity level (equivalent to 0.5 g L^{-1} of NaCl) the pH of the algal solution dropped to about 8.5. The control and the algal solutions that were subjected to a higher electric potential with a higher salinity (equivalent to 2.0 g L^{-1} of NaCl), had a lower impact on pH change from 10.5 to 9.4. In all cases the pH change in the system was in the range which *C. vulgaris* can thrive.

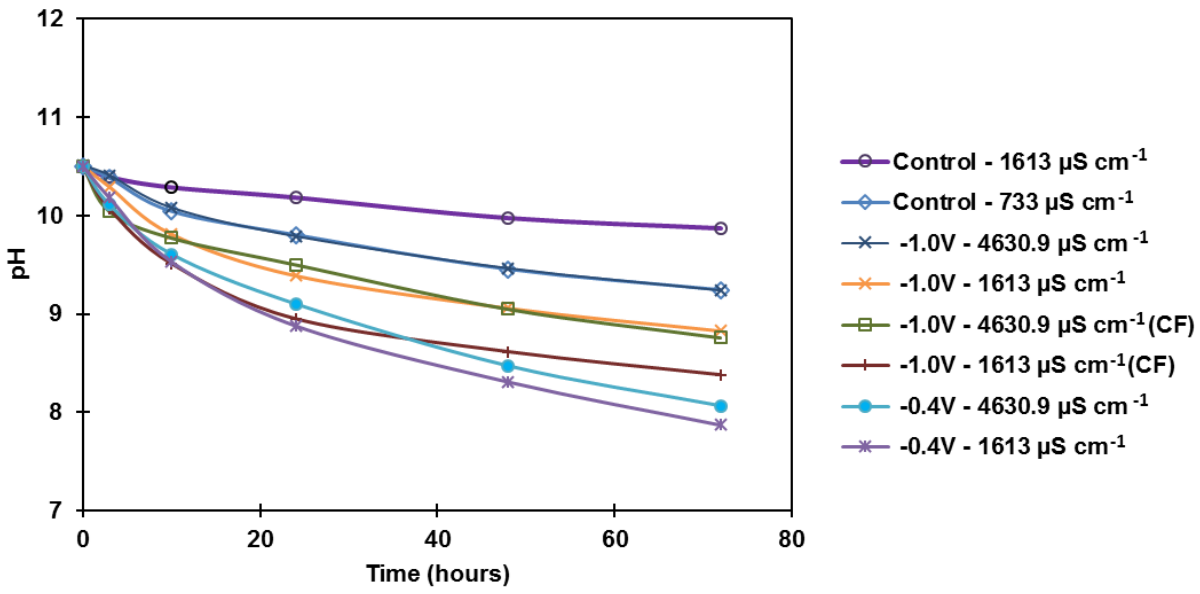

Figure 5-7: pH changes in FS solutions at different applied potentials and salinity levels. The control with a conductivity of 733 µS cm^{-1} was from the photo-bioreactor; the control with the conductivity of 1,613 µS cm^{-1} (conductivity increased by adding NaCl); 1,613 and 4,630 µS cm^{-1} conductivities were used to correspond to potential low and high RSF conductivity levels in an EFFO system. Initial algae concentration was 0.5 g L^{-1} dry algal biomass.

Conductivity

While high DS concentration can increase the osmotic pressure in the EFFO process, the increased osmotic pressure can accelerate RSF (Faris M. Munshi et al., 2018). The initial conductivity of the algal FS was around 800 µS cm^{-1}, after operating a FO system for 24 hours, dewatering and RSF caused conductivity to increase to about 10 mS cm^{-1} in the FS solution. The increased conductivity in the FS solution can reduce the osmotic pressure by 2.14% (e.g., from 19.8 kPa to 19.4 kPa). This change in salinity can not only reduce the flux, but also increase the conductivity of electric current which may affect algal morphology and growth.

In controlled batch experiments running for 72 hours, the effect of conductivity change was measured for different conditions in table 2. In the original algal culture, the conductivity

decreased from 733 µS cm^{-1} to about 670 µS cm^{-1} within two days (Fig. D5). This change can be considered as the baseline where the algal biomass is cultivated in a BBM without aeration (no CO_2 input) and under 11.5-13.5 µmoL m^{-2} s^{-1} PAR of light intensity.

Controlled conductivity levels which represented RSF and dewatering in a FO system, 1,613 µS cm^{-1} (equivalent to 0.5 g L^{-1} of NaCl) and 4,630 µS cm^{-1} (equivalent to 2.0 g L^{-1} of NaCl) were tested with different applied potentials. The higher electric potential of -1.0 V had a loss conductivity effect on the solution by a maximum of 4%. Whereas, the lower applied potentials had a lower degree in conductivity change of about 0-2% (Fig. D6 and D7). These slight change in conductivity were not critical to the growth of algae culture.

Lipid content

The changes of lipid contents in algal biomass can indicate whether the algal species are stressed by the applied electric potentials (Ördög, Stirk, Bálint, van Staden, & Lovász, 2012; Wang, Ullrich, Joo, Waffenschmidt, & Goodenough, 2009). Lipid analyses after two days under EF conditions showed an increase in lipid content along with increase in salinity, and a further increase in lipid content with a higher applied potential (Fig. 5-8). Harvesting *C. vulgaris* in an EFFO system may result in higher lipid in algal biomass contents by stressing the algae cells or improving lipid extraction (Sydney et al., 2018), which are beneficial in biofuel and biodiesel production.

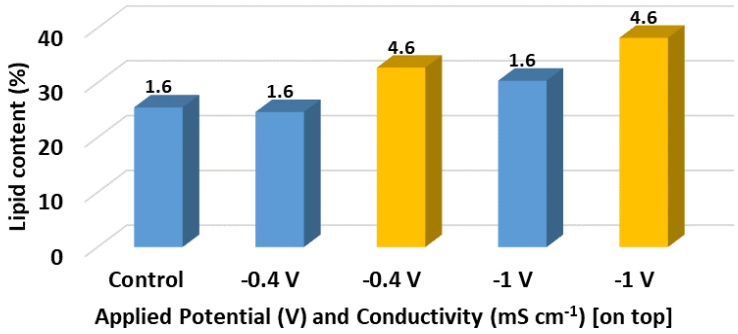

Figure 5-8: Lipid content in the algae culture after being subjected to different electrical fields for 72 hours under different salinity levels.

Settling velocity

Settling velocity is a parameter that was monitored to determine the effect of the EFFO on the algal cells in terms of settleability. This would provide information for a secondary separation stage (e.g., settling basin) which has low operation and maintenance costs. After running the EFFO at a potential of -1.0 V (on/off - 10/10sec) for 24 hours, the volume of the FS (0.5 g L^{-1} dry algae biomass) was 65% dewatered, the settling velocity was reduced from 0.56 m day^{-1} (Sample was from the bioreactor; 0.5 g L^{-1} dry algae biomass) to 0.24 m day^{-1} (Fig. D8). This showed that the increase in algal concentration in addition to other factors like the increase in salinity due to RSF, light intensity change, no aeration and dosing of oxidized metals from the anode can reduce the settleability. For the experiment running on a CFV of 10.7 cm sec^{-1}, the control (no EFFO) had a settling velocity of 0.30 m day^{-1}, as the -0.4 V applied electric potential run had a settling velocity of 0.33 m day^{-1}. The applied electric field can change the settling properties of the algal solution. This showed that the main factor reducing the settling velocity was the increase in algal concentration due to dewatering.

Further batch tests were conducted to find the effect of the electric field on biomass settling. Aggregate or floc formation would develop by a three step mechanism; algae wall charge neutralization, blanket sweep and bridging (Vandamme, Foubert, & Muylaert, 2013; Vandamme, Muylaert, Fraeye, & Foubert, 2014). It was found that there was an increase of settling velocity with the high salinity (conductivity equivalent to 2 g L^{-1} of NaCl) compared to low salinity (conductivity equivalent to 0.5 g L^{-1} of NaCl) (Fig. 5-9). At a low salinity of 0.5 g L^{-1} (1.6 mS cm^{-1}) and a low applied potential of -0.1 V, the algal settling had a settling resistant as algae cell walls maintained a stable charge, which can prevented the natural blanket sweep to occur (Lam, 2017). Large algae cells settled while small algae cells were suspended in the supernatant, compared to the control. The low salinity (0.5 g L^{-1} NaCl) and an applied electric potential of -0.1 V were not ideal conditions with poor algae settling.

At the high potential of -1.0 V while using stainless steel mesh electrodes, the algae promptly sunk to the bottom. The blanket sweep line could not be distinguished from the supernatant. This was due to the metals release form the oxidized anode (i.e. electrocoagulation). The applied potentials of -0.1 and -0.4 V can affect the constituents in the algae solution while the supernatant would have more suspended algae cells (i.e. slight green color) compared to the control and the high applied potential of -1 V.

The two-day period under the batch experimental conditions adversely affected the algae settling characteristics (Fig. 5-10). It was also noticed that algae subjected to a salinity dose can reduce settling characteristics.

Overall the increase in the intensity of the electric field can lead to improving the settling velocity (Fig 5-9). Salinity is also a major factor in improving the settle-ability of the algae cells. From Figure 5-10, it shows that the settling velocity for the unprocessed algae culture was affected with salt addition, but further addition of salt would again increase the settling velocity (Fig. 5-9). The use of -1 V with stainless steel anode can cause electrocoagulation leading to further increase in settle-ability.

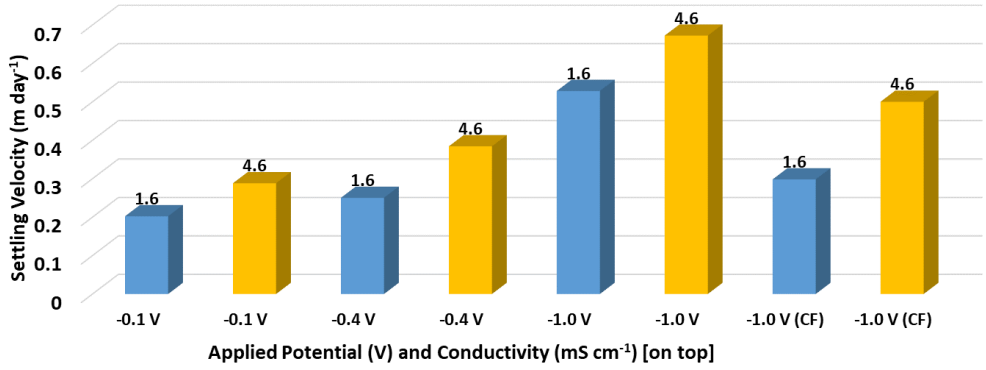

Figure 5-9: Settling velocity after 72 hours for different applied potentials (-0.1, -0.4 and -4.6 V on an algae solution (0.3 g L^{-1} dry algae biomass) with a conductivity of 1,630 and 4,630.9 µS cm^{-1} (equivalent to 0.5 and 2.0 mg L^{-1} of NaCl, respectively).

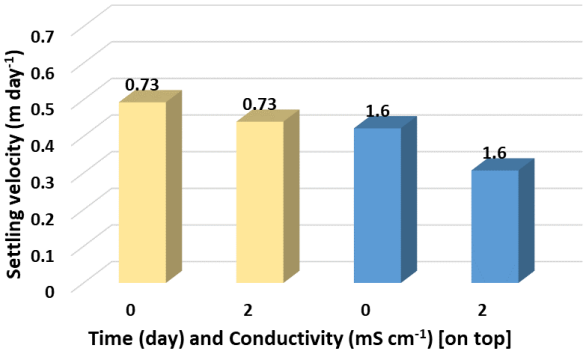

Figure 5-10: Settling velocity for algae solution (0.3 g L^{-1} dry algae biomass) at day 0 and after 3 days, with a conductivity of 730 and 1630 µS cm^{-1}.

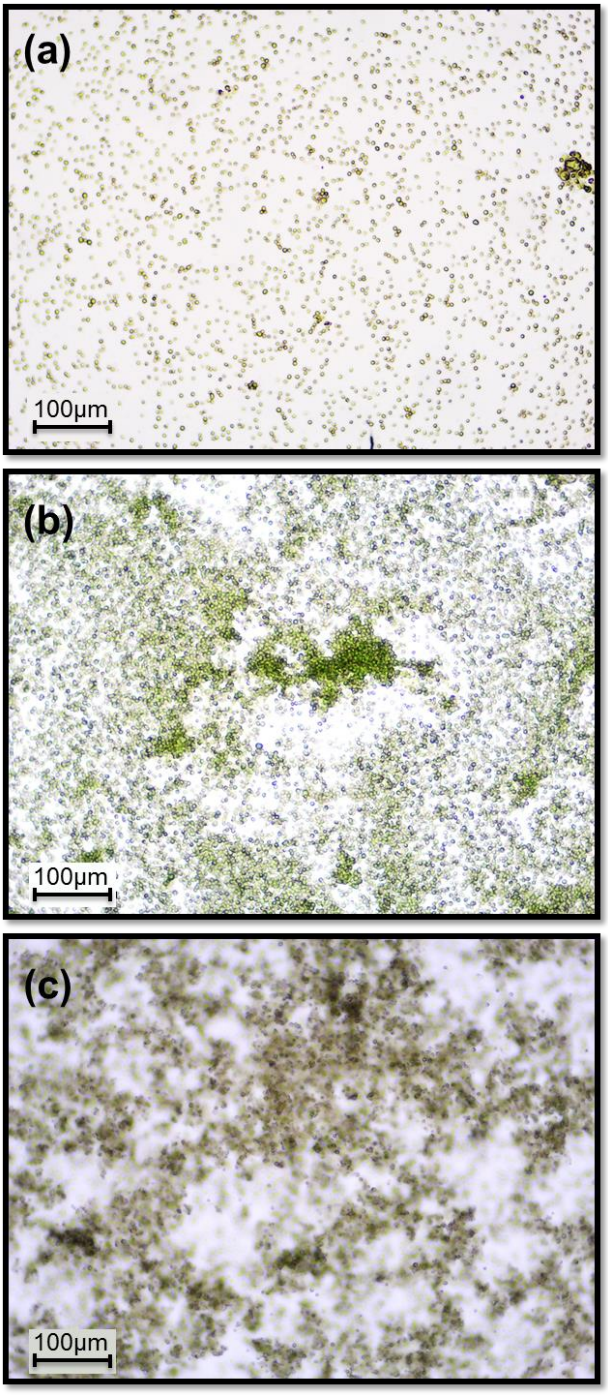

Figure 5-11: Microscopic imaging of the feed solution after algal dewatering; (a) Dewatering in a FO system, (b) EFFO dewatering under a potential of -0.4 V (on/off - 10/10sec), and (c) EFFO dewatering under a potential of -1.0 V (on/off - 10/10sec)

Microscopic images of the effect of the electric field on algae

Microscopic images of the algal biomass in a control (no EFFO) and EFFO algal biomass were examined under a microscope. The samples collected from the control FO system showed suspended algal cells that were scattered with rare formation of algal aggregates after 48 hours of dewatering (Fig 5-11(a)). The EFFO algal samples (-0.4 V, on/off - 10/10sec) showed the tendency to form algal aggregates (Fig 5-11(b)), this can be considered as a side reaction of the applied electric field (e.g. electrocoagulation or electrochemical-coagulation). The passing electric current had disturbed the outer charges on the algal cells and promote agglomeration (Lam, 2017; Vandamme, Foubert, Meesschaert, & Muylaert, 2010). When running the EFFO dewatering under the potential of -1.0 V (on/off - 10/10sec) (Fig 5-11(c)), the color of the algae turned brownish-green and under the microscope, the algal cells showed aggregates and floc formations of algae with metallic particles released from the stainless-steel anode.

In an attempt to further study the effect of the electric field on the algal solution, separate batch tests were conducted with different electric potentials (-0.1, -0.4 and -1.0 V) and conductivity levels (1,613 and 4,630.9 µS cm^{-1}). The electrode type unless other stated was a SS mesh. Fig D9 shows the experimental setup and visual images of each batch after 48 hours application. With -1 V with high and low salinity, dissolved metals have changed the color of the algae culture which may results in the contamination of the final algae product. It was found that the algae cells in the control had healthy algae cells throughout the 48 hours (Figures D10(a)). At the applied electric potential of -0.1 V and conductivity of 1,613 µS cm^{-1}, the algae morphology was similar to the control with no abnormalities (Figures D10(b)), but with an increase of salt concentration with a conductivity of 4630.9 µS cm^{-1}, the aggregate formation was present in low

a frequency (Figures D10(c)). With an increase in the applied electric potential to -0.4 V and with the higher conductivity level, there was occurrences of lysed algae cells (Figures D10(d)).

At the high applied potential of -1.0 V with both conductivity levels, cells lysing was visible with higher occurrence in the high conductivity level (Figures D10(e) and (f)). With the higher potential and higher salinity, algae deterioration was accelerated. After 10 hours, floc formation was observed and after 24 hours there was clear change in the color of the solution (greenish brown). The conditions promoted algae cells to lyse and release organelles. This can affect the quality of the algae. While the electrochemical reaction added SS particles to the solution which can promote settling of the algae cells, the high potential and salinity can also assist in the breakdown of the cell's membrane wall leading to the release of the lipids (Figures D10(f)).

When carbon fiber sheet anodes were used to develop the electric field, the high potential of -1 V with low salinity had a minor impact on the algae cells. Visible lysis or algae organelles were not observed. The algae cells were spread from each other indicating a development of a charge build up around the algae cells (Figures D10(g)). With the higher salinity, the algae cells were also spread out from each other. There were some cells that appeared to be lysed. The organelles (soluble intracellular matter) assisted in the formation of grouped algae cells (Carullo et al., 2018; Goettel, Eing, Gusbeth, Straessner, & Frey, 2013). In this case, the carbon fiber anode did not chemically react with solution which reduced the level of change in the algal product (e.g., lysis, floc formation, introducing chemicals by electrolysis) (Figures D10(h)).

Conclusions

This modified FO system coupled with an electric field was able to increase the permeate flux and the flux recovery. The EFFO algae was able to reduce fouling formation in addition to altering algae characteristics. Overall the higher applied potential produced higher flux.

The settling velocity increased with the increase in salinity. It was found that higher potentials and higher salinity can provide better conditions to promote algae settling. The algae can attach to the oxidized particles from the anode and form aggregates of dense algae that promote algae settling. Furthermore, the EFFO system can stress the algae culture affecting lipid content in the algae cell. The anode can degrade with time, further control measures can be addressed to control the quality of the final product. Novel inert anode material is required to reduce cost and control the addition of metal ions in the solution. This can be done using carbon-based anode electrodes. High applied potential with high salinity can cause algae cell lyses, leading to release intercellular cell matter that can contribute in algae cell aggregate formation. Lipid content was found to also increase, possibly from the added stress and enhanced extraction applied from the electric field.

References

Ahmad, A., Yasin, N. M., Derek, C., & Lim, J. (2011). Microalgae as a sustainable energy source for biodiesel production: a review. *Renewable and Sustainable Energy Reviews*, *15*(1), 584-593.

Akamatsu, K., Lu, W., Sugawara, T., & Nakao, S.-i. (2010). Development of a novel fouling suppression system in membrane bioreactors using an intermittent electric field. *Water Research, 44*(3), 825-830.

Alfafara, C. G., Nakano, K., Nomura, N., Igarashi, T., & Matsumura, M. (2002). Operating and scale-up factors for the electrolytic removal of algae from eutrophied lakewater. *Journal of*

Chemical Technology & Biotechnology: International Research in Process, Environmental & Clean Technology, 77(8), 871-876.

Bani-Melhem, K., & Elektorowicz, M. (2011). Performance of the submerged membrane electro-bioreactor (SMEBR) with iron electrodes for wastewater treatment and fouling reduction. *Journal of Membrane Science, 379*(1-2), 434-439.

Bechhold, H. (1904). Die Ausflockung von Suspensionen bzw. Kolloiden und die Bakterienagglutination. *Zeitschrift für Physikalische Chemie, 48*(1), 385-423.

Bligh, E. G., & Dyer, W. J. (1959). A rapid method of total lipid extraction and purification. *Canadian journal of biochemistry and physiology, 37*(8), 911-917.

Buckwalter, P., Embaye, T., Gormly, S., & Trent, J. D. (2013). Dewatering microalgae by forward osmosis. *Desalination, 312*, 19-22. doi:http://dx.doi.org/10.1016/j.desal.2012.12.015

Carullo, D., Abera, B. D., Casazza, A. A., Donsì, F., Perego, P., Ferrari, G., & Pataro, G. (2018). Effect of pulsed electric fields and high pressure homogenization on the aqueous extraction of intracellular compounds from the microalgae Chlorella vulgaris. *Algal Research, 31*, 60-69. doi:https://doi.org/10.1016/j.algal.2018.01.017

Chang, I.-S., Le Clech, P., Jefferson, B., & Judd, S. (2002). Membrane fouling in membrane bioreactors for wastewater treatment. *Journal of Environmental Engineering, 128*(11), 1018-1029.

Goettel, M., Eing, C., Gusbeth, C., Straessner, R., & Frey, W. (2013). Pulsed electric field assisted extraction of intracellular valuables from microalgae. *Algal Research, 2*(4), 401-408. doi:https://doi.org/10.1016/j.algal.2013.07.004

Hwang, J.-H., Church, J., Lim, J., & Lee, W. H. (2018). Photosynthetic biohydrogen production in a wastewater environment and its potential as renewable energy. *Energy, 149*, 222-229. doi:https://doi.org/10.1016/j.energy.2018.02.051

Kline, L. M., Hayes, D. G., Womac, A. R., & Labbe, N. (2010). Simplified determination of lignin content in hard and soft woods via UV-spectrophotometric analysis of biomass dissolved in ionic liquids. *BioResources, 5*(3), 1366-1383.

Lam, G. P. t. (2017). *Harvesting and Cell Disruption of Microalgae.* Wageningen University & Research, Retrieved from https://www.wur.nl/en/activity/Harvesting-and-Cell-Disruption-of-Microalgae-1.htm

Liu, J., Liu, L., Gao, B., & Yang, F. (2012). Cathode membrane fouling reduction and sludge property in membrane bioreactor integrating electrocoagulation and electrostatic repulsion. *Separation and Purification Technology, 100*, 44-50.

Liu, L., Liu, J., Gao, B., & Yang, F. (2012). Minute electric field reduced membrane fouling and improved performance of membrane bioreactor. *Separation and Purification Technology, 86*, 106-112.

Liu, L., Liu, J., Gao, B., Yang, F., & Chellam, S. (2012). Fouling reductions in a membrane bioreactor using an intermittent electric field and cathodic membrane modified by vapor phase polymerized pyrrole. *Journal of Membrane Science, 394*, 202-208.

Mi, B., & Elimelech, M. (2010a). Gypsum Scaling and Cleaning in Forward Osmosis: Measurements and Mechanisms. *Environmental Science & Technology, 44*(6), 2022-2028. doi:10.1021/es903623r

Mi, B., & Elimelech, M. (2010b). Organic fouling of forward osmosis membranes: Fouling reversibility and cleaning without chemical reagents. *Journal of Membrane Science, 348*(1–2), 337-345. doi:http://dx.doi.org/10.1016/j.memsci.2009.11.021

Munshi, F. M., Church, J., McLean, R., Maier, N., Sadmani, A. A., Duranceau, S. J., & Lee, W. H. (2018). Dewatering algae using an aquaporin-based polyethersulfone forward osmosis membrane. *Separation and Purification Technology, 204*, 154-161.

Munshi, F. M., Church, J., McLean, R., Maier, N., Sadmani, A. H. M. A., Duranceau, S. J., & Lee, W. H. (2018). Dewatering algae using an aquaporin-based polyethersulfone forward osmosis membrane. *Separation and Purification Technology, 204*, 154-161. doi:https://doi.org/10.1016/j.seppur.2018.04.077

Ördög, V., Stirk, W. A., Bálint, P., van Staden, J., & Lovász, C. (2012). Changes in lipid, protein and pigment concentrations in nitrogen-stressed Chlorella minutissima cultures. *Journal of Applied Phycology, 24*(4), 907-914. doi:10.1007/s10811-011-9711-2

Oukarroum, A., Bras, S., Perreault, F., & Popovic, R. (2012). Inhibitory effects of silver nanoparticles in two green algae, Chlorella vulgaris and Dunaliella tertiolecta. *Ecotoxicology and Environmental Safety, 78*, 80-85. doi:https://doi.org/10.1016/j.ecoenv.2011.11.012

Pahl, S. L., Lee, A. K., Kalaitzidis, T., Ashman, P. J., Sathe, S., & Lewis, D. M. (2013). Harvesting, thickening and dewatering microalgae biomass. In *Algae for biofuels and energy* (pp. 165-185): Springer.

Rosenhahn, A., Finlay, J. A., Pettit, M. E., Ward, A., Wirges, W., Gerhard, R., . . . Callow, J. A. (2009). Zeta potential of motile spores of the green alga Ulva linza and the influence of electrostatic interactions on spore settlement and adhesion strength. *Biointerphases, 4*(1), 7-11.

Sing, S. F., Isdepsky, A., Borowitzka, M., & Lewis, D. (2014). Pilot-scale continuous recycling of growth medium for the mass culture of a halotolerant Tetraselmis sp. in raceway ponds under

increasing salinity: a novel protocol for commercial microalgal biomass production. *Bioresource Technology, 161*, 47-54.

Son, J., Sung, M., Ryu, H., Oh, Y.-K., & Han, J.-I. (2017). Microalgae dewatering based on forward osmosis employing proton exchange membrane. *Bioresource Technology*, *244*, 57-62. doi:https://doi.org/10.1016/j.biortech.2017.07.086

Stein, J. R. (1979). *Handbook of phycological methods: culture methods and growth measurements* (Vol. 1): CUP Archive.

Sydney, T., Marshall-Thompson, J.-A., Kapoore, R., Vaidyanathan, S., Pandhal, J., & Fairclough, J. (2018). The Effect of High-Intensity Ultraviolet Light to Elicit Microalgal Cell Lysis and Enhance Lipid Extraction. *Metabolites, 8*(4), 65.

Ursua, A., Gandia, L. M., & Sanchis, P. (2012). Hydrogen production from water electrolysis: current status and future trends. *Proceedings of the IEEE, 100*(2), 410-426.

v Zumbusch, P., Kulcke, W., & Brunner, G. (1998). Use of alternating electrical fields as anti-fouling strategy in ultrafiltration of biological suspensions–Introduction of a new experimental procedure for crossflow filtration. *Journal of Membrane Science, 142*(1), 75-86.

Valladares Linares, R., Yangali-Quintanilla, V., Li, Z., & Amy, G. (2012). NOM and TEP fouling of a forward osmosis (FO) membrane: Foulant identification and cleaning. *Journal of Membrane Science, 421–422*, 217-224. doi:http://dx.doi.org/10.1016/j.memsci.2012.07.019

Vandamme, D., Foubert, I., Meesschaert, B., & Muylaert, K. (2010). Flocculation of microalgae using cationic starch. *Journal of Applied Phycology, 22*(4), 525-530.

Vandamme, D., Foubert, I., & Muylaert, K. (2013). Flocculation as a low-cost method for harvesting microalgae for bulk biomass production. *Trends in Biotechnology, 31*(4), 233-239.

Vandamme, D., Muylaert, K., Fraeye, I., & Foubert, I. (2014). Floc characteristics of Chlorella vulgaris: influence of flocculation mode and presence of organic matter. *Bioresource Technology, 151*, 383-387.

Wang, Z. T., Ullrich, N., Joo, S., Waffenschmidt, S., & Goodenough, U. (2009). Algal Lipid Bodies: Stress Induction, Purification, and Biochemical Characterization in Wild-Type and Starchless <em>Chlamydomonas reinhardtii</em&gt. *Eukaryotic Cell, 8*(12), 1856. doi:10.1128/EC.00272-09

Yeh, K.-L., & Chang, J.-S. (2012). Effects of cultivation conditions and media composition on cell growth and lipid productivity of indigenous microalga Chlorella vulgaris ESP-31. *Bioresource Technology, 105*, 120-127. doi:https://doi.org/10.1016/j.biortech.2011.11.103

CHAPTER 6: CONCLUSION

Forward osmosis (FO) showed the ability to produce clean water and concentrate the algal solution with low energy requirements. Through the works done, a better understanding of algae dewatering was determined when using a novel and specific aquaporin PES membrane. Different natural solutions were used as draw solutions under different CFVs. The effect of the RSF from the FO system on the algae was evaluated. Furthermore, a novel electrical field fouling mitigation system was embedded and evaluated in the FO system. The effect of the electrical field was evaluated on the FO dewatering efficiency and the algae culture.

When harvesting algae using the aquaporin FO membrane, it was found that the osmotic pressure gradient in the FO system provided a driving force for the dewatering process. This gives high potential for FO to be used as for algae dewatering aimed for biofuel production. In a short term, the increase in CFVs from 1.5 to 10.7 cm sec^{-1} was able to increase the average permeate flux by 5–10% depending on the DSs tested in this study. The accumulation of *C. vulgaris* microalgae on the surface had a minimal impact on flux throughout the duration of 8-hour experiment. The increase of DS concentration from 0.5–0.6 to 1.0 M increased the flux by 85.5% for NH_4Cl, whereas for NaCl and KCl the flux increase was only 47.3 and 33.2%, respectively. In the continuous long-term run, while the fluxes declined with time, sudden recovery of flux was periodically observed, which may be attributed to dislodging of relatively 'loose' layers of algal biofilm without additional cleaning processes.

Chlorella vulgaris microalgae which was subjected to low doses of salts within short time frames which simulated RSF in a FO system showed algal morphological and

compositional changes. The introduction of the different salts caused C. *vulgaris* to inhibit growth and photosynthesis. Although growth was limited, the lipid increased. The settling velocity of the algae feed solution was found to increase with the increase of the salt content. NH_4Cl caused the algae solution to accelerate cell division which hindered algae settling.

The electric field forward osmosis (EFFO) configuration was found to successfully increase the permeate flux and the flux recovery. Water flux was maintained and fouling formation was reduced. It was found that as the applied potential increased the produced flux increased. The application of a high potential of -10 V for 60 seconds was able to remove fouling/biofouling from the surface of the membrane with about 99% flux recovery.

With a low salinity of 0.5 g L^{-1} and low applied potential of -0.1 V, the algae settling had settling resistant from electrostatic charge build up on the surface of the particles. The increase in the applied potentials was able to improve algae settling. The high applied potential of -1.0 V caused oxidized particles to be released from the anode, which worked as an electrochemical coagulant that helped form groups of dense algae. The EFFO system was found to also stress the algae culture and increasing lipid content. Lyse algae cells were observed (-1 V and 4,631 µS cm^{-1}) when the stainless steel (SS) anode was used, this also led to the release of organelles and lipids from the algal cell which had contribute in aggregate algae formation and lipid extraction.

CHAPTER 7: IMPACTS AND OUTLOOK

This study provided a better understanding of the capabilities of an aquaporin FO membrane in terms of *Chlorella vulgaris* microalgae harvesting using natural draw solutions that can further be recycled and reused after dilution. The effect of reverse salts flux in the FO system on the microalgae was also analysed in terms of changes in pH, conductivity, algal cell growth, lipid accumulation, settling velocity and algae cell morphology. In addition, the incorporating of an electric field in a FO system was found to have high potential in fouling control. The novel EFFO system also has the capacity to recover flux by applying a high electric field intensity for short periods. Furthermore, the applied electric potential, the type of DS, and electrode material were found modify the quality of the algae product.

Future works can be suggested on enhancing FO membrane (e.g., antibacterial TiO_2 coating) or other commercial and lab made FO membranes can be tested for compatibility for algae dewatering. Further attempts can be approached for FO membrane cleaning to mitigate fouling and concentration polarization, while maintaining permeate flux like using continuous and pulsing vibrating FO cells.

Additional analyses can be implemented by monitoring algal cell components (e.g., protein, carbohydrates and lipid content) in a continuous FO operation, with microbial fatty acid profiles and amino acid composition analyses to determine the optimal algae use as a product.

Extended runs with different CFV can be examined for economic and durable conditions in terms of washing frequency and FO life span. Also, systematic cleaning needs to be further studied using high electrical potentials (-5 to -10 V). Novel anode materials are recommended to

reduce cost and control any metal ions releases in the system. This can be done using carbon-based anode electrodes. Lastly, the effect of DS and applied potential can be further studied for different microalgae specie in relation to cell constituents and morphology.

APPENDIX A: COPYRIGHT USE OF PUBLISHED MANUSCRIPTS

From the Elsevier author and user right - web page:
https://www.elsevier.com/__data/assets/pdf_file/0007/55654/AuthorUserRights.pdf

AUTHOR AND USER RIGHTS

INTRODUCTION

Elsevier requests transfers of copyright, or in some cases exclusive rights, from its journal authors in order to ensure that we have the rights necessary for the proper administration of electronic rights and online dissemination of journal articles, authors and their employers retain (or are granted/transferred back) significant scholarly rights in their work. We take seriously our responsibility as the steward of the online record to ensure the integrity of scholarly works and the sustainability of journal business models, and we actively monitor and pursue unauthorized and unsubscribed uses and re-distribution (for subscription models).

In addition to authors' scholarly rights, anyone who is affiliated with an institution with a journal subscription can use articles from subscribed content under the terms of their institution's license, while there are a number of other ways in which anyone (whether or not an author or subscriber) can make use of content published by Elsevier, which is free at the point of use or accessed under license.

Author Rights

As a journal author, you have rights for a large range of uses of your article, including use by your employing institute or company. These rights can be exercised without the need to obtain specific permission.

How authors can use their own journal articles

Authors publishing in Elsevier journals have wide rights to use their works for teaching and scholarly purposes without needing to seek permission.

Table of Author's Rights

	Preprint version (with a few exceptions- see below *)	Accepted Author Manuscript	Published Journal Articles
Use for classroom teaching by author or author's institution and presentation at a meeting or conference and distributing copies to attendees	Yes	Yes	Yes
Use for internal training by author's company	Yes	Yes	Yes
Distribution to colleagues for their research use	Yes	Yes	Yes
Use in a subsequent compilation of the author's works	Yes	Yes	Yes
Inclusion in a thesis or dissertation	Yes	Yes	Yes

APPENDIX B: SUPPLEMENTAL INFORMATION: DEWATERING ALGAE USING AN AQUAPORIN-NASED POLYETHERSULONE FORWARD OSMOSIS MEMBRANE

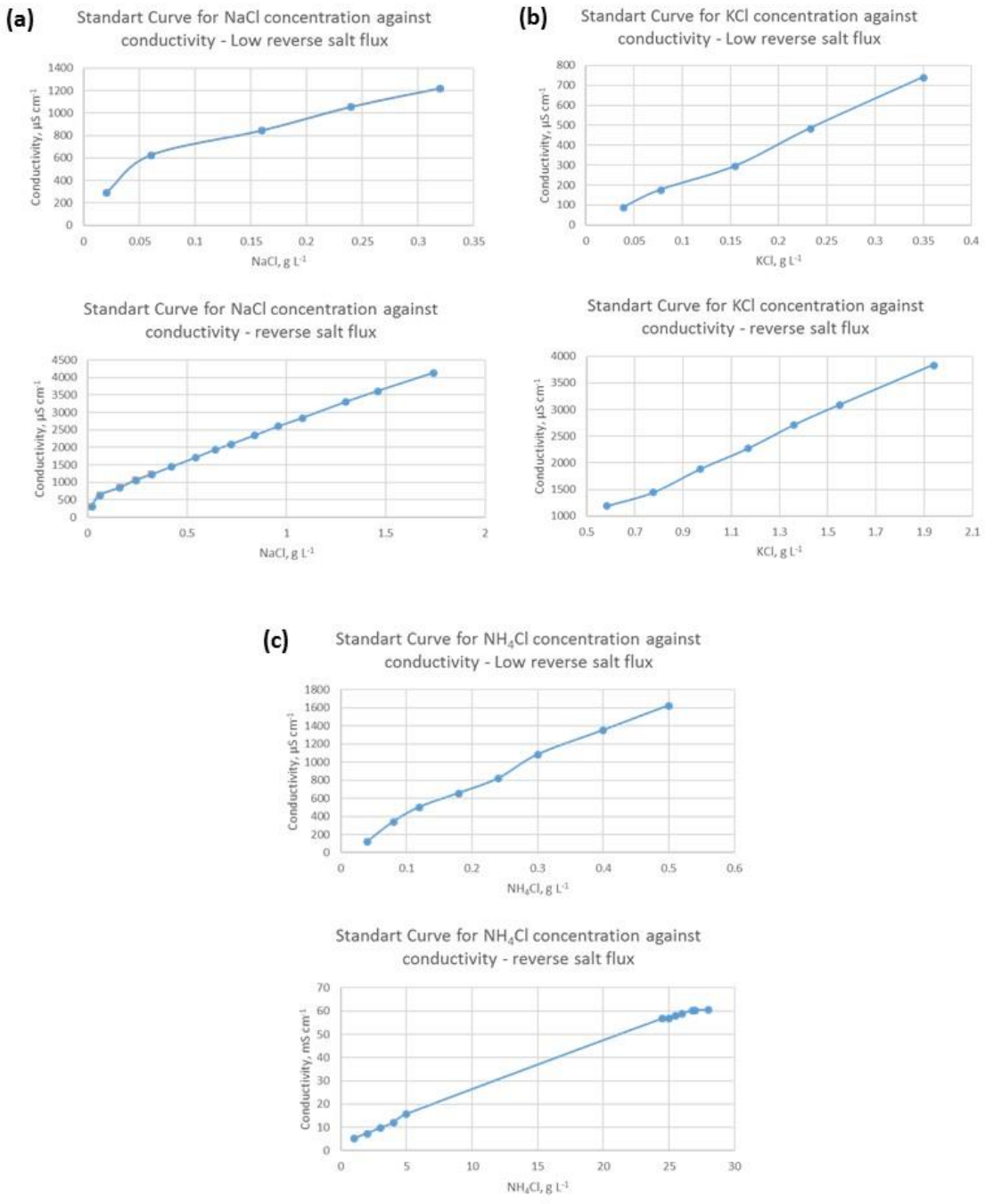

Figure. B1. Standard curves for conductivity with various concentrations of (a) NaCl, (b) KCl and (c) NH_4Cl. Low range of salt concentrations was used to determine the concentration of reverse salt flux, while high range of the concentrations was used for calibration for the conductivity of DS.

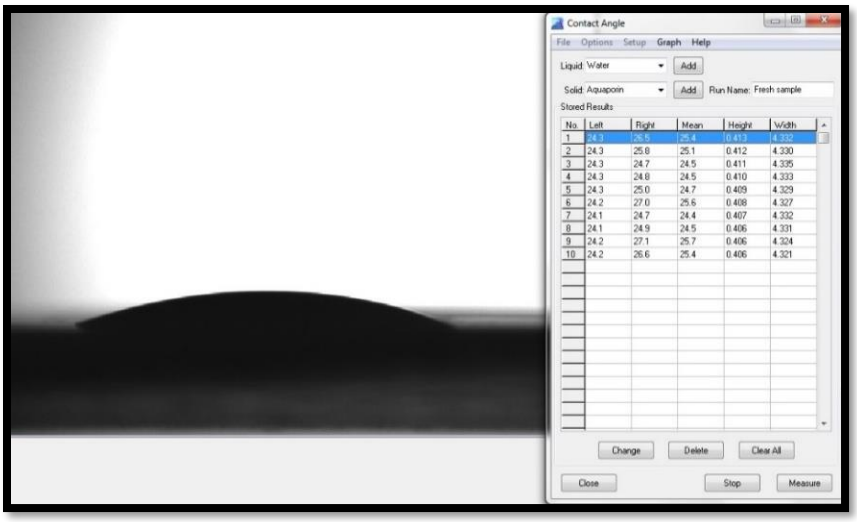

Figure. B2. Contact angle using a sessile drop method on a fresh FO membrane – active layer side.

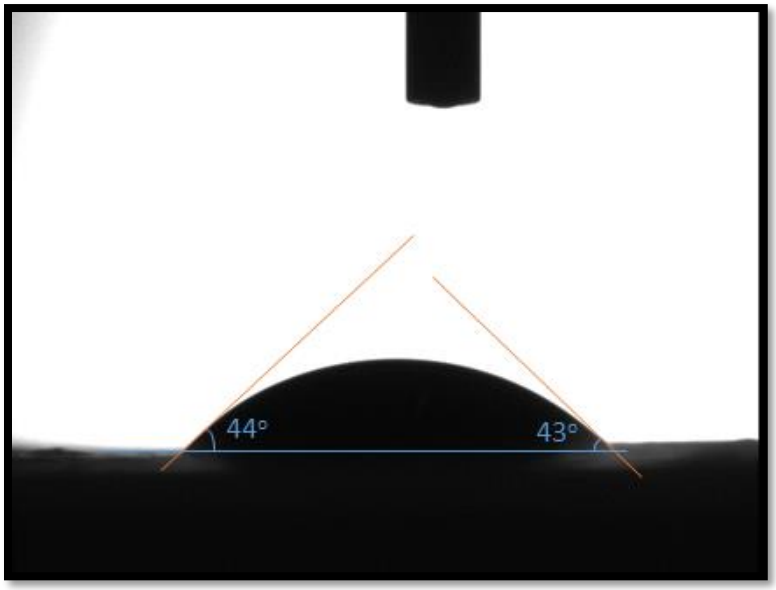

Figure. B3. Contact angle using a sessile drop method for a FO membrane fouled with algae – active layer side.

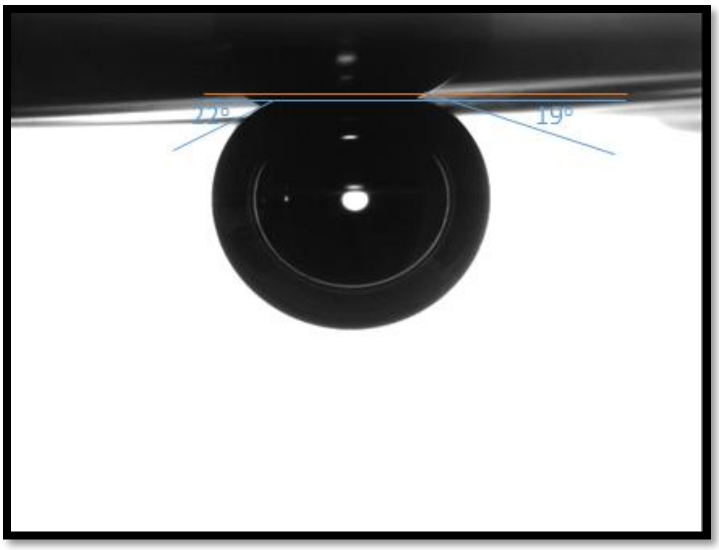

Figure. B4. Contact angle using a captive bubble technique for a fresh FO membrane – PES support side.

Sessile drop and captive bubble methods for contact angle measurement

The sessile drop method is the common method used to measure contact angle. It is measured using a horizontal cell to hold the membrane. A micro-pipette is used to drop DI water on the membrane. The measurement of the contact angle is analyzed by a software (DROPimage Advanced, Rame-hart instrument Co.) after applying a light source and capturing the image using a telescopic camera. In the captive bubble method, and air bubble is used. The membrane is submersed upside down and the air bubble is injected using a U-shape micro-pipette. The angle created by the air bubble and the membrane is recorded by the telescopic camera and analyzed by the software [1].

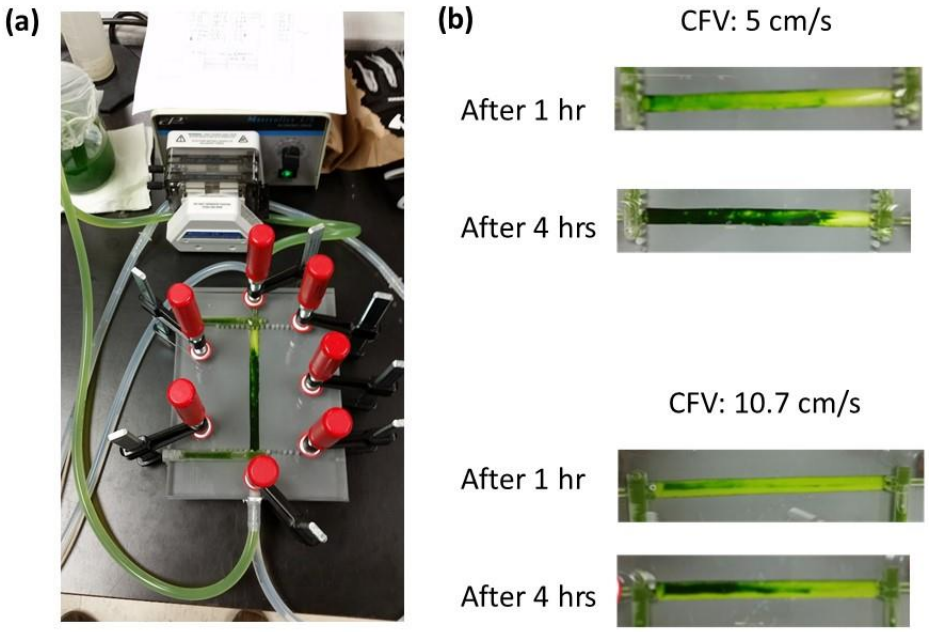

Figure. B5. (a) Photographs of a FO membrane separation unit and (b) the visual observation of temporal algal biomass build ups on the FO membrane surface with different CFVs.

Table B1: Comparing literature that used FO membranes (i.e. HTI) to dewater algae. The focus in the comparison starts with similar DS types and concentrations, in addition to the FS being microalgae.

Membrane type	Membrane manufacturer	Flux, L m^{-2} h^{-1}	Reverse salt flux, g m^{-2} h^{-1}	CFV, cm sec^{-1}	Dimensions	Membrane surface area, cm^2	DS	FS	Dewatering reached	Reference
X-Pack Hydration bags: Cellulose triacetate	Hydration Technology Innovations, HTI (Albany, OR, USA)	2.2	Not reported	Bath mode	250 mL	90.0	750 mL of 0.6 M NaCl (35 g L^{-1})	*Chlorella vulgaris*; 250 mL, 0.5 - 2 g L^{-1} in BG-11	87%	[2]
Cellulose triacetate (CTA) membrane		16.0		22.3	Not reported	29.2	0.5 M of NaCl	*Chlorella sorokiniana*; 0.1 g L^{-1} with a total ionic strength 10 mM	-	[3]
		27.0					1 M of NaCl		-	
		6.7 - 10.0		9.6	Commercial FO spiral wound module	200.0	6 L of 1.2 M NaCl (70 g L^{-1})	*Scenedesmus obliquus*; 1 L, 0.2 g L^{-1} of algae suspension	75%	[4]
		7.0		9.6	Not reported	Not reported	6 L of 1.2 M NaCl	*Scenedesmus obliquus*; 1 L, 0.2 g L^{-1} of algae suspension	75%	[5]
Aquaporine active layer with a PES support layer	Aquaporine™, (Kongens Lyngby, Danmark)	5.2	0.66	5.0	1 cm [W] × 12.5 cm [L] × 0.3 cm [H]	12.5	15 L of 0.6 M NaCl	*Chlorella vulgaris*; 500 mL of 1 g L^{-1} dry algae biomass	81%	This work
		7.7	0.75				15 L of 1 M NaCl			

References

1. Yuan, Y. and T.R. Lee, *Contact angle and wetting properties*, in *Surface science techniques*. 2013, Springer. p. 3-34.
2. Buckwalter, P., et al., *Dewatering microalgae by forward osmosis.* Desalination, 2013. **312**: p. 19-22.
3. Zou, S., et al., *Direct microscopic observation of forward osmosis membrane fouling by microalgae: Critical flux and the role of operational conditions.* Journal of Membrane Science, 2013. **436**: p. 174-185.
4. Larronde-Larretche, M. and X. Jin, *Microalgae (Scenedesmus obliquus) dewatering using forward osmosis membrane: Influence of draw solution chemistry.* Algal Research, 2016. **15**(Supplement C): p. 1-8.
5. Larronde-Larretche, M. and X. Jin, *Microalgal biomass dewatering using forward osmosis membrane: Influence of microalgae species and carbohydrates composition.* Algal Research, 2017. **23**(Supplement C): p. 12-19.

APPENDIX C: SUPPLEMENTAL INFORMATION: REVERSE SALT FLUX EFFECT ON *CHLORELLA VULGARIS* IN A FORWARD OSMOSIS SYSTEM

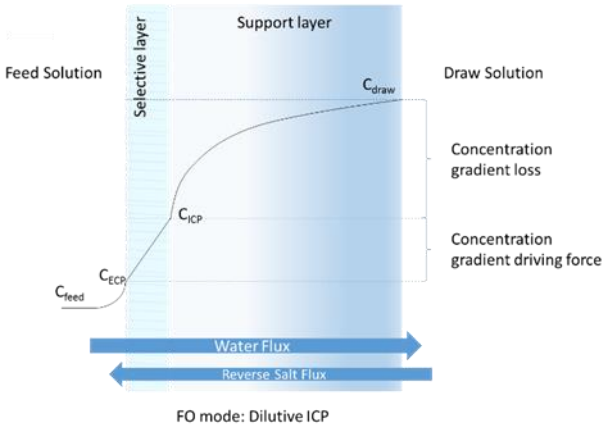

Figure C1: Permeate flux and reverse salt flux on a FO membrane configuration. Internal and external concentration polarization (ICP and ECP) in a FO membrane selective layer FO.

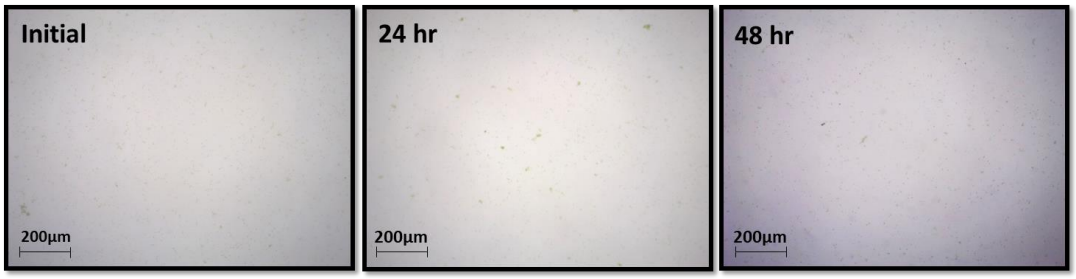

a) Microscopic imaging: 100 time magnification; for the original algae culture.

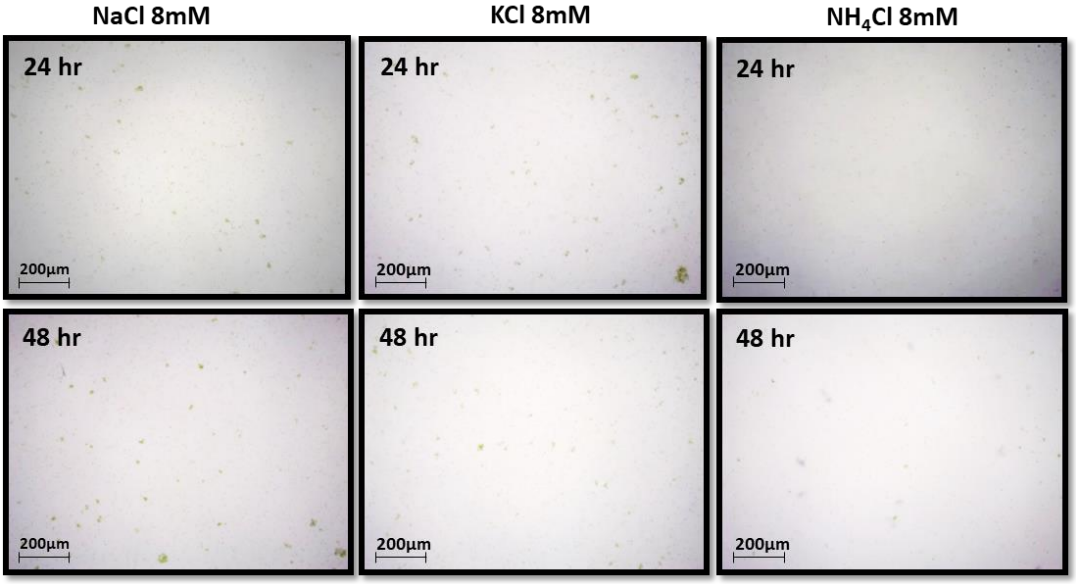

b) Microscopic imaging: 100 time magnification; Salt dose of NaCl, KCl and NH_4Cl of 8 mM after 24 and 48 hours.

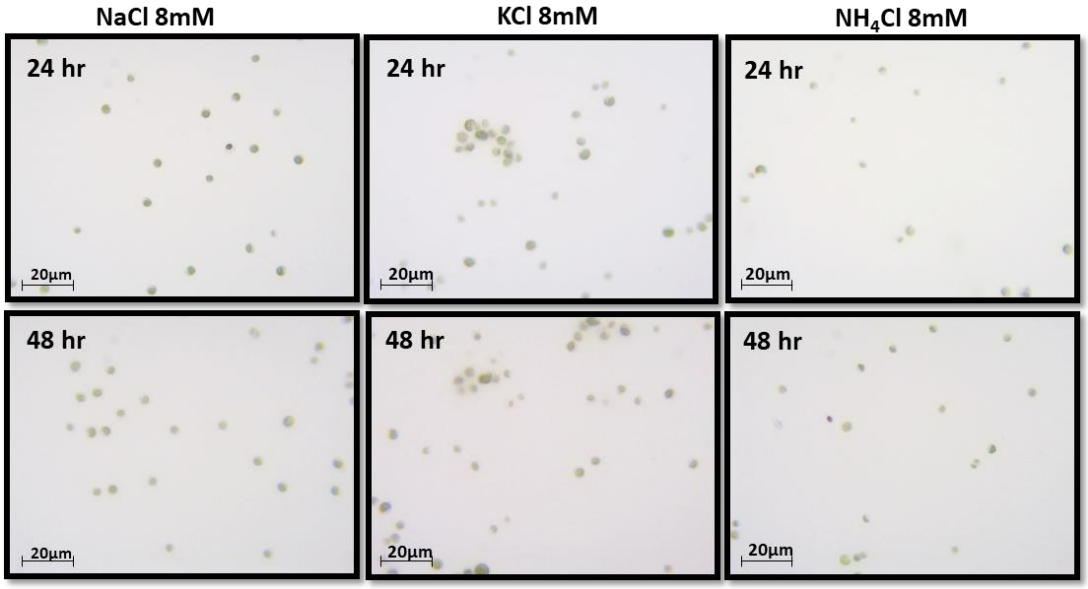

c) Microscopic imaging: 1,000 time magnification; Salt dose of NaCl, KCl and NH_4Cl of 8 mM after 24 and 48 hours.

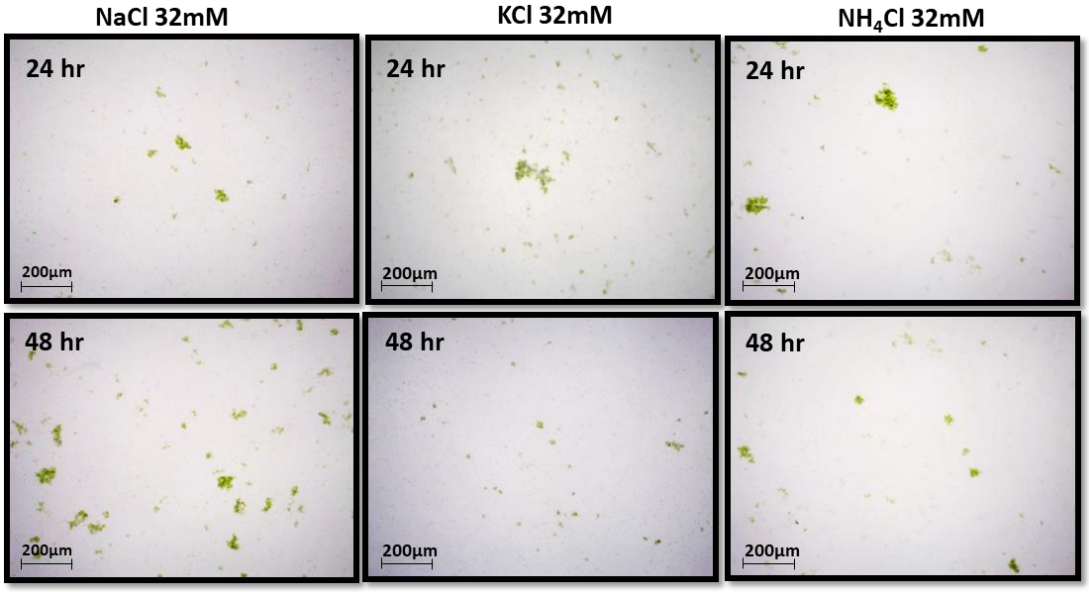

d) Microscopic imaging: 100 time magnification; Salt dose of NaCl, KCl and NH_4Cl of 32 mM after 24 and 48 hours.

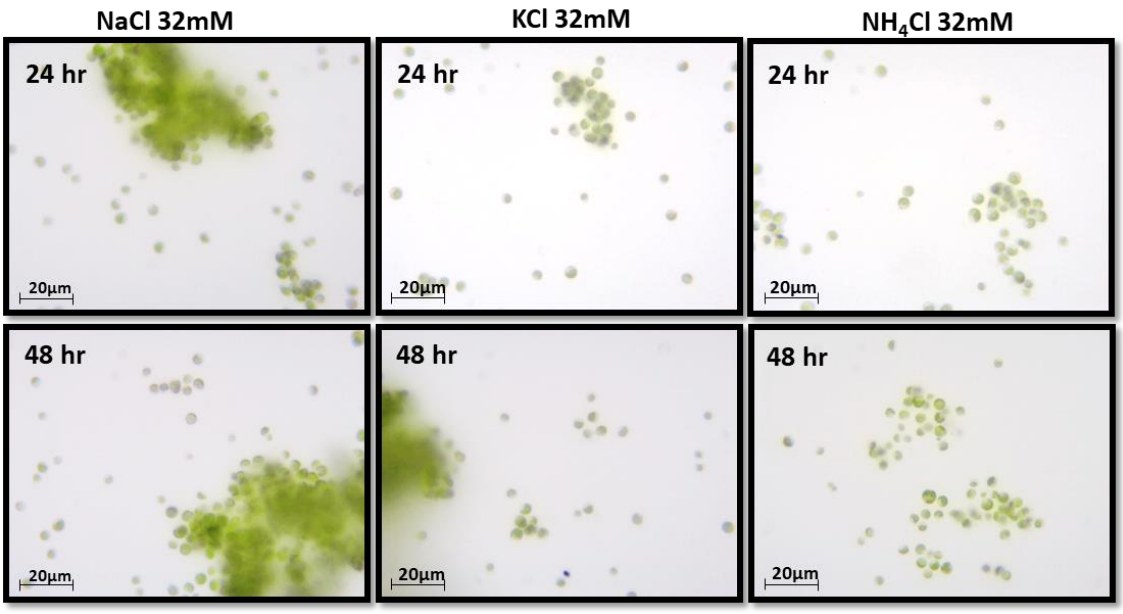

e) Microscopic imaging: 1000 time magnification; Salt dose of NaCl, KCl and NH_4Cl of 32 mM after 24 and 48 hours.

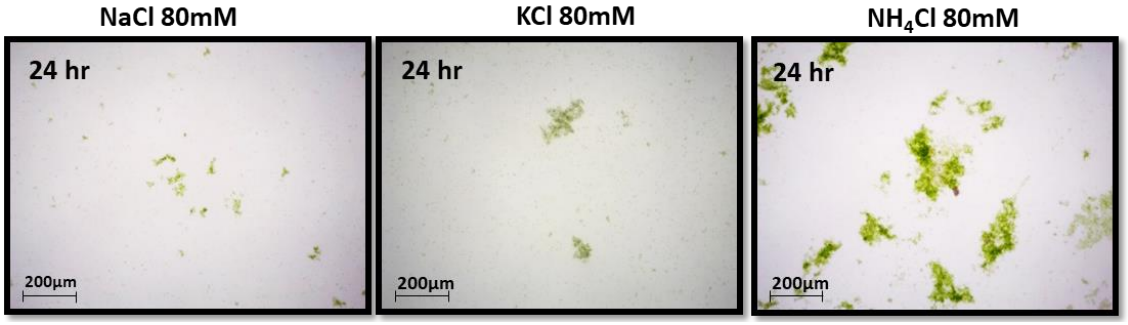

f) Microscopic imaging: 100 time magnification; Salt dose of NaCl, KCl and NH_4Cl of 80 mM after 24 hours.

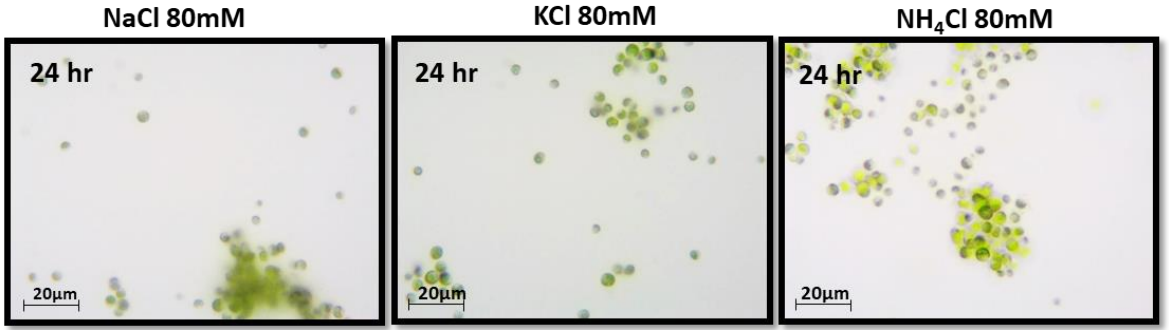

g) Microscopic imaging: 1,000 time magnification; Salt dose of NaCl, KCl and NH_4Cl of 80 mM after 24 hours.

Figure C2: Microscopic imaging of the algae feed solution after 24 and 48 hours of being subjected to different salts and concentrations.

APPENDIX D: SUPPLEMENTAL INFORMATION: THE USE OF ELECTRIC FIELD FORWARD OSMOSIS FOR THE MITIGATION OF FOULING DURING ALGAE HARVESTING

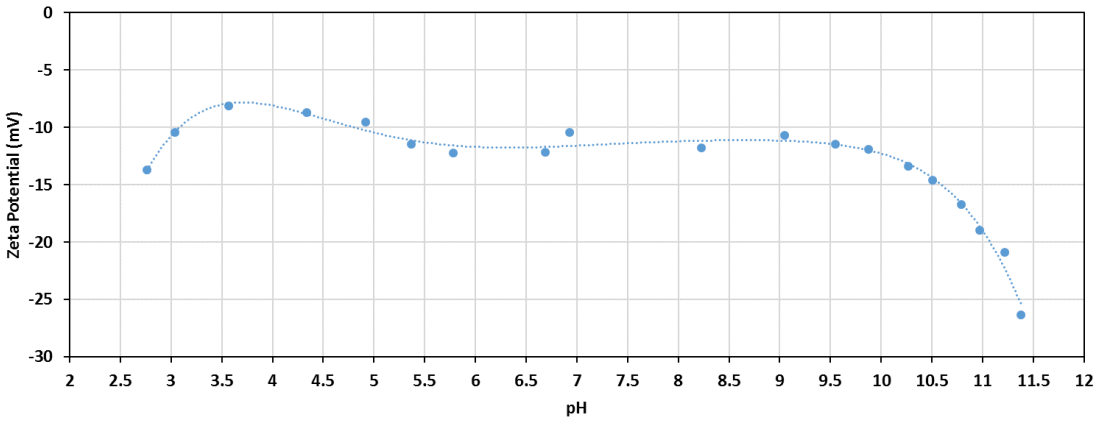

Figure D1: Zeta potential (mV) for a FO aquaporin TFC membrane. Electrolyte: KCl 1.0 mM, pH 6.3 ± 0.4, Temp. 23.0 ± 0.5 ˚C.

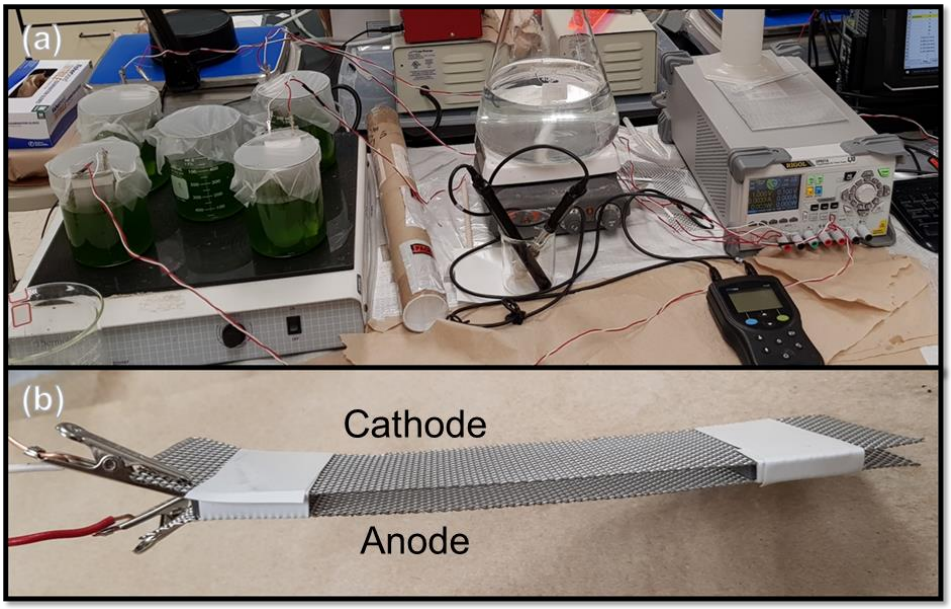

Figure D2. FO electric field test experimental setup. (a) An image of the batch experimental setup to study the effect of the electric field on the algal solution. (b) The mesh cathode and anode which were inserted in the algal culture solution to develop the electric field.

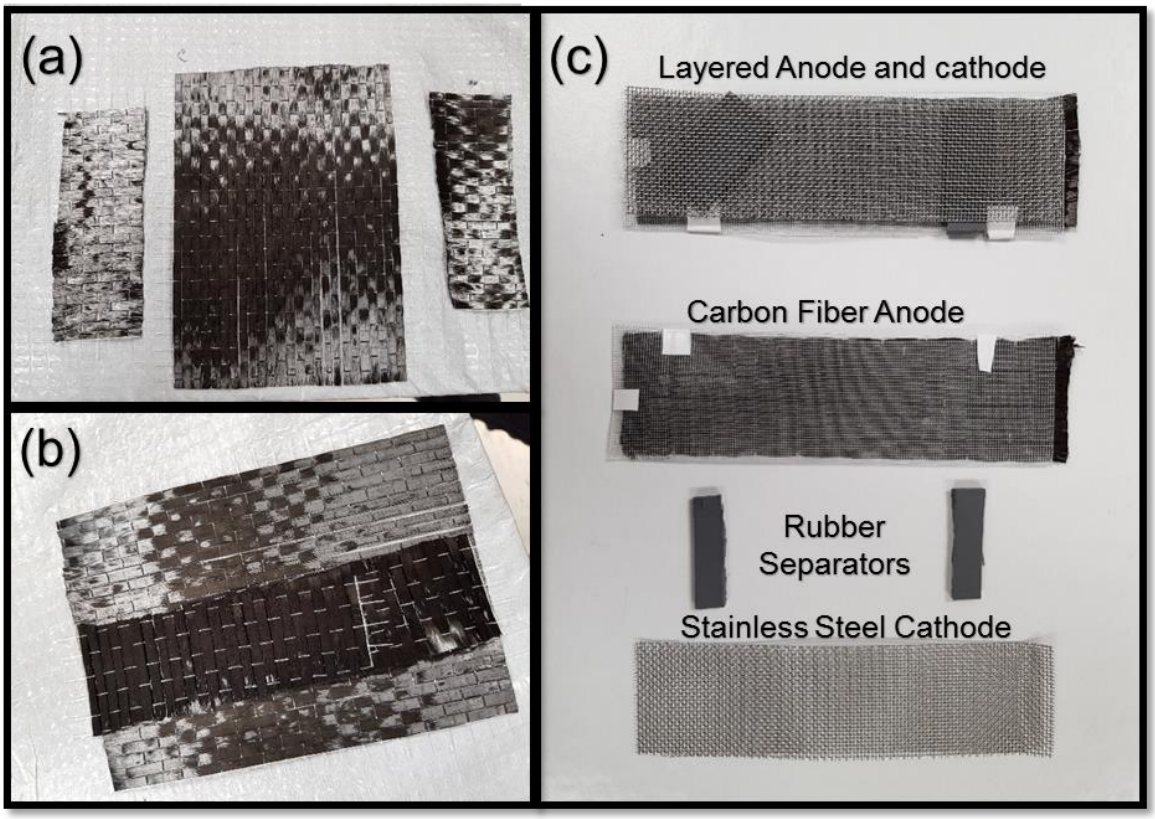

Figure D3: Fabrication of the carbon fiber anode electrode. (a) Carbon fiber layers used to fabricate a conductive electrode used as an anode. (b) Cross-connecting of the carbon fiber fabric to a defined surface area. (c) (Top) carbon fiber anode and stainless-steel cathode spaced with a 3 mm rubber (50A, Rubber-Cal, Santa Ana, CA); (Middle) The carbon fiber sheet electrodes covered with a polypropylene permeable mesh (FM100, Diversified Biotech, Dedham) to maintain the electrodes shape.

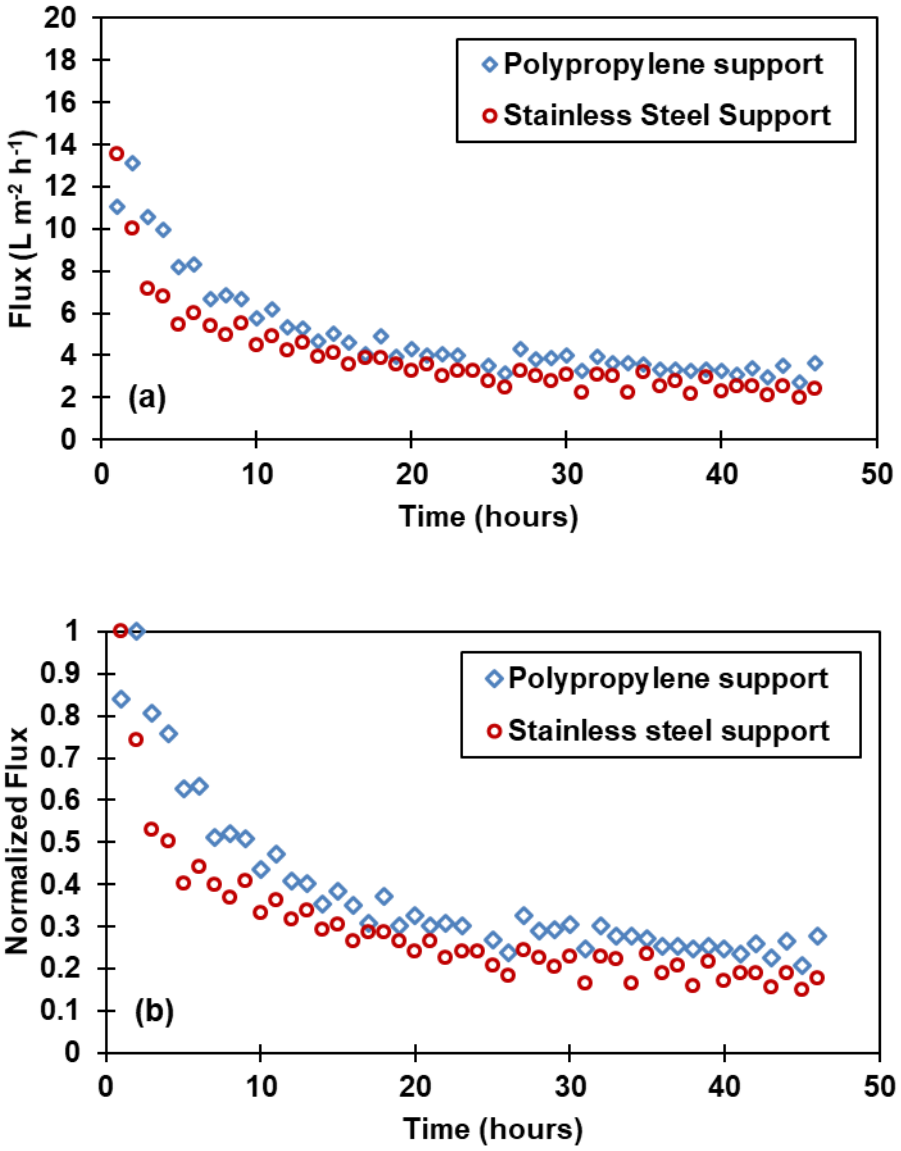

Figure D4: Effect of different FO membrane support materials on water flux during algae dewatering. (a) Actual flux against time and (b) Normalized flux against time. The FO batch experiment was conducted with 0.5 g L^{-1} of dry biomass *C. vulgaris* as FS and 4 M of NaCl as DS and at 5 cm sec^{-1} CFV. The measured (actual) water flux was normalized by dividing each flux at a given time by the initial flux.

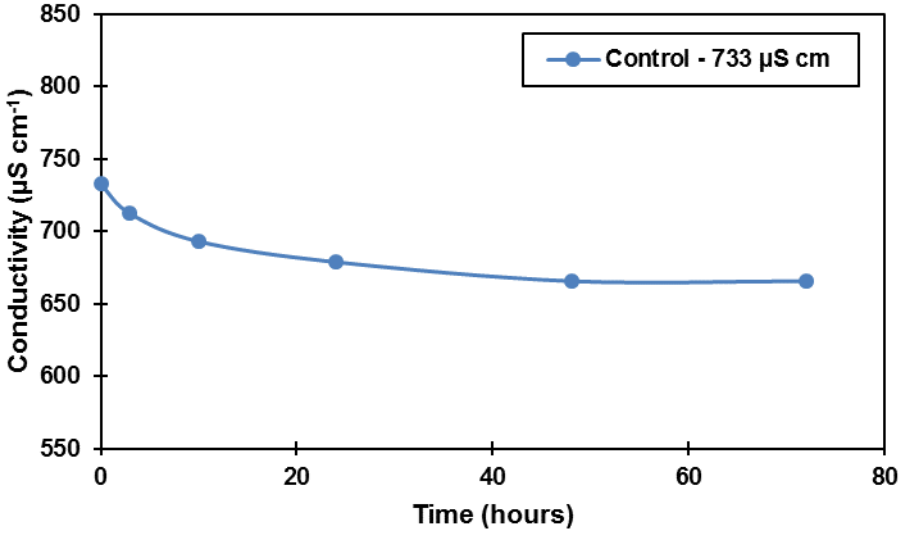

Figure D5: The change of conductivity in original algal culture (0.37 g L^{-1} dry algae biomass) over time. Algae cultivated in BBM without aeration and under 11.5-13.5 µmoL m^{-2} s^{-1} PAR of light intensity.

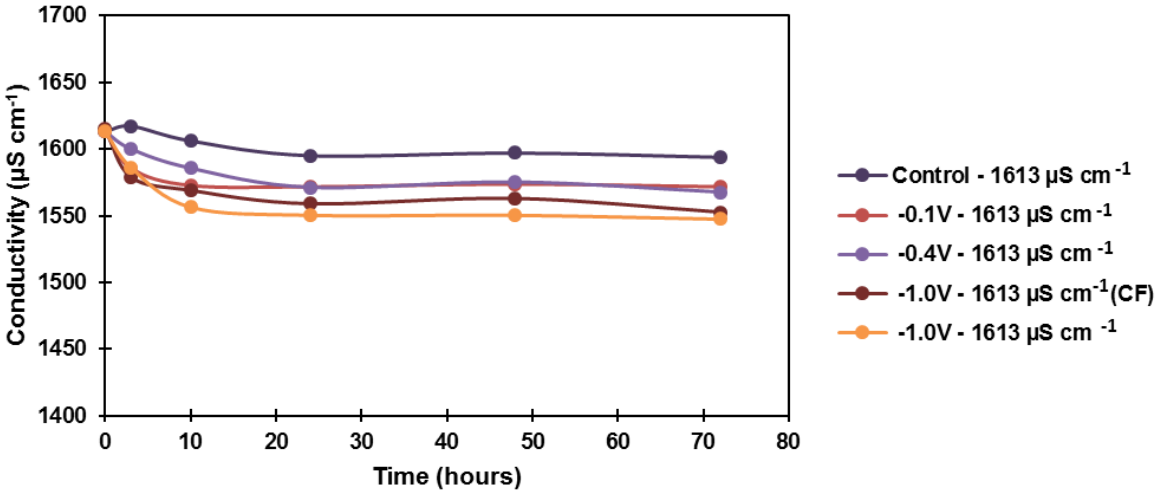

Figure D6: Conductivity change over time for different applied potentials on an algal solution (0.3 g L^{-1} dry algae biomass) with a conductivity of 1,613 µS cm^{-1} (equivalent to 0.5 g L^{-1} of NaCl).

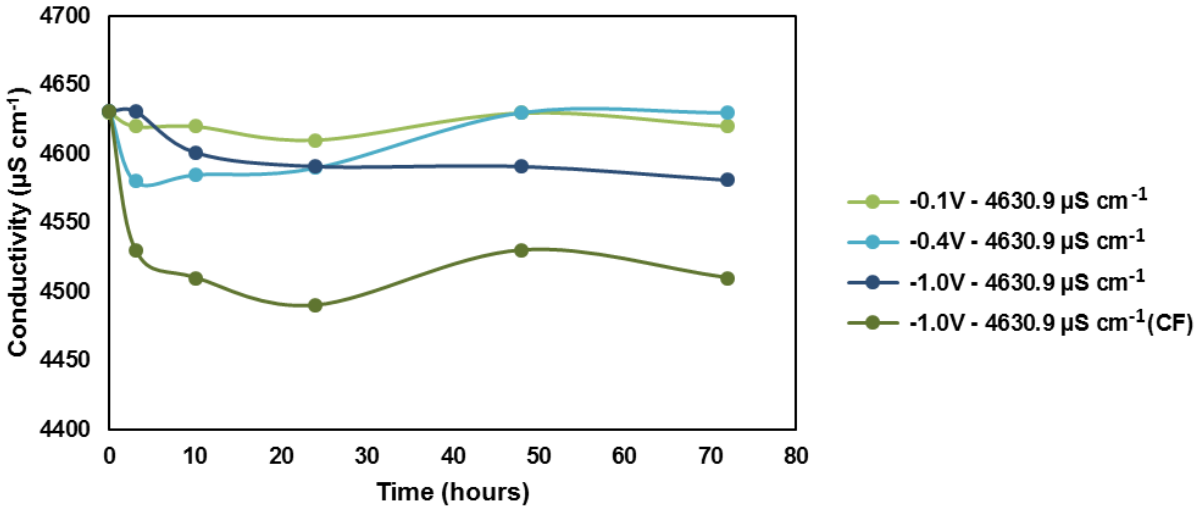

Figure D7: Conductivity change over time for different applied potentials on an algae solution (0.3 g L^{-1} dry algae biomass) with a conductivity of 4630.9 µS cm^{-1} (equivalent to 2.0 g L^{-1} of NaCl).

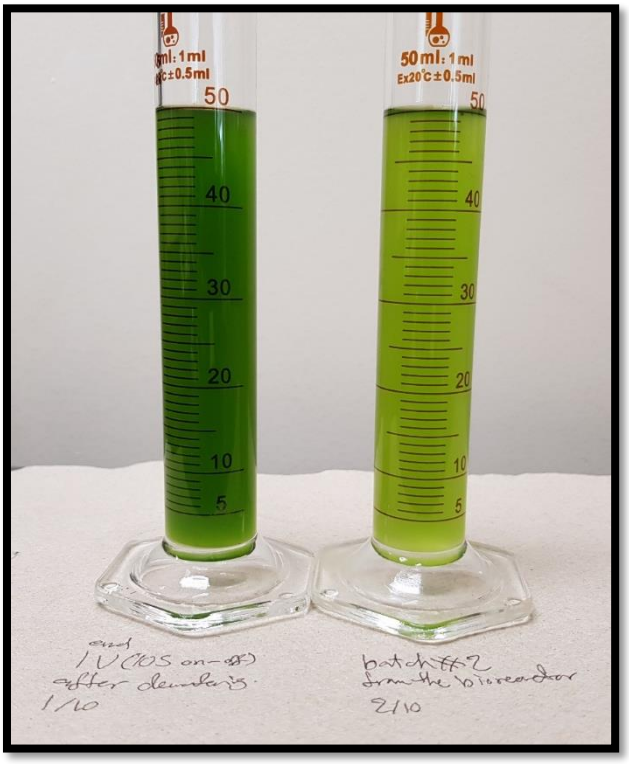

Figure D8: Left: 65% dewatered micro algae running under EFFO at a potential of -1.0V (10 sec on-off), conductivity in the concentrated FS had a 10 fold increase which required double the time to settle. Right: Original algae solution from the bioreactor.

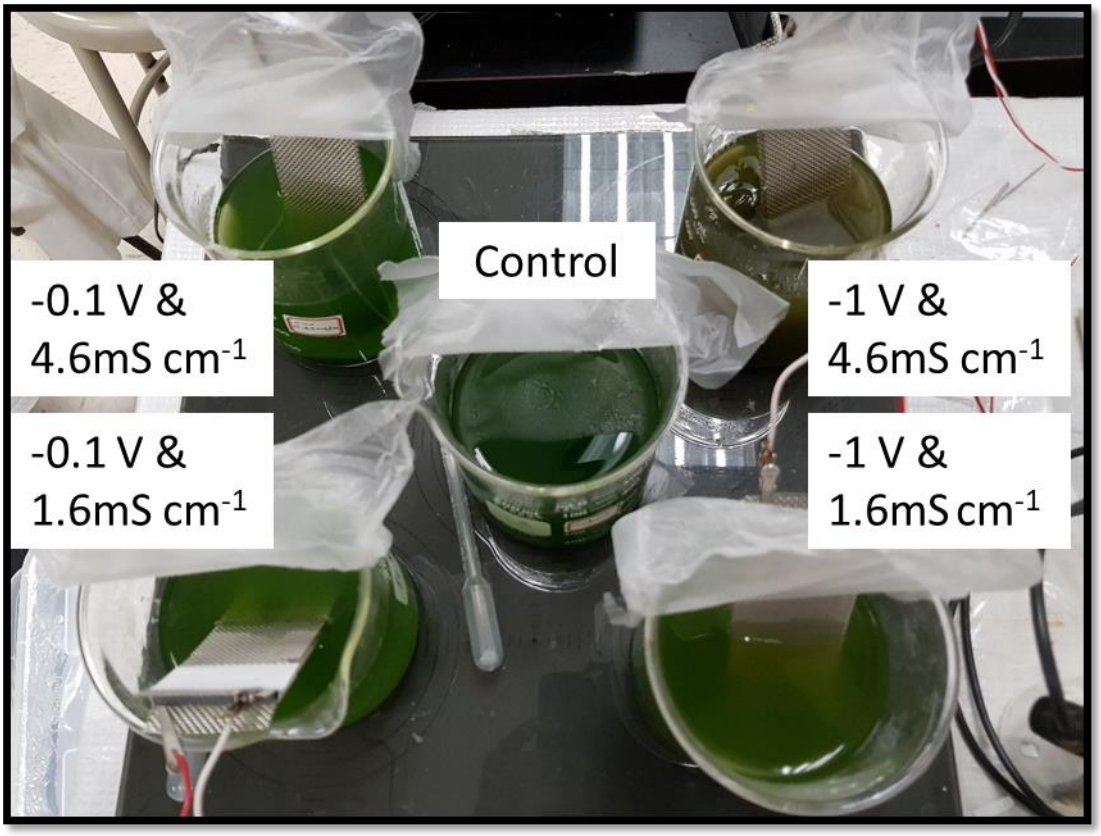

Figure D9: Applied EF on algae (0.3 g L^{-1}) batch experiments. 48 hours after running different electric potentials with different conductivity ranges. Stainless steel meshes cathodes and anodes.

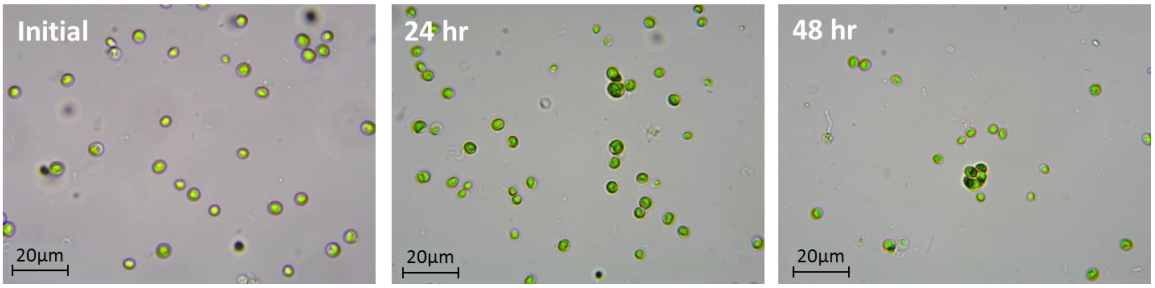

(a) Control: Original algae culture.

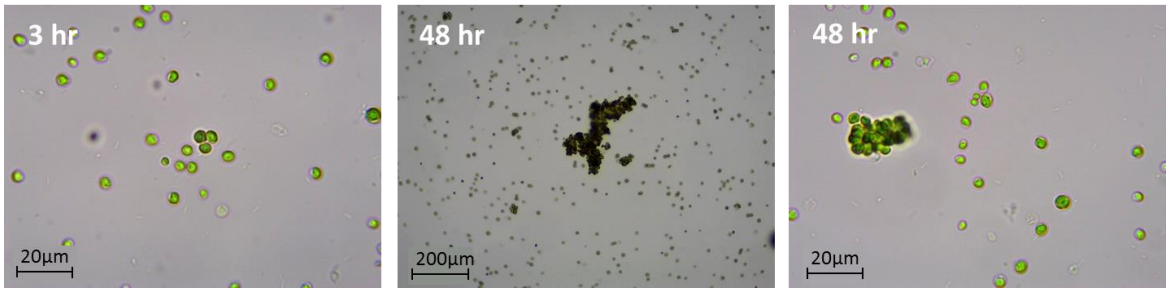

(b) Applied potential: -0.1 V; conductivity: 1613 µS cm^{-1}, Electrode type: Stainless steel mesh.

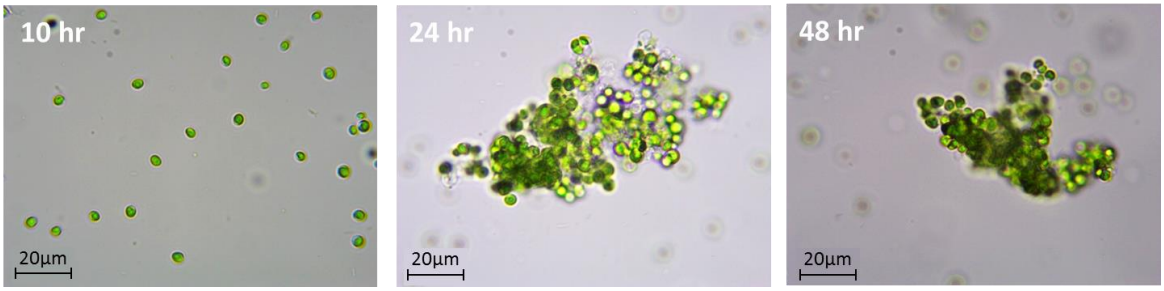

(c) Applied potential: -0.1 V; conductivity: 4630.9 µS cm^{-1}, Electrode type: Stainless steel mesh.

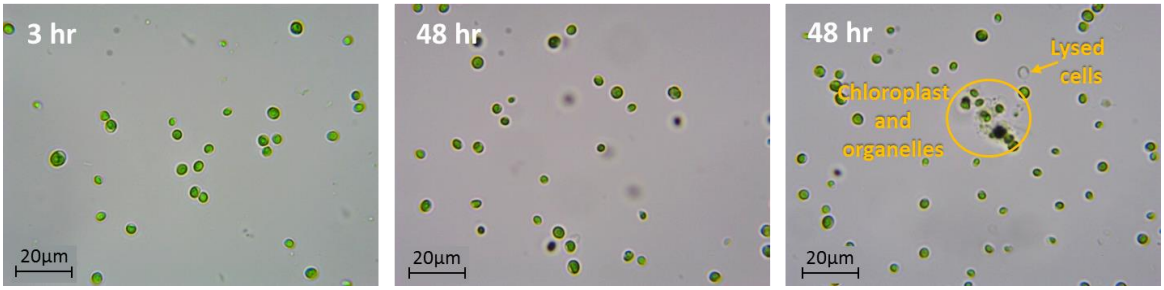

(d) Applied potential: -0.4 V; conductivity: 4630.9 µS cm^{-1}, Electrode type: Stainless steel mesh.

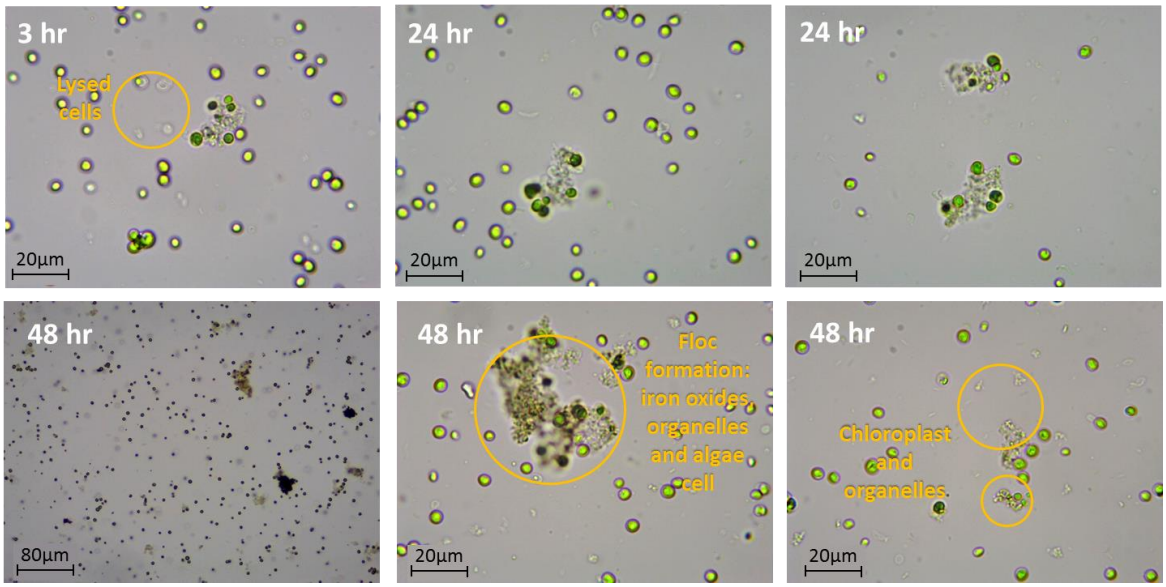

(e) **Applied potential: -1.0 V; conductivity: 1630 µS cm^{-1}, Electrode type: Stainless steel mesh.**

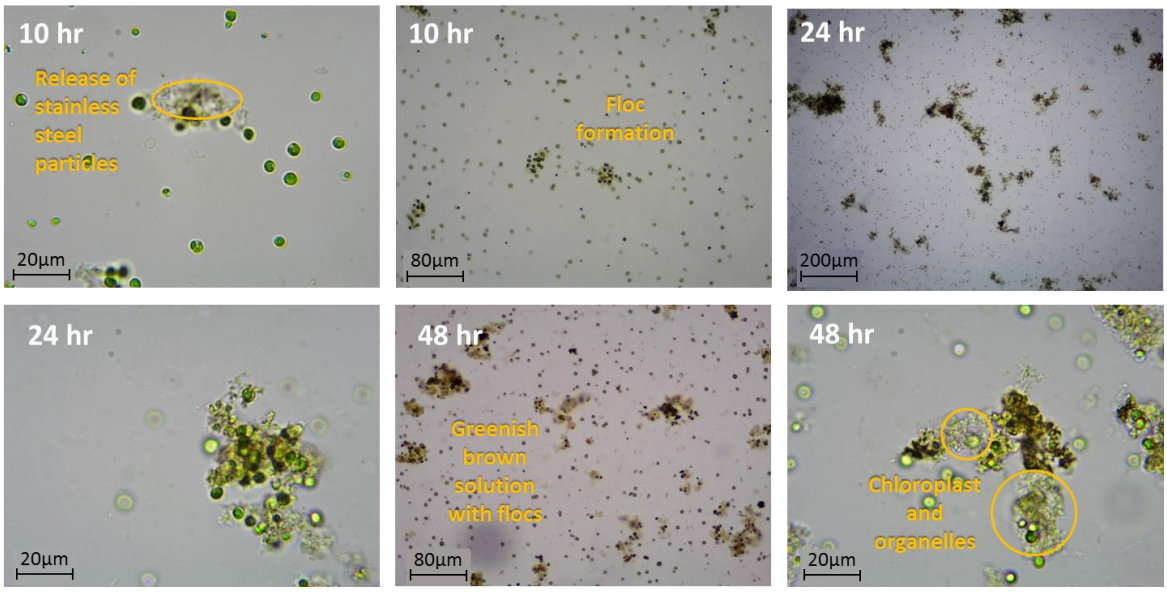

(f) Applied potential: -1.0 V; conductivity: 4630.9 µS cm^{-1}, Electrode type: Stainless steel mesh.

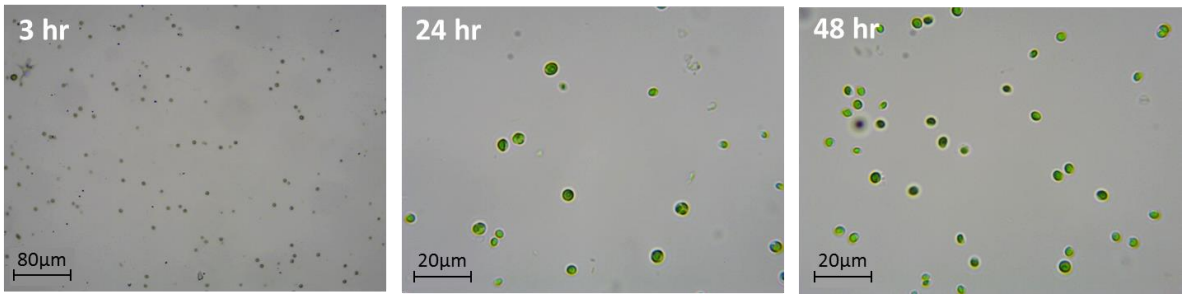

(g) Applied potential: -1.0 V; conductivity: 1630 µS cm^{-1}, Electrode type: Carbon fiber sheet.

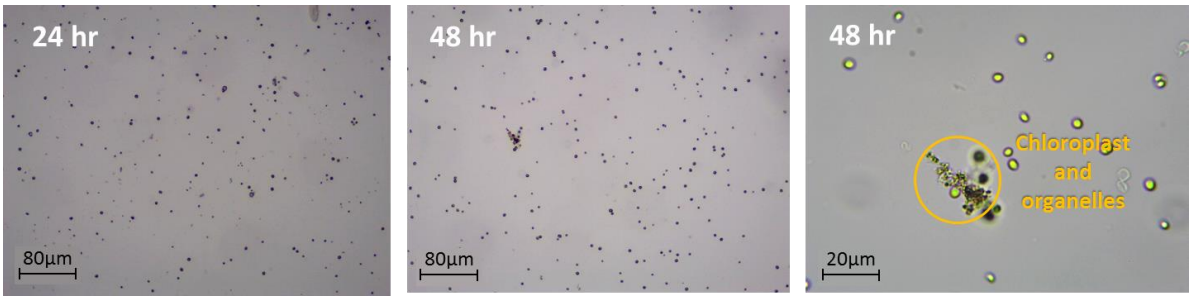

(h) Applied potential: -1.0 V; conductivity: 4630.9 µS cm^{-1}, Electrode type: Carbon fiber sheet.

Figure D10: Microscopic imaging of the algae feed solution after 3 days of being subjected to different applied potentials, with different salinity levels and electrode mesh type.